

Mineralogical and Geochemical Studies of Carbonaceous Shale Deposits from Egypt

Vorgelegt von

M.Sc.

Mostafa Gouda Mohamed Attia Temraz

aus Ägypten

an der Fakultät VI

Bauingenieurwesen und Angewandte Geowissenschaften
der Technischen Universität Berlin

zur Erlangung des akademischen Grades

Doktor der Naturwissenschaften

-Dr. rer. nat.-

genehmigte Dissertation

Promotionsausschuss:

Vorsitzender: Prof. Dr. H. Burkhardt

Berichter: Prof. Dr. Wilhelm Dominik

Berichter: Prof. Dr. Brian Horsfield

Tag der wissenschaftlichen Aussprache: 29. März 2005

Berlin 2005

D 83

Zusammenfassung

Die vorliegende Arbeit konzentrierte sich auf die integrierte sedimentologische, mineralogische und geochemische Analyse von kohlehaltigen Tonsteinabfolgen aus Ägypten. Die Untersuchungen der Schwarzschiefer der Ataqa Formation des Karbon und der Safa Formation des Jura im südlichen und nördlichen Sinai erlauben Rückschlüsse auf optimale Bedingungen zur Zeit der Ablagerung. Die Dominanz an detritischem Kaolinit, die Anreicherung an den chemisch immobilisierenden Elementen SiO_2 , Al_2O_3 und TiO_2 sowie die hohen Werte im Chemischen Alterierungs-Index (CIA = Chemical Index of Alteration), liefern Hinweise auf eine intensive chemische Verwitterung der Ausgangsgesteine und auf tropische bis subtropische, feuchtwarme Klimabedingungen im Hinterland. Das Auftreten von Kohleflözen in der Ataqa Formation in Abu Zinema und in der Safa Formation in Al Maghara (hier mit abbauwürdigen Kohleflözen) sowie das Fehlen von marinen Mikrofossilien weisen auf eine Sedimentation unter kontinentalen bis lagunären Bedingungen hin.

Die Schwarzschiefer der Duwi Formation, des Dakhla Shale und des Esna Shale (Oberkreide bis Tertiär) in Abu Tartur, im Nile Valley und in Quseir zeichnen sich durch einen sehr hohen Anteil an detritischem Smektit aus. Kaolinit und Chlorit treten nur untergeordnet auf. Das erhöhte Auftreten von Smektit belegt deutliche marine Einflüsse während der Ablagerung der Sedimente in Südagypen im Vergleich zur Region des Sinai. Der Ursprung der Sedimente, abgeleitet von granitischen bis basaltischen Ausgangsgesteinen und die Verwitterungsbedingungen im Hinterland waren in beidem Regionen gleich. Die Duwi Formation war unter eingeschränkt flachmarinen Bindungen, vorwiegend in einem reduzierenden Milieu zur Ablagerung gekommen. Die fortschreitende Campan-Maastricht Transgression wurde unterbrochen durch eine mehrphasige intensive Aufarbeitung von Sedimenten und der resultierenden Anreicherung von Phosphatlagen in dieser Formation. Charakteristisch ist das Fehlen von Mikrofossilien in der Duwi Formation, während reiche Foraminiferen-Vergesellschaftungen im darüber liegenden Dakhla Shale und im Esna Shale das Wiedereinsetzen und den Höhepunkt der Transgression unter offenmarinen Bedingungen aufzeigen.

Die untersuchten Schwarzschiefer der Ataqa Formation (Karbon), der Safa Formation (Jura) und der Duwi Formation (Oberkreide) zeigen deutliche Anreicherungen an organischer

Substanz (Total Organic Content, TOC). Im Dakhla Shale und im Esna Shale ist die organische Substanz durch tiefgründige Verwitterung und Oxidation deutlich reduziert.

Alle untersuchten Schwarzschiefer-Proben sind immatur hinsichtlich einer Kohlenwasserstoffgenerierung mit niedrigen Werten in Hydrogen Potential (HI)-Index vom Kerogen-Typus III.

Abstract

The present investigations focus on an integrated sedimentological, mineralogical and geochemical evaluation of the carbonaceous shales from Egypt.

The analysis of the black shales of the Ataqa Formation and the Safa Formation in both, Southern and Northern Sinai, indicate improved depositional environmental conditions during Carboniferous and Jurassic in Egypt. The dominance of detrital kaolinite, the enrichment in chemically immobile elements SiO_2 , Al_2O_3 and TiO_2 and high values of Chemical Index of Alteration (CIA) suggest intensive chemical weathering of the source rocks under tropical to subtropical humid climatic conditions. The occurrence of coal seams within the Ataqa Formation in Abu Zinema and within the Safa Formation in Al Maghara (here with mineable coal beds), as well as the absence of foraminifera in both formations indicate their deposition in a continental lagoonal environment.

In the black and carbonaceous shales of Duwi Formation, Dakhla Shale and Esna Shale of Upper Cretaceous and Lower Tertiary age in Abu Tartur, Nile Valley and Quseir, detrital smectite is the dominant clay mineral in addition to minor kaolinite and chlorite contents. The smectite content gives evidence of considerable marine influence during the sedimentary processes in South Egypt in comparison to Sinai, whereas the origin of detrital sedimentary input derived from granitic to basaltic source rock, and the weathering conditions were the same for both areas. The Duwi Formation in Abu Tartur was deposited in a shallow and restricted marine environment under prevailing reducing conditions. There, the Campanian/Maastrichtian transgression was interrupted by multiple regressive phases which caused intensive reworking of sediments and enrichment of the phosphate layers in this formation. The Duwi Formation is characterized by absence of foraminifera, compared to the abundance of foraminifera's assemblages in Dakhla and Esna shales which suggest open marine environments and prograding marine transgression during the deposition of these formations.

The studied shales show significant enrichment in organic matter in the black shale of Ataqa and Safa formations of Carboniferous and Jurassic age and Duwi Formation of Cretaceous age whereas the total organic carbon content (TOC) of Dakhla Shale and Esna Shale was depleted by oxidation under surface conditions in outcrops. All studied shales are immature for hydrocarbon generation with a fair hydrocarbon potential of kerogen type III.

Acknowledgement

First and above all, I would like to express my great thanks to my God, for helping me to accomplish this work.

I wish to express my sincere gratitude and appreciation to my academic supervisor Prof. Dr. Wilhelm Dominik, Faculty of Civil Engineering and Applied Geosciences, Technical University of Berlin for his supervision and guidance and for his encouragement. He supervised this study and helped to direct the research toward success by numerous discussions and informative reviews of reports and manuscripts.

This work would not have been possible without the most patient help and support of Dr. Robert Bussert during the laboratory analyses and the preparation of the thesis. Special thanks are due to Dr. Mathies for his help and achievement of my acceptance at the Institute of Applied Geosciences. Special thanks are also due to all colleagues of the Institute, particularly to Mrs. Lange, Mrs. Glowa and Mr. Thiel.

Personal appreciations are due to Prof. Dr. M. El Batanony, Manager of the Egyptian Petroleum Research Institute (EPRI), Prof. Dr. A. Abu Elezz, Head of the Exploration Department at EPRI and Prof. Dr. S. Awad, Ain Shams University.

My profound acknowledgement and thanks are due to the Government of Egypt for the financial support. I would like to thank all colleagues of Exploration Department for their help during the field seasons, particularly to Dr. A. Ahmed and Dr. I. Hasanein.

This thesis would never have been completed without the help and support of my mother and the support of my wife, Dr. Mona Khalaf and my son dear Ahmed. They were an important source of motivation. The great interest of my brothers Gamal, Khaled and Mohamed was very helpful for the successful accomplishment of the study.

TABLE OF CONTENTS

Zusammenfassung	I
Abstract	III
Acknowledgement	IV
Table of contents	V
List of Figures	IX
List of Tables	X
 1 Introduction	 1
1.1 General geographical and geological setting of Egypt	1
1.2 Location of the studied areas	2
1.2.1 Abu Zinema area in Southwest Sinai(Carboniferous)	2
1.2.2 Al-Maghara coal mine in North Sinai (Jurassic)	2
1.2.3 Abu Tartur phosphate mine in Western Desert (Cretaceous-Eocene)	4
1.2.4 Esna-Idfu region in Nile Valley (Cretaceous-Eocene)	4
1.2.5 Qusier phosphate mine in the Red Sea coast (Cretaceous-Eocene)	4
1.3 Distribution of carbonaceous shales in Egypt	5
1.4 Previous studies on black and carbonaceous shales in Egypt	6
1.5 Scope of the present work	6
 2 Lithostratigraphy	 7
2.1 The area of Abu Zinema in Southwest Sinai (Carboniferous)	8
2.1.1 Um Bogma Formation (Lower Carboniferous)	8
2.1.2 Ataq Formation (Lower Carboniferous)	10
2.2 The area of Al-Maghara coal mine North Sinai (Jurassic)	10
2.2.1 Mashaba Formation (Lower Jurassic)	11
2.2.2 Rajabiah Formation (Lower Jurassic)	11
2.2.3 Shusha Formation (Lower Jurassic)	11
2.2.4 Bir Maghara Formation (Middle Jurassic)	13
2.2.5 Safa Formation (Middle Jurassic)	13
2.2.6 Masajid Formation (Upper Jurassic)	13

2.3 The area of Qusier phosphate mines in Red Sea coast (Cretaceous - Eocene)	13
2.3.1 „Nubia Sandstone” (Pre-Campanian)	15
2.3.2 Quseir Variegated Shale (Pre-Campanian)	15
2.3.3 Duwi Formation (Campanian-Maastrichtian)	16
2.3.4 Dakhla Shale (Danian–Lower Paleocene)	17
2.3.5 Tarawan Chalk (Landanian-Late Paleocene)	18
2.3.6 Esna Shale (Early Eocene)	18
2.3.7 Thebes Formation (Early Eocene)	19
2.3.8 Nakheil Formation (Oligocene)	19
3 Methods of Investigation	20
3.1 Mineralogical analysis	20
3.1.1 Separation of clay size fraction	20
3.1.2 X-ray diffraction (XRD)	20
3.1.3 Petrographic microscopy	21
3.1.4 Scanning Electron Microscopy (SEM)	21
3.2 Geochemical analysis	21
3.2.1 X-ray Fluorescence (XRF)	21
3.2.2 Determination of total organic carbon content (TOC)	22
3.2.3 Rock Eval pyrolysis	22
4 Mineralogy	23
4.1 Clay mineralogy	23
4.1.1 The importance of clay minerals	23
4.1.2 Structure and chemistry of clays	23
4.1.2.1 Smectite group minerals	24
4.1.2.2 Kaolinite group minerals	24
4.1.2.3 Chlorite group minerals	24
4.1.2.4 Illite/Mica group minerals	25
4.2 Clay minerals in the studied shale samples	25
4.2.1 Smectite	26
4.2.2 Kaolinite	29

4.2.3	Chlorite	30
4.2.4	Illite	32
4.3	Whole rock samples	33
4.3.1	Quartz	33
4.3.2	Carbonates	33
4.3.3	Sulphates	33
4.3.4	Pyrite	34
4.3.5	Carbonate fluorapatite	34
5	Geochemistry	36
5.1	Major and trace elements	37
5.1.1	Silica (SiO ₂)	40
5.1.2	Alumina (Al ₂ O ₃)	41
5.1.3	Calcium (CaO)	41
5.1.4	Magnesium (MgO)	43
5.1.5	Iron Oxide (Fe ₂ O ₃)	45
5.1.6	Titanium (TiO ₂)	45
5.1.7	Phosphorous (P ₂ O ₅)	46
5.1.8	Sodium (Na ₂ O)	47
5.1.9	Potassium (K ₂ O)	47
5.1.10	Sulphate (SO ₃)	47
5.2	Distribution of significant trace elements	48
5.2.1	Vanadium	48
5.2.2	Nickel	48
5.2.3	Chromium	50
5.2.4	Cobalt	52
5.2.5	Strontium	52
5.2.6	Zinc	52
5.2.7	Copper	53
5.2.8	Zirconium	53
5.3	Discussion of chemical effects	54
5.4	Weathering effects	55
5.5	Provenance analysis for sedimentary rocks	56
5.6	Distribution of major and trace elements in phosphate rocks	59

6	Petrography and SEM investigations	62
6.1	Organic matter-rich black shale facies	63
6.2	Foraminifera-rich shale facies	65
6.3	Carbonate facies	65
6.4	Phosphatic facies	66
7	Organic Geochemistry	68
7.1	Total organic carbon (TOC) content	68
7.2	Rock-Eval pyrolysis	70
7.2.1	Hydrocarbon source potentials	72
7.2.2	Determination of thermal maturity (Tmax)	72
8	Summary and conclusions	73
9	References	75
10	Appendix	90
A	Tables	91
B	Figures	102
C	Plates	105

List of Figures

Fig. 1: Location map of the study areas in Egypt.....	3
Fig. 2: Stratigraphic column and regional distribution of the studied formations.....	7
Fig. 3: Lithostratigraphic section of the Paleozoic in central Sinai showing the position of Ataqa Formation (after Said 1990).....	9
Fig. 4: Generalized lithostratigraphic column of Jurassic and Cretaceous rocks exposed at Gebel Maghara (after Jenkins et al. 1982).....	12
Fig. 5: Sedimentary sequences of Upper Cretaceous-Lower Tertiary rocks showing the position of the samples in the studied areas.....	14
Fig. 6: Smectite average at the studied locations.....	26
Fig. 7: Kaolinite average at the studied locations.....	29
Fig. 8: Chlorite average at the studied locations.....	31
Fig. 9: Illite average at the studied locations.....	32
Fig. 10: Major elements variation of the studied samples including 7 phosphate samples.....	37
Fig. 11: The relationships between SiO_2 with Al_2O_3 , TiO_2 , Zr & K_2O and Al_2O_3 with TiO_2 & K_2O for the studied samples.....	42
Fig. 12: The relationship between CaO with Na_2O , P_2O_5 , MgO, K_2O , SiO_2 & Al_2O_3 for the studied samples.....	44
Fig. 13: The relationship between TiO_2 with Al_2O_3 and Zr for the studied samples.....	46
Fig. 14: The relationships between V with Ni, Cr, Al_2O_3 , clay & TOC and Ni with clay, TOC & Al_2O_3 for the studied samples.....	49
Fig. 15: The relationship between Cr with Zn, Al_2O_3 , V, clay, Cu and TOC for the studied samples.....	51
Fig. 16: TiO_2 / Al_2O_3 binary plot of the studied shale samples.....	58
Fig. 17: Distribution of P_2O_5 in the studied phosphate samples.....	59
Fig. 18: The relationship between P_2O_5 with TiO_2 , CaO & Al_2O_3	61
Fig. 19: Stratigraphic position of the studied shales and composite TOC (%) profile	69
Fig. 20: Van Krevelen-type plot of Rock-Eval data for the studied bulk samples.....	71

List of Tables

Table 1: Average semi-quantitative clay mineralogy of the studied shales (by XRD).....	25
Table 2: Comparison of chemical composition of the studied shales with published average shales (1 to 4) and regional average composition (5 to 8).....	38
Table 3: The major and trace elements average of formations at the studied locations.....	39
Table 4: The TOC and Rock-Eval results of the studied shales.....	70

1. Introduction

Carbonaceous shales have a wide distribution on the Egyptian surface and in subsurface sedimentary sequences e.g. in sediments of predominantly Carboniferous, Jurassic, Cretaceous, Paleocene and Eocene age. The carbonaceous and black shales in Egypt gained interest since five decades when the phosphorite deposits were discovered and exploited. The phosphorites are intercalated with and capped by black shales that contain considerable amounts of organic matter and are enriched in trace elements, which may be of economic potential. The interest in the black shales all over the world in the last decades principally stem from the widespread recognition that black shales are important source rocks for petroleum or may be used as natural fuel resources. Various previous studies of the carbonaceous shales in Egypt concentrated on an individual location or an individual geological age. In this work the shales of the variety of Egyptian locations and stratigraphic ages are investigated focusing on their mineralogical and geochemical characteristics.

1.1 General geographical and geological setting of Egypt

Egypt forms the north-eastern part of the African continent and is situated between latitudes 22° and 31° north. The country covers an area of about one million km² and occupies nearly one-thirtieth of the total area of Africa. The largest part of Egypt consists of desert, the so called Western Desert, to the west of the Nile, the Eastern Desert, east of the Nile Valley and the Sinai Peninsula, delineating the north-eastern extension of the Sahara.

The structural elements of the Precambrian of the north-eastern margin of the African Shield (Arabian-Nubian massif) are the principal features that controlled the structural development of Egypt (Said 1962). The reactivation of these elements during the Paleozoic resulted in the development of large NNW–SSE striking interacratonic depressions (Klitzsch 1984).

From Late Precambrian to Mid-Cretaceous sediments all over Egypt were deposited in largely shallow and nearshore marine environments, interbedded with continental (fluvial) and deltaic sediments (Gindy 1983). At the end of the Lower Carboniferous, the post-Visean uplifting was accompanied by E–W fault systems and affected a large part of the NE African plate. As a result, most of the pre-Visean deposits were eroded from uplifted areas and were only preserved in the western part of Egypt. Marine strata in the northern Gulf of Suez (Said 1962) and fluvio-glacial sediments in the south were also encountered or preserved in the

Carboniferous (Klitzsch 1980, 1983a and 1983b). During the Permian and until the Lower or Middle Jurassic, continental to shallow marine sediments covered the northern part of Egypt.

After the disintegration of the large continent „Pangaea” in Jurassic time, the old structural patterns of Precambrian age, which had influence in the Early Paleozoic, were reactivated (Schandelmeier et al. 1987). The result was a stepwise subsidence of the intracratonic depocenters that gave rise to the formation of the Dakhla and Assiut basins (Hendriks et al. 1987). Until Early Cretaceous time, clastic sedimentation was predominant. Starting from the Cenomanian and ending in the Senonian, the structural differentiation of the NE African plate was increased and the major marine transgression of the Tethys, that deepened to the north and advanced southwards, reached its maximum extension in the Lower Eocene. The Upper Cretaceous sediments in southern Egypt consist of variegated shales upon which, (in the intracratonic depocenters), a thick sedimentary succession follows. The sediments are of shallow marine origin with some lateral and vertical lithological changes, in which the phosphate deposits are intercalated.

1.2 Location of the studied areas

In this work 144 samples were selected from five different locations and different geological ages to represent all the carbonaceous shales of Egypt (Fig.1).

1.2.1 Abu Zinema area in Southwest Sinai (Carboniferous)

In this location 12 samples were selected from the carbonaceous (black) shale located within the middle part of sandstones of the Ataq Formation of Carboniferous age at Bedaa–Um Thora district (long. 33° 13' East and lat. 29° 3' North) in Southwest Sinai. The Paleozoic sediments are exposed in the south-central parts of Sinai, primarily in the Um Bogma area east of Abu Zinema and at Abu Durba.

1.2.2 Al-Maghara coal mine in North Sinai (Jurassic)

From Al-Maghara coal mine about 70 km south of the Mediterranean Sea at long. 33° 10' and 33° 35' E and latitudes 30° 35' and 30° 10' N. North Sinai, five samples of carbonaceous (black) shale which is associated with the main coal bed of Safa Formation of the Jurassic age (Al Far 1966), were collected.



Fig. 1: Location map of the study areas in Egypt.

In North Sinai a complete Jurassic section is exposed at Gebel Al-Maghara. During the Jurassic and Cretaceous periods there was no significant change in the depositional framework. The Jurassic sequence below the Cretaceous at Gebel Al-Maghara can be divided into six alternating continental and marine formations.

1.2.3 Abu Tartur phosphate mine in Western Desert (Cretaceous - Eocene)

The Abu Tartur phosphorites, which were first described by Hermina et al. (1961), are situated in the middle latitudes of Egypt about 60 km to the west of El Kharga town (lat. 25° 26' N and long. 30° 02' E). The Abu Tartur plateau forms an extended escarpment which bounds the Dakhla–El Kharga depression to the north. The semi-oval plateau covers an area of 1200 km². It is covered by Early Tertiary limestones. From the long wall sector at Abu Tartur phosphate mine 12 samples from the carbonaceous (black) shale of Duwi Formation were collected. It is of Upper Campanian to Lower Maastrichtian age (Said 1962).

1.2.4 Esna-Idfu region in Nile Valley (Cretaceous - Eocene)

The Esna-Idfu region is situated east of the Nile Valley between latitude 25° 05' and 25° 30' N and longitude 32° 30' and 32° 50' E. About 80 samples were collected to represent the exposed rock units, as a composite section stratigraphically subdivided from top to base into:

Esna Formation	Paleocene - L. Eocene
Tarawan Formation	U. Palaeocene
Dakhla Shale	Maastrichtian - Paleocene
Duwi Formation	U. Campanian - L. Maastrichtian
„Nubia Sandstone“	Pre-Campanian

1.2.5 Qusier phosphate mine in the Red Sea coast (Cretaceous - Eocene)

The Qusier and Safaga areas are part of the Eastern Desert of Egypt at the Red Sea Coast, and gained importance since five decades when the phosphate deposits of the Gebel Duwi Range were discovered and exploited. The region extends in a northwest direction along the western coast of the Red Sea from south of Qusier to Safaga, between latitude 25° 50' and 26° 67' N and longitude 33° 45' and 34° 25' E, covering an area of about 500 km².

At present, most of the mines in Quseir and Safaga are abandoned due to the low grade of the remaining phosphate deposits, the current exploitation of phosphates from Abu Tartur phosphate mine and the effect of international competition of Moroccan and Jordanian ores. The phosphate in some mines is usually intercalated with and capped by shales. Typically, the Egyptian phosphates are shallow marine deposits of a general Upper Cretaceous age. Their maximum intensity of deposition was associated with a transgressive shoreline of the Late Campanian or Early Maastrichtian Sea which encroached from North to South over the northern slope of Africa. From Quseir phosphate mines 35 samples from Duwi and Dakhla formations were collected.

1.3 Distribution of carbonaceous shales in Egypt

The black shales are widely distributed in Egypt in several horizons of different geologic ages. No serious approach had been made to evaluate their geological as well as their economic significance. This may have been due to the lack of interest in developing and using these economically important deposits as a source of fuel, most probably due to the competition of oil. Ball (1916) and Hume (1927) were the first authors who recorded in outcrops Cenomanian marls and sandstones which contain hydrocarbons in the form of oil and asphaltic matter at many localities, e.g. Wadi Abu Quda, Itala el-Zur and Nazzazat, Gulf of Suez area.

Said (1962) mentioned that some carbonaceous shale bands containing plant remains of Paleozoic age are recorded at Rod El Hammal, Wadi Araba. Oil shales were also reported from Cabal Tanka, Wadi Matulla, North Ras Gharib, Abu Shaar, Judal, and Ras Dib. In the Fayum region to the west of Gharaq and Wadi Maela, the Middle Eocene limestone is bituminous. The middle chalky limestone to the east of Tura is distinctively bituminous.

The oil shales are present in different Upper Cretaceous-Lower Tertiary formations: Duwi Formation (Phosphate bearing rock), Dakhla Shale and Esna Shale in the region between Safaga and Quseir in the Red sea coast. The Dakhla Shale possesses the horizon richest in organic matter. The Dakhla Shale directly overlies the upper phosphate bed. The average amount of oil yielded by Fischer assay from Cretaceous oil shale amounts to 20 - 45 gal/ton (Robison and Tröger 1983; Tröger 1984). Black shales also occur in many localities in the Western Desert. Among the important localities of oil shale is the one recorded in Abu Tartur area which yield considerable amount of oil (Tröger 1984).

1.4 Previous studies on black and carbonaceous shales in Egypt

Various authors have attempted to provide some information on the geology and the sedimentology of the black and carbonaceous shales in Egypt. However, many points concerning their origin and potential still need further clarification. Higazy and Hussein (1955) measured the uranium content of some black shales and phosphates from the Quseir - Safaga district. Mustafa and Ghaly (1964) studied the carbonaceous shales from different localities in Egypt (Galala area, Buda Valley and Quseir area). Malak et al. (1977) studied the mineralogical, petrography and organic geochemical characteristics of black shale in Safaga-Quseir area. Robison and Tröger (1983) studied the geology and organic geochemistry of Dakhla shale from Quseir, Sibaiya and Abu Tartur. Tröger (1984) determined the oil yield by Fischer assay and estimated the total volume of all potential organic-rich Cretaceous strata of Quseir-Safaga and Abu Tartur areas. Ganz (1984) proposed a genetic model for the organic rich phosphate-bearing Dakhla Shale. Darwish (1984) studied the stratigraphy and organic chemistry of the black shales in the Quseir-Safaga area. Khaled et al. (1987) studied the geochemical characters of the oil shales and their extractable bitumina within the Duwi Formation in the Quseir-Safaga district.

The black shales in Egypt were also studied petrographically, mineralogically and geochemically by many workers (El-Kammar 1987; Ganz 1987; Germann et al.1987; El-Kammar et al.1990; Ibrahim 1992; El-Kammar 1993; Ismael 1996; Ahmed 1997; Sediek and Amer 2001; Ghandour et al 2003; Ibrahim et al.2004). Most of the previous studies were carried out on black shales of the Eastern Desert (Quseir-Safaga district); however, little was done on the Western Desert and Sinai. Thus this study focuses on the carbonaceous and black shales from both, the Eastern and the Western Desert as well as Sinai.

1.5 Scope of the present work

Egyptian carbonaceous and black shales have drawn the attention because of their geological and economic significance (as a source rock and raw material). The present work aims to provide detailed geological, mineralogical, geochemical, petrographical information and to determine the economic potential of some Egyptian carbonaceous shale, which stem from five different geological ages. For these carbonaceous shales the depositional conditions are studied.

2 Lithostratigraphy

In the following, the regional distribution of the different lithofacies types of the carbonaceous shales of Carboniferous to Eocene age for the five locations will be discussed.

	Sinai		Western Desert	Nile Valley	Red Sea coast	
	Abu Zinema Az. (1)	Al – Maghara Mg (2)	Abu Tartur AT (3)	Esna-Idfu N (4)	Quseir Q (5)	
Early Eocene				Esna Shale		
Late Paleocene				Tarawan Chalk		
Lower Paleocene - Upper Cretaceous				Dakhla Shale		
Upper Cretaceous			Duwi Formation			
Pre Campanian					Varigated Shale	
Middle Jurassic				Safa Formation		
Lower Carboniferous	Ataqa Formation					

Fig. 2: Stratigraphic column and regional distribution of the studied formations.

2.1 The area of Abu Zinema in Southwest Sinai (Carboniferous)

The Paleozoic sediments are exposed in the southern central parts of the Sinai, primarily in the Um Bogma area east of Abu Zinema and at Abu Durba (Fig. 3). These sediments have been studied in detail by Abdallah and Adindani (1963), Hassan (1967), Weissbrod (1969), Said (1980) and Issawi and Jux (1982). The lack of diagnostic fossils has made accurate dating and correlation extremely difficult and additional confusion has been created by the use of various formation names. The basal Cambro-Ordovician sequence comprises the Araba, Naqus and Wadi Malik Formations of Issawi and Jux (1982), which are equivalent to the Yam Suf Group and the Netafim Formation of Weissbrod (1969). These clastic sediments were deposited on the peneplained surface of the pre-Cambrian basement and are dominated by grits, siltstones, subarkoses and conglomerates, with few dolomite beds (Said 1990).

Issawi and Jux (1982) have interpreted some of the conglomerates to be of fluvioglacial origin, suggesting that some of these sediments may be of Silurian age whilst the upper parts are interpreted as Devonian. However, these age datings are not based on direct faunal evidence and therefore may not be totally correct. These basal Paleozoic sediments were deposited under fluvial paralic conditions and probably represent relics of a very large sediment body which originally extended over a large area, but was deeply eroded before the deposition of upper Paleozoic strata. The Carboniferous at southwest Sinai was divided from base to top into two formations, the Um Bogma Formation and the Ataqa Formation.

2.1.1 Um Bogma Formation (Lower Carboniferous)

The Um Bogma Formation provides the first reliable date for the Paleozoic sequence in Sinai. These marine carbonates are highly fossiliferous, especially in foraminifera, and have been dated as Tournaisian-Visean (Said 1990). The Um Bogma Formation lies conformably over nonfossiliferous sandstones which are generally believed to be of lower Paleozoic age. Ferromanganese minerals within the basal part of the carbonates at Um Bogma have been extensively mined for many years. South of Abu Durba the Um Bogma Formation is represented by black marine shales (122 m thick) which have yielded a similar fauna comparable to that of Um Bogma area.

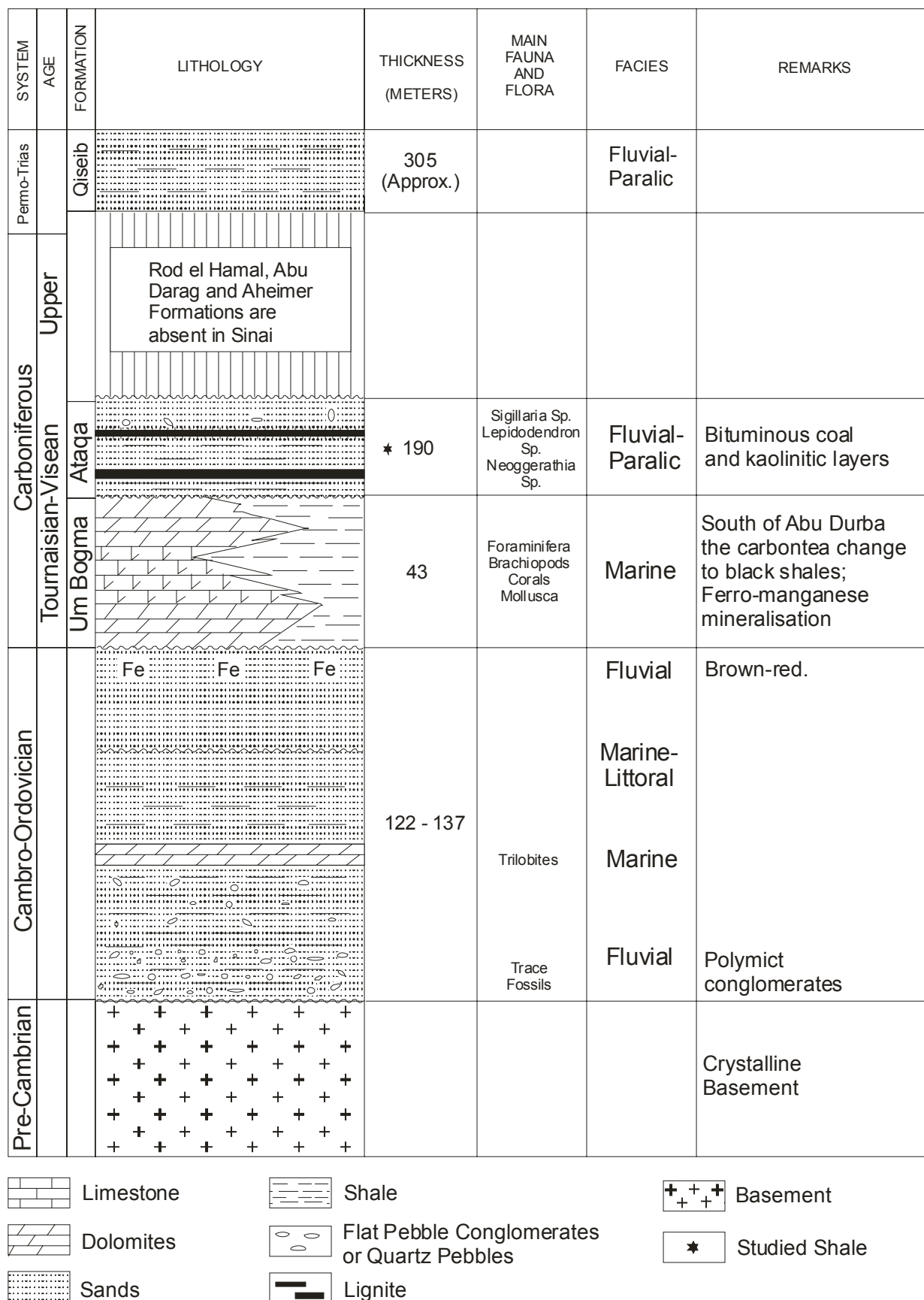


Fig. 3: Lithostratigraphic section of the Paleozoic in central Sinai showing the position of Ataqa Formation (after Said 1990)

2.1.2 Ataqa Formation (Lower Carboniferous)

The Ataqa Formation is unconformable overlying the Um Bogma Formation and consists of thick cross-bedded, very fine to fine grained sandstones. Visean flora and fauna have been identified within these sediments by Horowitz (1973). Kaolinitic layers are present within the Ataqa Formation and these are exploited commercially in the Wadi Abu Natash area. At Um Bogma the Ataqa Formation contains bituminous coal seams and is capped by a basaltic sill. Several carbonaceous shale beds (black shales) are located within the middle part of the Carboniferous sandstones of the Ataqa Formation at Bedaa-Um Thora district. Upper Carboniferous sediments were previously thought to be absent which they have described in Sinai. However, Issawi and Jux (1982) have reported the presence of Upper Carboniferous Aheimer Formation at Um Bogma.

2.2 The area of Al -Maghara coal mine North Sinai (Jurassic)

During the Jurassic period, north and central Sinai was a coastal plain and shallow shelf of low relief, separating the continental Arabo-Nubian shield to the south from the deep marine Tethyan Sea to the north. The most complete Jurassic sequence (1980 m) is exposed in northern Sinai at Gebel Maghara, which is a large breached anticline with a gentle north flank and a steep, often vertical or overturned, southern flank. Locally there are indications for a reverse thrust fault is developed through the southern flank. Gebel Al-Maghara has been subjected to many geological studies such as of Barthoux and Douville (1913), Shata (1951), Arkell (1956), Al Far (1966), Barakat (1970) and Said (1962 &1990).

Al Far (1966) subdivided the Jurassic sequence below the Cretaceous at Gebel Al-Maghara into six formations of 1.980 m total thickness:

Masajid Formation (575 m)	Marine deposits	Upper Jurassic
Safa Formation (215 m)	Continental deposits	Middle
Bir Maghara Formation (444 m)	Marine deposits	Middle Jurassic
Shusha Formation (272 m)	Continental deposits	Lower
Rajabiah Formation (293 m)	Marine deposits	Lower
Mashaba Formation (100 m)	Continental deposits	Lower Jurassic.

Mashaba, Shusha and Safa Formations are supposed to be of continental origin and represent fossil plant bearing formations. Economically, significant coal seams have been found only

in the Safa Formation. The coal reserves are more than 40 million ton of sub-bituminous coal. Said (1962 &1990) mentioned that in north Sinai the complete Jurassic section is exposed at Gebel Maghara and during the Jurassic and Cretaceous periods there was no great change in the depositional framework. The dominant rocks are limestones and dolomites. The stratigraphic column at Gebel Maghara belongs to Jurassic and Cretaceous age (Fig. 4). In the following, a lithofacies description from the base to the top of the succession is given.

2.2.1 Mashaba Formation (Lower Jurassic)

The lowermost Jurassic sediments exposed at Gebel Maghara belong to the Mashaba Formation. These clastic sediments are of Liassic age and were deposited by north flowing braided streams carrying detritus shed off the Arabian-Nubian massif. The dominance of continental clastics was probably the result of a low eustatic sea level coupled with tectonic uplift to the south. The thin basal fluvial sandstones containing large wood fragments are succeeded by interbedded shallow marine carbonates and nearshore marine clastics of the Rajabiah and Shusha formations. The carbonates are rich in lime mud having been poorly winnowed in low energy environments. Rare interbeds of well-sorted oolitic limestone are present, suggesting higher energy conditions, commonly with quartz sand grains indicating proximity to the shoreline. The interbedding of carbonates and clastics might have been caused simply by the shifting of different depositional facies across a low energy shelf (Said 1990). The Mashaba Formation consists of lime, clay and sandstone with a thickness of about 100 m. It is exposed at Wadi Sadd El-Mashaba at the base of the El-Maghara section.

2.2.2 Rajabiah Formation (Lower Jurassic)

The Rajabiah Formation is composed of a thickly bedded limestone with some marl and sandstone interbeds. This formation is of Liassic age and its thickness attains about 293 m. It is exposed at Wadi El-Mashaba and Wadi Rajabiah.

2.2.3 Shusha Formation (Lower Jurassic)

This formation consists of clastic sediments (sandstones) with thin carbonate intercalations. The formation is of Liassic age and its thickness attains about 272 m. It is exposed around Shusht Al-Maghara.

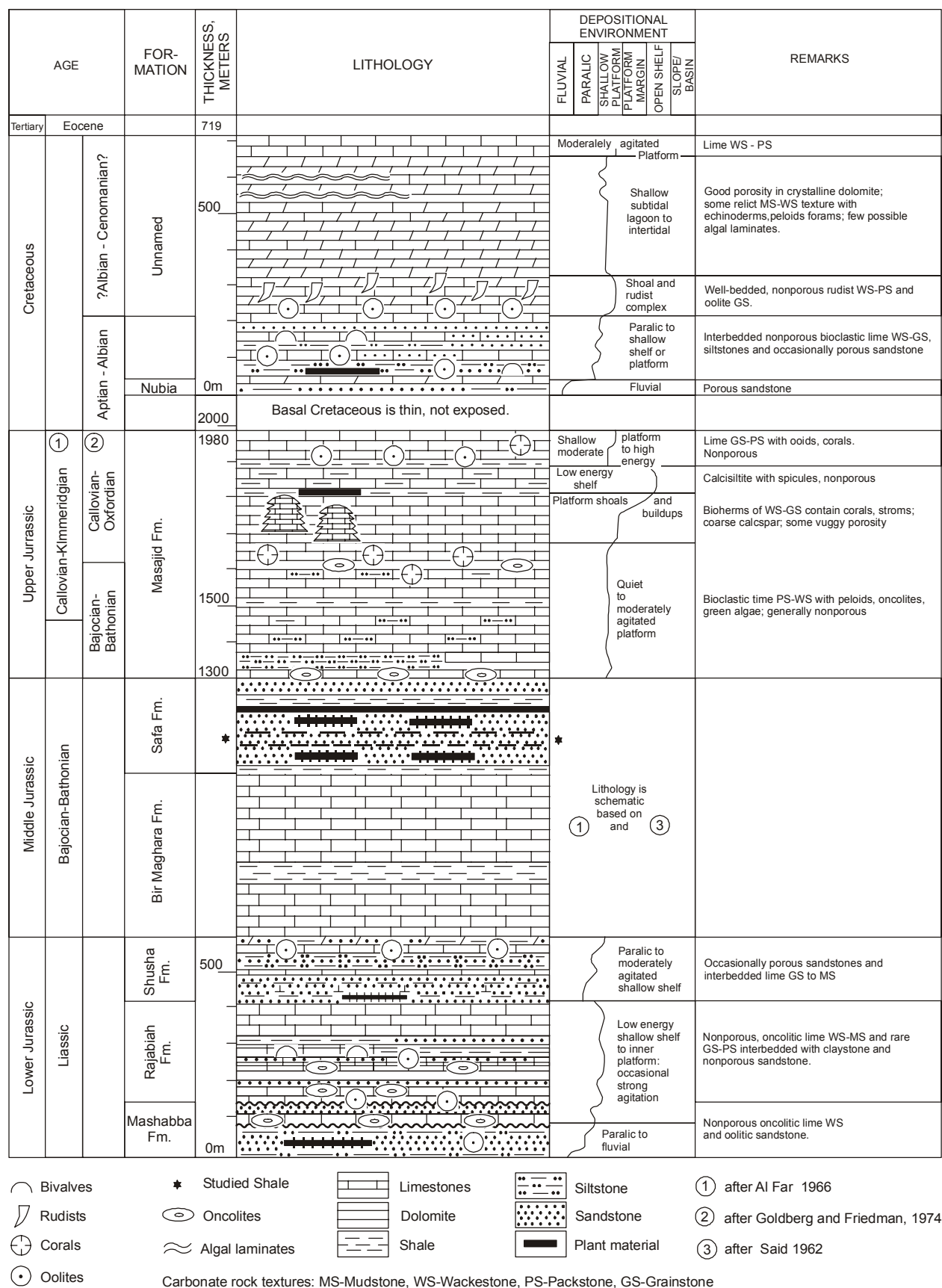


Fig. 4: Generalized lithostratigraphic column of Jurassic and Cretaceous rocks exposed at Gebel Maghara (after Jenkins et al. 1982).

2.2.4 Bir Maghara Formation (Middle Jurassic)

The Middle Jurassic sediments at Gebel Maghara can be subdivided into a lower carbonate unit (Bir Maghara Formation) and an upper clastic unit (Safa Formation) which attain a thickness of approximately 701 m (Said 1990). The Bir Maghara Formation is exposed at Bir Maghara and at Mowerib; it is of Bajocian-Bathonian age. Al Far (1966) divided the Bir Maghara Formation into three members: the Mahl Member which consists of lime and clay (type locality at Wadi Mahl), the Bir Member (located around Bir Maghara) consists of clay with some limestone interbeds, and the Mowerib Member, which consists of lime, clay and sandstone.

2.2.5 Safa Formation (Middle Jurassic)

The Safa Formation is composed of well bedded silty sandstones with some beds of limestone, clay and marl. It is of Bathonian age and is exposed at Wadi El Safa and Wadi Al-Maghara. It contains sub-bituminous coals near its base which are interpreted as having been deposited in lakes or lagoons adjacent to the coastline (Said 1990).

2.2.6 Masajid Formation (Upper Jurassic)

The Upper Jurassic Masajid Formation is dominated by carbonates representing a southerly marine transgression at the end of Bathonian–Callovian times. At Gebel Maghara these carbonates are 680 m thick and consist of bioclastic, oncolitic, peloidal packstones and wackstones and isolated bioherms (Al Far 1966).

2.3 The area of Qusier phosphate mines in Red Sea coast (Cretaceous –Eocene)

Geologically and stratigraphically the Abu Tartur area, Esna-Idfu region (Nile Valley) and Qusier have similar sedimentary successions (Fig. 5).

The complex geology which characterizes the Qusier region is attributed to its confinement to the boundary between the Arabian-Nubian massif and the Gulf of Suez rift. Faulting with a dominant NW trend is the main feature in the region and forms complicated horsts and grabens with outcropping basement rocks covering the major part of this region.

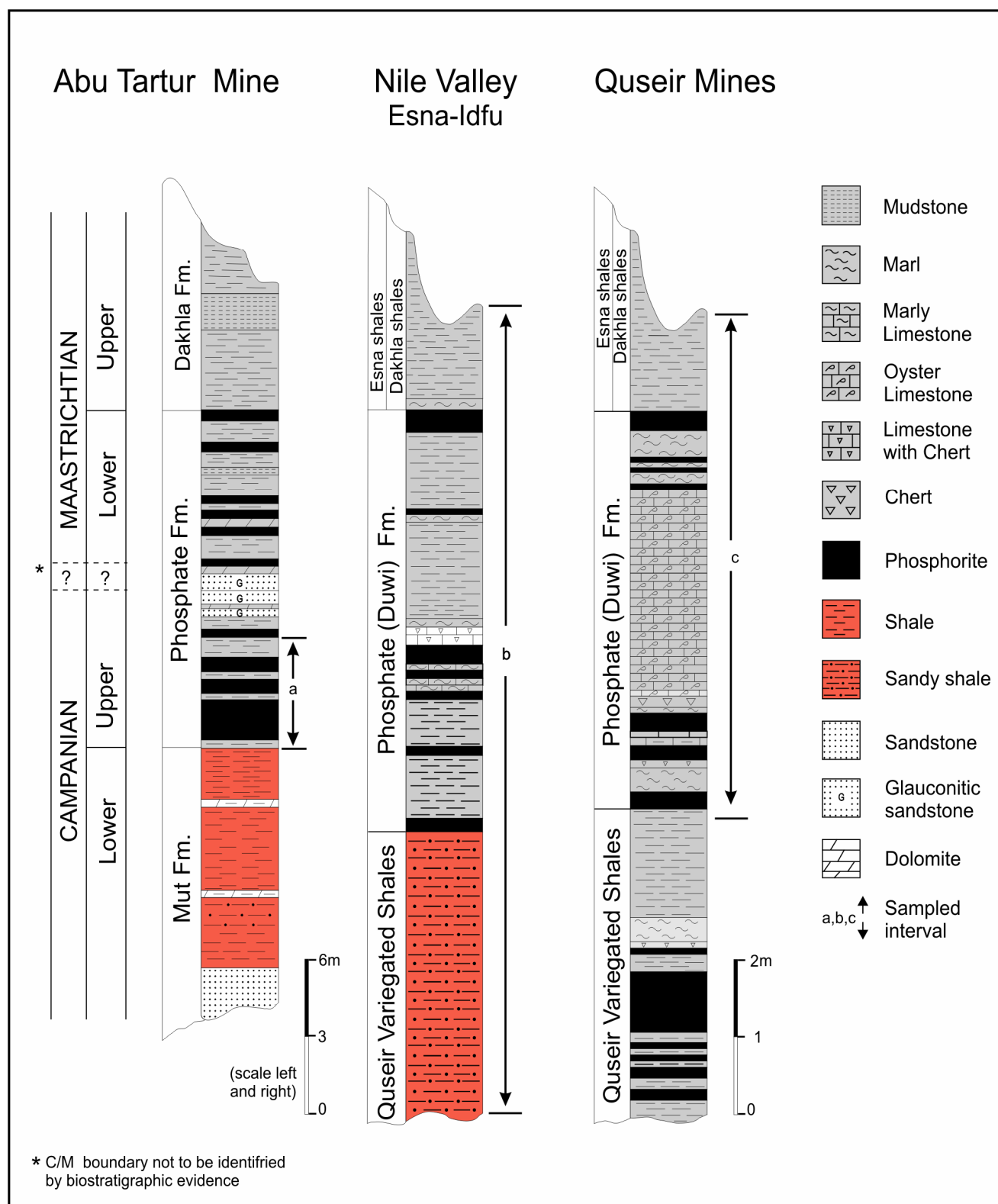


Fig. 5: Sedimentary sequences of Upper Cretaceous – Lower Tertiary rocks showing the position of the samples in the studied areas.

The Upper Cretaceous and Lower Eocene sediments are preserved mostly in synclinal structures. They form isolated hills. The sections in Qusier and Safaga areas were described by many authors including Barron and Hume (1902), Ball (1913), Youssef (1957), Faris and Hassan (1959), El Akkad and Dardir (1966), Abdel Razik (1967& 1972), Issawi et al. (1968 &1971), Hassaan et al. (1979), Mohammed (1982), Saad (1983), Philobos et al. (1985), Ramadan (1992) and Ismael (1996).

The stratigraphy of the exposed sedimentary rocks was described under the following rock units according to Said (1962) from base to top as follows:

Nakheil Formation	top
Thebes Formation	
Esna Shale	
Tarawan Chalk	
Dakhla Shale	
Duwi Formation	
Quseir Variegated Shale	
„Nubia Sandstone”	base

2.3.1 Nubia Sandstone (Pre-Campanian)

The term „Nubia sandstone” was first introduced to the Egyptian stratigraphy by Russegger (1937), who used the term "Sandstein von Nubien" to designate nonfossiliferous sandstone sections of Paleozoic or Mesozoic age. It is the oldest sedimentary unit and rests unconformably over the basement complex. The bed occupies many of the topographic lows in Qusier area (Said 1962). It consists mainly of well sorted, fine to coarse grained, brownish to yellowish sandstone. The thickness of this unit is about 130 m in Qusier area (Issawi et al. 1968). According to Ward et al. (1979) and Van Houten et al. (1984), this unit can be divided into three members. This unit is assigned of Pre-Campanian age (Issawi et. al.1968).

2.3.2 Qusier Variegated Shale (Pre-Campanian)

This formation was introduced by Ghorab (1956), who considered it as a separate formation and named it "Quseir Variegated Shale". The variegated shale consists of multicoloured shale (grey, brownish yellow, green, reddish, violet and blackish) alternating with yellowish sandstone at Gebel Duwi. The Quseir Variegated Shale is considered by earlier authors

(Awad and Ghobrial 1965; Abdel Razik 1970; El Naggar and Ashor 1983) as a part of the "Nubia Sandstone". The thickness of this unit is in the range of 70 m in Gebel Atshan (Said 1990). It is unfossiliferous, with the exception of rare plant remains, bone fragments and fish teeth. Seward (1935) concluded that these plants must have grown in nearby places under a humid tropical climate. The upper part of the Quseir Variegated Shale contains some phosphate bands. These phosphate bands, which range between 10 – 20cm thicknesses, are exposed within indurated sandstone in Gebel Duwi, while they are associated with shale in Wasif section (Glenn 1980). Lithologically, the upper part of the Quseir Variegated Shale is very similar to the shale lithofacies of the Duwi Formation (Glenn and Mansour 1979). The age of this formation is regarded to be Pre-Campanian (Said 1962).

2.3.3 Duwi Formation (Campanian – Maastrichtian)

In 1900, Barron noted the presence of phosphate beds in the Eastern Desert. Youssef (1949 & 1957) described the Duwi Formation and classified the exploited phosphate in Gebel Duwi into three beds, the upper (Atshan bed), the middle (Duwi bed) and the lower (Hammadat bed). Said (1962) extended the use of the term Duwi Formation to laminated gray clays and chert phosphatic bands at Safaga and subdivided the whole section in the Red Sea area into three members: Atshan or "A" member separated from the middle Duwi or "B" member by an oyster limestone bed 6-16 m in thickness, and lower Abu Shegela or "C" member, separated from the middle member by a shale unit of variable thickness (6-10 m).

The Duwi Formation in the Quseir-Safaga coastal region comprises a heterogeneous suite of shallow marine rocks that lies stratigraphically above the Quseir Variegated Shale and below the Dakhla Shale. The Duwi Formation consists of phosphorite, shale, siliceous claystone, glauconitic sandstone, chert, dolostone, marl and reefal limestone (Glenn and Mansour 1979).

The Duwi Formation can be subdivided into three members, the lower "C" member, separated from the middle member by variegated shale of non marine to marginal marine origin, similar to those of the underlying Quseir Formation. In some places such as the Younis mine this member comprises three beds separated from each other by shale beds. It ranges in thickness from 20 cm to 1 m. In Zoug El Bohar mine the "C" member forms a lens that ranges in thickness from 3 to 7 m. The phosphorites of the "C" member are characterized by medium to coarse grains, reddish in colour and of friable consistence. This member is exploited in Abu Shegala, Younis and Zoug El Bohar Mine. The middle "B" member is well developed at

Gebel Duwi. It is made up of three phosphate beds, separated by thin shale, marl, and silicified limestone beds. Its thickness ranges from 20 to 90 cm and colour from gray, pale gray to yellowish. An important marker in this member is a thick oyster limestone bed which caps and intercalates this member. This member is exploited in Galal, Um Resifa and Zoug El Bohar mines in Quseir area and in Rabbah mine in Safaga area. The upper member "A" is made up of three phosphate beds separated by thin shale, chert and marl beds. It ranges in thickness from 10-120 cm. The colour varies from pale white to pale gray. It is exploited in Younis, Galal, Wadi El Anz and Um Resifa mines in Quseir area, Wasif and Rabbah mines in Safaga area and "B" mine in Hamrawin area. The Duwi Formation in Quseir–Safaga region is of Campanian age in its lower part and Maastrichtian in the upper part (Youssef 1957).

A Maastrichtian age is given for this formation by Youssef (1949, 1957), Said and Sabry (1964), El Akkad and Dardir (1966) and Issawi et al. (1968, 1971). Dominik and Schaal (1984) assigned the age of the Phosphate Formation (Duwi Formation) to Upper Campanian to possibly Early Maastrichtian on the basis of ammonites and vertebrate remains. The microflora content of drilled cores from the Younis mine puts a Maastrichtian age to the upper part of the black shales which lay on top of the Duwi Formation. An Upper Campanian to Early Maastrichtian age, therefore, may be assigned to the underlying Duwi Formation in this area (Schrack and Ganz 1984).

2.3.4 Dakhla Shale (Danian – Lower Paleocene)

The term Dakhla Shale was first introduced by Said (1961) to describe 130 m of gray shale becoming calcareous toward the top, exposed at Mut in the Dakhla Oasis, conformably overlying the Duwi Formation and underlying the Tarawan Chalk. It consists of a series of marls and shales which vary in thickness from one place to another. It is subdivided into two members namely Beida Shale Member (10 m) at the top and Hamama Marl Member 27 m at the base (Abdel Razik 1972). The lower member at Wasif is usually composed of argillaceous gray or reddish limestone with gypsum veinlets, while at Gebel Duwi it is composed of varicoloured (yellowish, white and brownish) marl. The upper member consists of gray to green shale, yellowish in some parts, and fissile with gypsum veinlets. This member is conformably overlain by the Tarawan Chalk. The contact is marked by an abrupt change from gray shale with gypsum veinlets into brownish, reddish limestone and chalky white limestone. The lower part of this formation is assigned to a Danian age, while the upper part is of lower Paleocene age (Youssef 1957).

A notable feature of Quseir, lower Dakhla and Duwi Formation is the presence of black shale within and above the phosphatic beds. Some of these shales are reported to have caught fire (Shahin et al. 1986). These shales often contain abundant foraminiferal tests, fish debris, pecten, scattered pyrite grains and phosphatic grains. The average oil content of weathered black shale samples is 19gal/t (Tröger 1984). Malak et al. (1977) suggested that these black shales were deposited in stagnating, reducing, slightly alkaline water with an upper oxygenated surface zone in which green algae lived and acted as the main source of organic matter.

2.3.5 Tarawan Chalk (Landanian-Late Palaeocene)

The term "Tarawan Chalk" was first introduced by Awad and Ghobrial (1965) to describe 45 m of chalk exposed at Gebel Teir in the Kharga Oasis. The Tarawan Chalk is 3.10 m thick at Wasif and 10 m thick at Gebel Duwi. It is conformably overlying the Dakhla Shale and underlying the Esna Shale. The boundary between the Tarawan Chalk and the underlying and overlying formations is marked by an abrupt change in lithology shown by compactness, carbonate content and colour (Ramadan 1992). Tarawan Chalk consists of chalky limestone, white, argillaceous in the lower part and chalky in the upper part. It is assigned to a Landenian age (Issawi et. al 1968).

2.3.6 Esna Shale (Early Eocene)

Beadnell (1905) introduced the term "Esna Shale" to describe a succession of laminated green and gray shaley clay at the locality Gebel Owenia, opposite Esna, northeast of Sebaiya. The Esna Shale lies conformably over the Tarawan Chalk with sharp contact, marked by white chalk limestone and is conformably overlain by the Thebes Formation, where the contact is marked by pink argillaceous limestone bands. It measures 14 m in thickness in Wasif and 32 m at Gebel Duwi (Ramadan 1992).

According to Hassaan et al. (1979) the Esna Shale is subdivided into two members: a calcareous shale member, consisting of gray to green, fissile and highly fossiliferous shale with gypsum veinlets, and an argillaceous limestone member of whitish gray colour. This Formation is assigned to the Upper Paleocene (Landinian) at the base and Lower Eocene (Ypressian) at the top (Issawi 1972).

2.3.7 Thebes Formation (Early Eocene)

Said (1960) introduced the term "Thebes Formation" to describe the thick limestone section which overlies the Esna Shale at the Thebes type section in Gebel Gurnah opposite Luxor. In the study areas, it attains about 285 m in thickness in the Duwi range, about 250 m in Hamadat and 166 m in Gebel Anz (Said 1990). It consists of thinly bedded limestone with noticeable flint bands or flint nodules and chert concentrations, interbedded toward the top by a marl bed.

Snively et al. (1979) divided the Thebes Formation of Gebel Duwi into three "informal members" representing different stages of deposition. The lower member rests conformably on the Esna Shale and consists of about 40-60 m of laminated to thinly bedded limestone and chalk as well as massive bioturbated chalk beds and chert bands. This member indicates a deep water phase of a predominately pelagic depositional environment. The middle member is made up of thinly bedded limestone and chalk, interbedded with nodular limestones, intraformational conglomerates, reworked and benthonic foraminifera, lime sands and rare chert. This unit is about 100 to 120 m thick according to Snively et al. (1979) and about 200 m thick according to Strougo and Abu Nasr (1981). This heterogeneous accumulation of carbonates is indicative of progressive shallowing and outward progradation of a shallow water depositional environment. The upper member is thin (10 to 15 m thick), if present. It is made up of fine grained limestone locally interbedded with oyster shells and shell hash. The distribution of this member probably indicates a period of local uplift coupled with a period of rapid sea level drop. This formation is assigned to the Early Eocene (Strougo and Abu Nasr 1981).

2.3.8 Nakheil Formation (Oligocene)

The Nakheil Formation was named by El Akkad and Dardir (1966). It is widely spread in the Quseir – Safaga district and may reach a thickness of about 60 m or more. This formation is made up of two types of deposits: very coarse breccias beds and fine grained lacustrine deposits. The Nakheil Formation occupies the slopes of the Thebes Formation on the down thrown side of the faults. It is closely associated with the early faulting which must have taken place after the deposition of the Thebes Formation. The Nakheil Formation is nonfossiliferous and assumed to be of Oligocene age (El Akkad and Dardir 1966).

3 Methods of investigation

The preparation of samples and the analyses of the samples were carried out in the laboratories of the Institute of Applied Geosciences at the Faculty of Civil Engineering and Applied Geosciences, Technical University of Berlin, Germany.

3.1 Mineralogical analysis

3.1.1 Separation of clay size fraction

From the original 144 samples, one hundred and one were chosen for powder XRD. Depending on the XRD powder results the samples were selected for clay mineralogy and XRF.

Forty eight shale samples were analyzed by X-ray diffraction. The clay size fraction (less than 2 μm) was investigated in order to give information about the clay mineralogy of the studied shales. About 25 g of the rock sample was soaked in distilled water after adding 5ml/l of 0.1M. $\text{Na}_4\text{P}_2\text{O}_7 \cdot 10\text{H}_2\text{O}$, and disintegrated with a shaker machine. The clay fraction (<2 μm) was separated out from the sample by centrifugation. The <2 μm suspension was dried on glass slides. The oriented mounts were run under three conditions:

- i) In air dry state.
- ii) After ethylene glycol treatment.
- iii) After heating to 550° C for 1 hour.

3.1.2 X – ray Diffraction (XRD)

The bulk samples and the clay fractions were examined by a Philips X-ray diffractometer PW1710, with Ni filtered $\text{CuK}\alpha$ radiation using 50 kV/30 mA.

X-rays are electromagnetic radiation, produced when an electron beam hits a substance and causes rapid deceleration of the electrons. In conventional diffraction, the X-ray tube is arranged so that electrons strike a target which produces X-rays of known wavelengths, which can be further filtered to produce radiation of a single wavelength which can be directed at the sample in the diffractometer. The wavelength of X-rays ranges from 0.05 to 0.25 nm. The sample is rotated in the beam so that crystallographic planes diffract X-rays as they reach the appropriate angle. The relationship of X-ray wavelength to the angle of diffraction and the characteristic lattice (or d) spacing of the mineral under examination forms the basis of all

X-ray diffraction (XRD) analysis and interpretation, and is known as Braggs Law (Dominic et al. 1993).

3.1.3 Petrographic microscopy

Thin sections were made both from the shales and from associated phosphate samples for mineralogical analysis with a petrographic microscope. The observed microfacies were described, discussed, interpreted and photographed.

Examination of standard and polished-thin sections is the mainstay of microscopic petrographic analysis. Because of the general softness of shales and mudstones, preparation of appropriate thin-sections often poses a challenge. The difficulty of preparing good petrographic thin sections of shales and mudstones is one of the reasons why acceptance and application of thin section microscopy of this rock type has been long delayed (Schieber and Zimmerle 1998)

3.1.4 Scanning Electron Microscopy (SEM)

Scanning Electron Microscopy (SEM) for selected samples of different lithofacies was performed in order to diagnose and understand the microstructure and the diagenetic relationships among the main constituents and the matrix of the studied sediments.

Identification of different minerals through SEM was facilitated by comparing their characteristic morphologies with those shown in the SEM Petrology Atlas of Welton (1984). Identification was verified by X-ray diffraction analysis when possible. SEM analyses were carried out using a Scanning Electron Microscope Type S-2700 HITACHI.

3.2 Geochemical analysis

The present study includes major and trace element analysis of 55 carbonaceous shales from Egypt. The samples were crushed by a crushing machine to reduce the rock aggregate to $<0.063\mu\text{m}$ particles. These samples were sieved to get the grain size fraction $<0.063\mu\text{m}$.

3.2.1 X-ray Fluorescence (XRF)

The crushed samples were used to determine the major element composition by XRF. Analyses were carried out with a Philips PW 1404 WD-XRF via program "POWDER".

Mixture of 6g of sample powder with 1.5g of "HOECHST C-Wax" homogenised in vibrating device and pressed into Al-cups (40mm diameter) at 20t-pressure. Analysed major elements

were SiO₂, TiO₂, Al₂O₃, Fe₂O₃, MgO, CaO, Na₂O, K₂O, SO₃ and P₂O₅. Trace elements analysed were F, Ag, As, Ba, Bi, Br, Cd, Cl, Co, Cu, Cr, Cs, Ga, Hg, Mn, Mo, Ni, Pb, Rb, Sb, Se, Sn, Sr, Th, U, V, W, Zn and Zr.

3.2.2 Determination of total organic carbon content (TOC)

The total organic carbon content was determined on each sample using a Hochtemperatur-TOC/TNb-Analysator (Liqui TOC) after decarbonating. The analyses were performed at the TU, Berlin, Germany. Twenty-seven whole rock samples were analysed for TOC concentrates. About 200 mg pulverised sample was used for this analysis. Carbonate was removed by treatment with 10 % aqueous hydrochloric-acid. The residual materials were used for the determination of TOC by combustion analysis of temperatures in excess of 850°C. The evolved gas (CO₂) was measured quantitatively and simultaneously by infrared detectors and recorded as percentage of carbon.

3.2.3 Rock-Eval pyrolysis

The Rock-Eval pyrolysis was performed in the Applied Petroleum Technology AS, Norway. The TOC and Rock-Eval were determined on each sample using a Rock-Eval 6 instrument. The all procedures follow NIGOGA, 4th Edition.

The pyrolysis method is described in detail by Espitalie et al. (1977). For analysis 100 mg of each rock sample was used. The sample was placed in the instrument and heated at a rate of 25°C/min in a helium stream from 250°C to 550°C. Free hydrocarbons contained in the rock are expressed as an S1 peak; those released by the thermal breakdown of kerogen appear as an S2 peak which is produced by pyrolysis between 300°C-550°C. The quantity of hydrocarbon is measured by a flame ionisation detector (FID). Finally, an S3 peak representing CO₂ produced from the kerogen appears as a reflection of the oxygen content of the organic matter. The quantity of CO₂ is registered by a thermal conductivity detector (TCD).

The method leads to the calculation or measurement of two kinds of parameters:

- i) Hydrogen and oxygen indices, which can be related to the type and thermal evolution of the organic matter.
- ii) The temperature at the maximum of the pyrolysis peak (S2 peak). This temperature is related to the thermal maturity of the organic matter (Espitalie et al. 1977; Peters, 1986).

4 Mineralogy

The identification of the mineralogical composition of shales can be easily approached through the use of X-ray analysis.

The present chapter deals with the mineralogical composition of shales of Carboniferous age from Abu Zinema in South Sinai, Jurassic age from Al-Maghara coal mine in North Sinai, Cretaceous age from Abu Tartur phosphate mine in Western Desert, Cretaceous to Early Eocene age from Esna-Idfu at Nile Valley and of Cretaceous age from Quseir phosphate mines at the Red Sea coast.

There are simple procedures for the semi-quantitative estimation of the clay mineral content. They involve the measurement of the height of the (001) reflections above the background with different correction factors used in this study or measurements of the peak areas (Johns et al. 1954; Weaver 1958). The following is a brief description of the minerals identified by means of X-ray diffraction analyses of the clay fraction and whole rock samples.

4.1 Clay Mineralogy

4.1.1 The importance of clay minerals

Clay minerals can be used as stratigraphic markers and environmental indicators. The type of clay found in shale is a function of provenance and diagenetic history. Depositional environment had a considerable influence on the clay mineralogy through early mineral transformations in the basin of deposition (Russell 1970).

4.1.2 Structure and chemistry of clays

There are two basic building blocks common to clay mineral structures:

- (i)- A sheet of silicate tetrahedra, consisting of two layers of oxygen atoms, and containing silicon in four-fold (tetrahedral) coordination.
- (ii)- An octahedral sheet, consisting of two layer of oxygen atoms or hydroxyl groups, between which aluminium, magnesium or iron are bounded in six-fold coordination.

The structural units of clays therefore consists of either alternating tetrahedral and octahedral sheets (OT or 1:1 structure), as in the kaolinite group of clay minerals; a sandwich of one octahedral sheet between two tetrahedral sheets (TOT or 2:1 structure), as in illite and

smectite clay minerals or an arrangement in which the three-layer TOT units alternate with a brucite layer (2:1:1 structure) as in chlorite.

The various clay minerals can be summarized as follows:

4.1.2.1 Smectite group minerals

These have a dioctahedral or a trioctahedral 2:1 layer structure. Smectites nearly always occur as fine-grained particles of clay size. The dioctahedral smectites are the phases which are often intimately associated (interlayering) with the mica-like minerals (Velde 1992). The main dioctahedral minerals are montmorillonite-beidellites (Al-rich) which are predominately octahedrally charged, and nontronites (Fe^{3+} -rich).

4.1.2.2 Kaolinite group minerals

This group consists of uncharged, dioctahedral layer units with a 1:1 structure of 7 Å in thickness. The individual mineral species considered are:

Kaolinite, which has varying degrees of crystallinity and a distinct, platy form; Dickite, which is similar to kaolinite, but with a different stacking arrangement of the unit layers; Halloysite, which consists of a poorly ordered arrangement of kaolinite-like units, with variable amounts of water between the layers, generally between 0.6 to 4H₂O per formula unit, and often with a tabular form.

4.1.2.3 Chlorite group minerals

These are sometimes dioctahedral but usually trioctahedral with a 2:1:1 layer structure of 14 Å in thickness. The 2:1 layer is negatively charged because of ionic substitutions, and is balanced by a positive charge on the interlayer hydroxide sheet. Chemically, the group is extremely variable, but it should suffice to concentrate on only three types:

- (i) Mg-rich chlorite (e.g. clinocllore) which is trioctahedral.
- (ii) Fe-rich chlorite (e.g. chamosite) which is also trioctahedral.
- (iii) Al-rich chlorite (e.g. sudoite) which is mainly dioctahedral.

Chlorite and kaolinite have very different structures and geological occurrences, but they sometimes are present in natural mixtures. Chlorite has a basal series of diffraction peaks superimposed or nearly superimposed on the members of the kaolinite 001 series. High-Fe chlorites have weak odd-order reflections, so weak that the 001 peak is easily obscured or not

noticed, so the distinction between chlorite and kaolinite is most difficult when Fe-rich chlorites are involved (Duane et al. 1997).

4.1.2.4 Illite/Mica group minerals

These have a di- or trioctahedral 2:1 layer structure of 10 Å in thickness. The structure is charged due to ionic substitution in both the tetrahedral and octahedral sheets, and contains interlayer non-exchangable cations (usually K⁺) that compensate for the charge deficit on the unit layers. The chemistry of the various members of the group is variable.

4.2 Clay minerals in the studied shale samples

Smectite, kaolinite and chlorite in addition to illite are the most abundant clay minerals encountered in the studied shale samples. The following is a discussion on the recognized clay mineral associations. Representative profiles and the semi-quantitative results obtained are shown in Appendix (Table 2 & 3 and Fig.1 to 5) and the following Table (Table 1).

Table 1: Average semi-quantitative clay mineralogy of the studied shales (by XRD)

Location	Formation	No. of samples	Smectite %	Kaolinite %	Chlorite %	Illite %
Nile Valley	Esna Shale	11	88	2	10	0
	Dakhla Shale	10	73	9	18	0
	Duwi	6	98	2	0	0
Quseire Mines	Dakhla and Duwi	11	80	20	0	0
Abu Tartur Mine	Duwi	4	100	0	0	0
Al Maghara Mine	Safa	3	traces	100	0	0
Abu Zinema Area	Ataqa	3	0	87	0	13

4.2.1 Smectite

Smectite is the dominant constituent of the clay mineral content of the studied shales in the Upper Cretaceous–Lower Tertiary sediments of Duwi Formation at Abu Tartur phosphate mine, Duwi Formation and Dakhla Shale at Quseir phosphate mines and Duwi Formation, Dakhla Shale and Esna Shale at Esna –Idfu at Nile Valley. The average content of smectite in the samples ranges from 100 % at Abu Tartur phosphate mine to 80 % at Quseir phosphate mine (Table 1); (Fig.6).

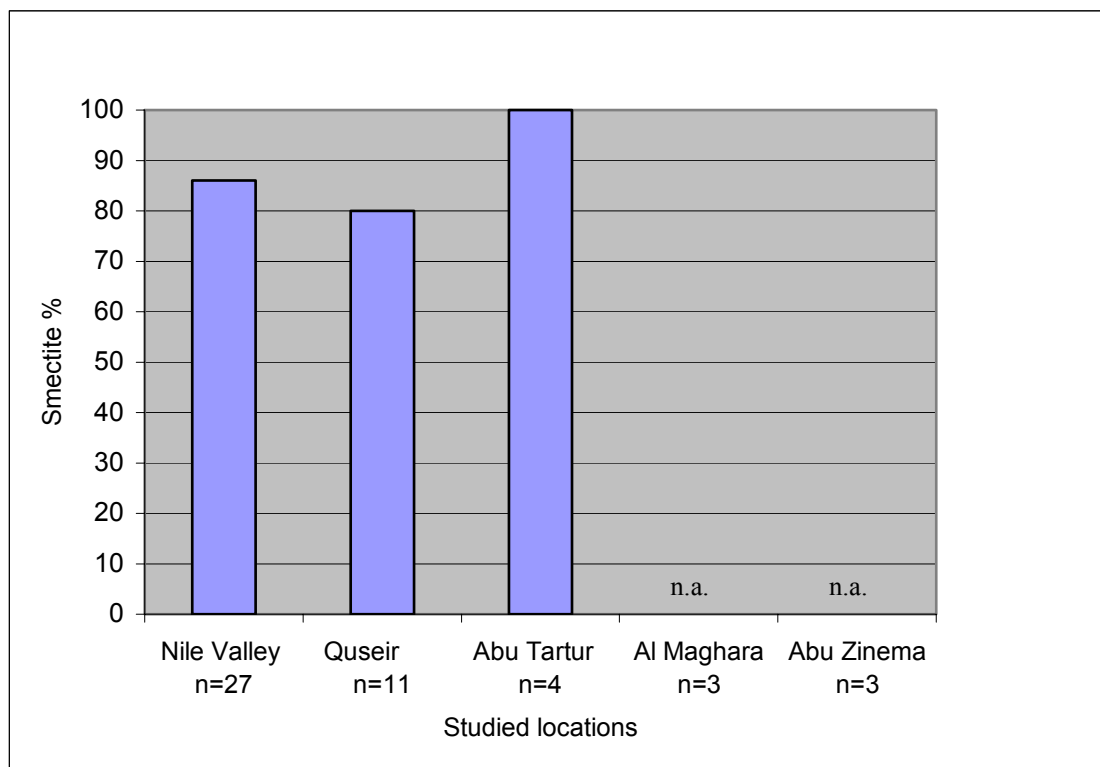


Fig. 6: Smectite average at studied locations

Terrigenous clay minerals are often transported great distances by wind and water before being deposited on the seafloor. The composition and the characteristics of clay minerals in well preserved sediments record the paleoclimatic and tectonic environments of their source areas (Chamley 1989; Ehrmann et al.1992; Velde 1995). Climate has strong influence on rock alteration, and clay minerals are often the main product of this process. For example, the global pedogenic and climatic zonation is reflected in the latitudinal distribution of certain clay minerals (Chamley 1989). However, other factors than climate such as assemblage,

topography, transport and diagenetic changes can modify the original clay assemblage (Yuretich et al. 1999). Clay minerals in marine sediments have been used to infer paleoenvironmental conditions (Jeong and Yoon 2001). In continental weathering environments, smectite and kaolinite are generally formed by active chemical weathering of rocks under humid temperate to tropical climates (Weaver 1989). Smectite and kaolinite occurrence in marine sediments was often ascribed to the chemical weathering in a warm humid environment. Chamley (1989) stated that in temperate arid regions the neoformation of smectite in vertisols often occurs simultaneously with negative transformations (e.g. open illite, irregular mixed-layer) and the preservation of some parent-rock minerals. In arid tropical areas smectite neoformation becomes exclusive. The pedogenic smectitization can extend over the humid intertropical zone, if the drainage conditions are poor and prevent the normal evacuation of ions. Smectite can also form diagenetically from illite, kaolinite, or chlorite (Moore and Reynolds 1989).

The dominance of smectites in the Upper Cretaceous-Lower Tertiary sediments in South Egypt has been described by Hendriks (1985, 1988), Hendriks et al. (1990), Ismael (1996) and Ahmed (1997). The dominance of smectite in the studied samples is in agreement with the obtained results from the other authors. The origin was believed by those authors to be due to continental pedogenesis as well as marine neoformation. Terrestrial smectite developed under warm and humid to seasonally humid conditions by the degradation of chlorite and illite or by crystallization from ion-enriched hydrolytic solutions in badly-drained alkaline soils. According to Moore and Reynolds (1997) there are two kinds of smectite, one produced by the kind of weathering found in soils and one by neoformation such as in the alteration of volcanic glass. Four main genetic hypotheses for the origin of smectite and mixed layer (I/S) exist: (1) reworking of soils and enrichment by differential settling, (2) alteration of volcanic material, (3) transformation of detritals, and (4) authigenesis (Chamley 1989; Thiry and Jaquin 1993). The absence of any conceivable volcanic precursor, such as tuff or glass in the studied shales indicates that smectite is mainly of a detrital origin. Smectite is the predominant clay mineral in many lacustrine settings. For example, it makes up to 100% of the shale minerals in some stratigraphic units of the Messel oil shale (Weber 1991). The author suggested a warm/humid climate proven by the smectite which corresponds with the existence of a diverse fauna and flora in south Egypt (Hendriks et al. 1990). Discrete smectite and mixed-layer illite/smectite (I/S) commonly forming from the weathering of ultrabasic or very basic rocks which produce magnesium minerals (Surdam and Stanley 1979).

The main sources of the studied shales lie in the rugged tectonic belt which forms the Precambrian basement complex and their weathering products in the South-Eastern Desert of Egypt and the northern part of Sudan. These basement rocks are mainly an association of metasediments, metavolcanics, metagabbros and serpentinites, constituting the ophiolitic melange (Shackleton et al. 1980) that is interrupted by gneisses in structural highs. This sequence is unconformably overlain by volcanics, and intruded by granite ranging in composition from quartz diorite to alkali-feldspar granite. Primarily the detrital material is carried to the shelf by streams and river system. Partially, however, aeolian transportation may have played a minor role. The detritus encountering the shelf environment undergoes further mechanical as well as chemical differentiation, and the transformation of detritus into deeper marine sediments results in further chemical and mineralogical changes.

The smectite-kaolinite association in the studied shales does not suggest the formation of kaolinite under the same conditions of smectite formation or the insitu formation of kaolinite by chemical precipitation. Smectite formation is compatible with alkaline reducing conditions, while kaolinite is generally thought to require acid conditions, and it may be unstable in alkaline environments. The occurrence of smectite together with kaolinite and chlorite indicates the alteration of feldspar in connection with an „arenization“ (Milot 1970) of crystalline basement rocks in a warm and semi-arid climate. Hendriks et al. (1990) stated that the clay mineral associations within the sedimentary succession of southern Egypt are attributed to a terrestrial provenance. They suggest a warm and semi-arid climate on the continent.

In the Duwi Formation at Abu Tartur phosphate mine, the abundance of smectite and the low content or absence of illite and kaolinite refer to a deposition under fluvio-marine environment. The presence of pyrite rombs indicates a reducing environment. These results are in agreement with these obtained by Sediek and Amer (2001). Dakhla and Esna Shale at Nile Valley section, Quseir phosphate mines, show an association of smectite with some kaolinite and chlorite, indicating the detrital origin and deposition in open marine environments. Generally, the clay mineral associations in the studied shales at Abu Tartur, Nile valley and Quseir with its smectite dominance suggest a terrestrial provenance that had not attained intensive weathering, a warm and semi-arid climate and the resulted materials were carried by fluvial action, which finally interfered and admixed with marine environments (marginal marine, low energy and reducing conditions of Duwi Formation and open marine facies of Dakhla and Esna Shale).

4.2.2 Kaolinite

Kaolinite is the dominant clay mineral of the studied shales of Safa Formation at Al Maghara coal mine and Abu Zinema. The average content of kaolinite in the shales of the 5 locations in Safa Formation at Al Maghara coal mine, in the Ataqa Formation at Abu Zinema, in the Duwi and Dakhla formations at Quseir phosphate mines and in the Duwi, Dakhla and Esna formations at Nile Valley varies between 0 and 100 % (Fig. 7); see also (Table 1).

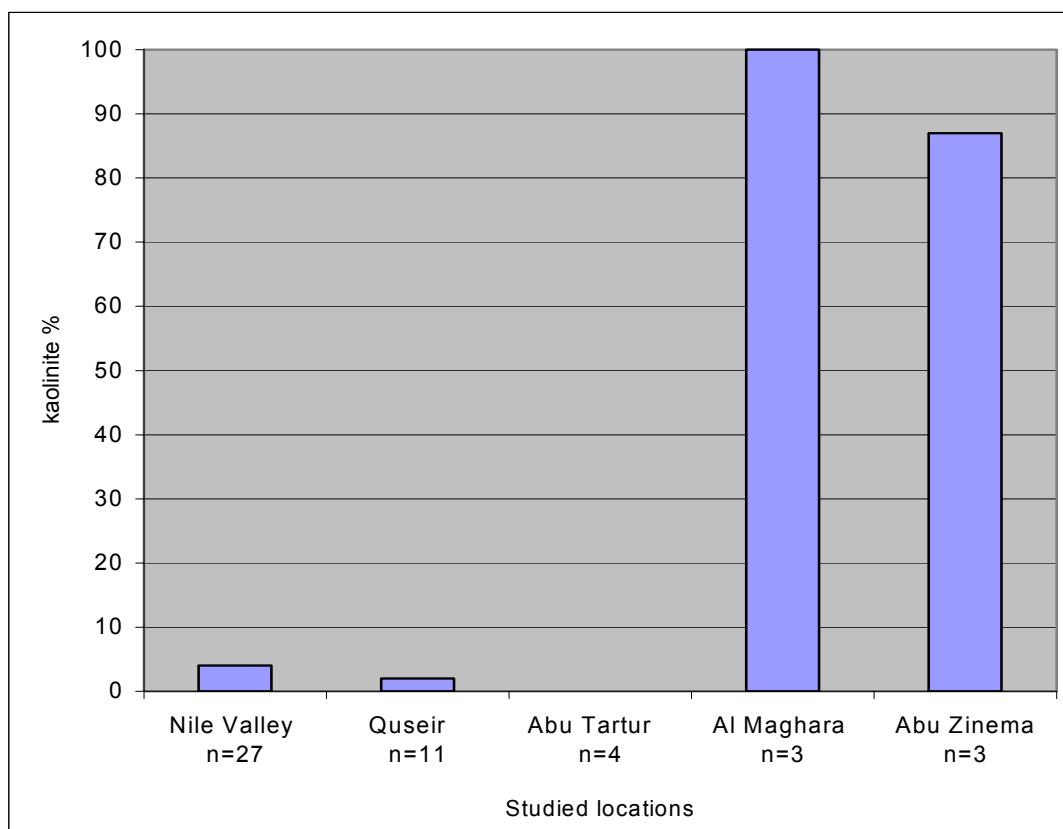


Fig. 7: Kaolinite average at the studied locations.

The origin of kaolinite in the studied shales has been interpreted for a long time as to be a product of chemical weathering of feldspars. Kaolinite formation is favoured under tropical to subtropical humid climatic conditions (Chamley 1989, Hallam et al. 1991). In addition to a detrital origin, kaolinite may also develop by diagenetic processes due to the circulation of acid solutions (Ghandour et al. 2003).

The dominance of kaolinite in the studied shales of Safa Formation at Al Maghara coal mine of Jurassic age immediately beneath the coal bed and the dominance of kaolinite also in the bituminous black shale at Ataqa Formation at Abu Zinema area of Carboniferous age are in

agreement with the results obtained by El-Anbaawy and Youssef (1989), Abd El Hameed (1997) and Ghandour et al. (2003). The kaolinite in Safa Formation at Al Maghara coal mine is interpreted to have been deposited in lakes or lagoons adjacent to the coastline (Said 1990). Kaolinite formed as a result of extensive chemical weathering and leaching of rocks which occur in the exposed granite-metamorphic basement area (granite intrusions ranging in composition from quartzdiorite to alkali-feldspar granite) of South Sinai. Mostafa and Younes (2001) stated that shales of Safa Formation at Al Maghara coal mine are generally immature for oil generation. Generally, mudstones which are immature for oil generation contain discrete minerals predominantly of detrital origin reflecting largely the character of parent rocks (Lindgreen and Surlyk 2000). During diagenesis, the morphology of kaolinite changes from vermicular or aggregates of books to individual blockier crystals (Ehrenberg et al. 1993). However, there is no SEM observation evidence for the role of diagenesis in the formation of kaolinite in Safa Formation. Ataqa Formation of Abu Zinema, i.e. the kaolinite is of primary or detrital origin.

The origin of kaolinite in the Upper Cretaceous-Lower Tertiary sediments of southern Egypt also was attributed by Gindy (1983) to the extensive chemical weathering and leaching of rocks which occur especially in the exposed granite-metamorphic basement areas in the south of Egypt and in northern Sudan. In the opinion of Hendriks et al. (1990) kaolinite in the marine deposits of Upper Cretaceous-Lower Tertiary age are products of terrestrial weathering and represent continental products of a warm and at least seasonally humid climate, being eroded and transported toward the sea by rivers.

The amount of kaolinite in the shales of Upper Cretaceous-Lower Tertiary age Dakhla and Esna Shale in the Nile Valley section and also in Duwi and Dakhla Shale at Quseir phosphate mine is in agreement with the results obtained by Hendriks et al. (1990), Ismael (1996) and Ahmed (1997). This kaolinite represents a continental weathering product at a warm and at least seasonally humid climate, being eroded and transported towards the sea by rivers.

4.2.3 Chlorite

Chlorite is the second most abundant clay mineral in the samples of Dakhla and Esna Shale at the Nile valley section. The average content of chlorite is 14 %. Chlorite varies between 0 and 14 % (Fig. 8); (see also Table 1). Chlorite has been interpreted to originate from the physical weathering of sedimentary, metamorphic and basic source rocks under cold climates (Ehrmann et al. 1992; Jeong and Yoon 2001).

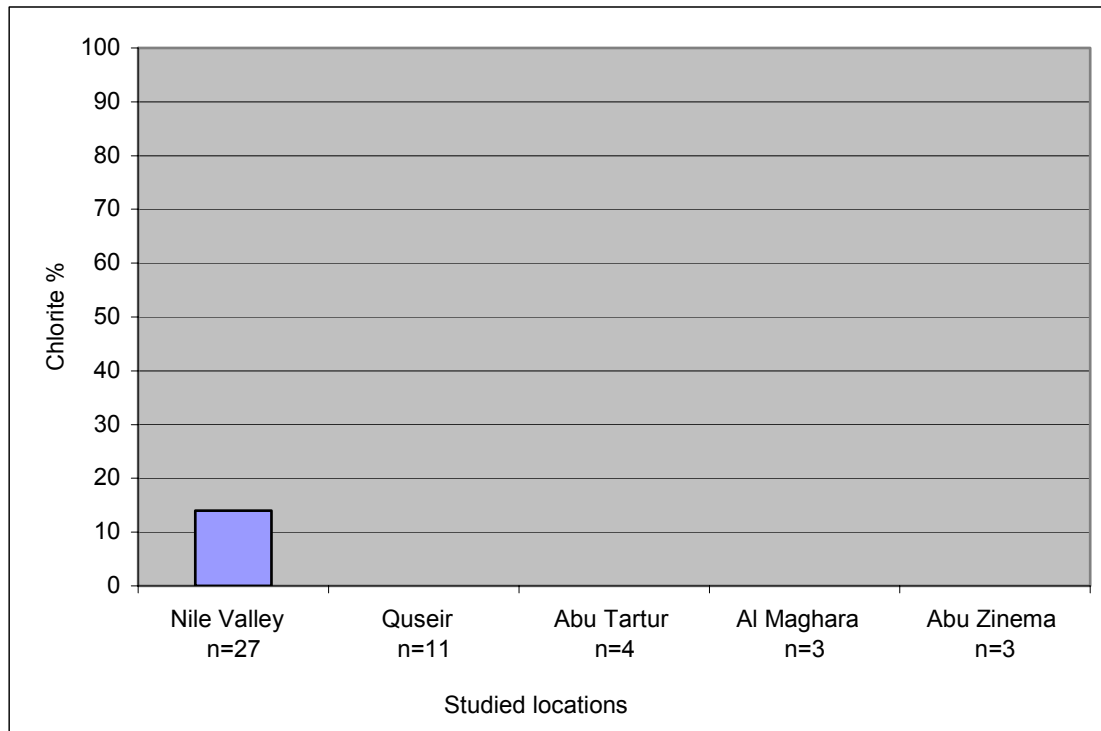


Fig. 8: Chlorite average at the studied locations.

Chlorite reacts very sensitively in continental chemical alteration processes and is easily transformed into smectite (Milot 1970). Walker (1993) concluded that most chlorites form diagenetically with burial especially in Mg-rich water in shales and slates, or can form directly at temperatures well below 200°C.

The origin of chlorite in South Egypt was attributed by Hendriks et al. (1990) to be exclusively of marine origin. The small amounts of chlorite in Dakhla and Esna Shale at Nile Valley, which are rich in Ca and Mg and characterized by the dominance of smectite, may indicate the neoformation of chlorite or may be formed by physical weathering. The main sources of chlorite in the studied shales lie in the Precambrian basement complex in the South-Eastern Desert of Egypt and the northern part of Sudan.

4.2.4 Illite

Illite was found to be a trace constituent only in the studied samples of Ataqa Formation which is of Carboniferous age (at Abu Zinema area, south-west Sinai). Illite average content is varies between 0 and 13 % (Fig. 9); (see also Table 1).

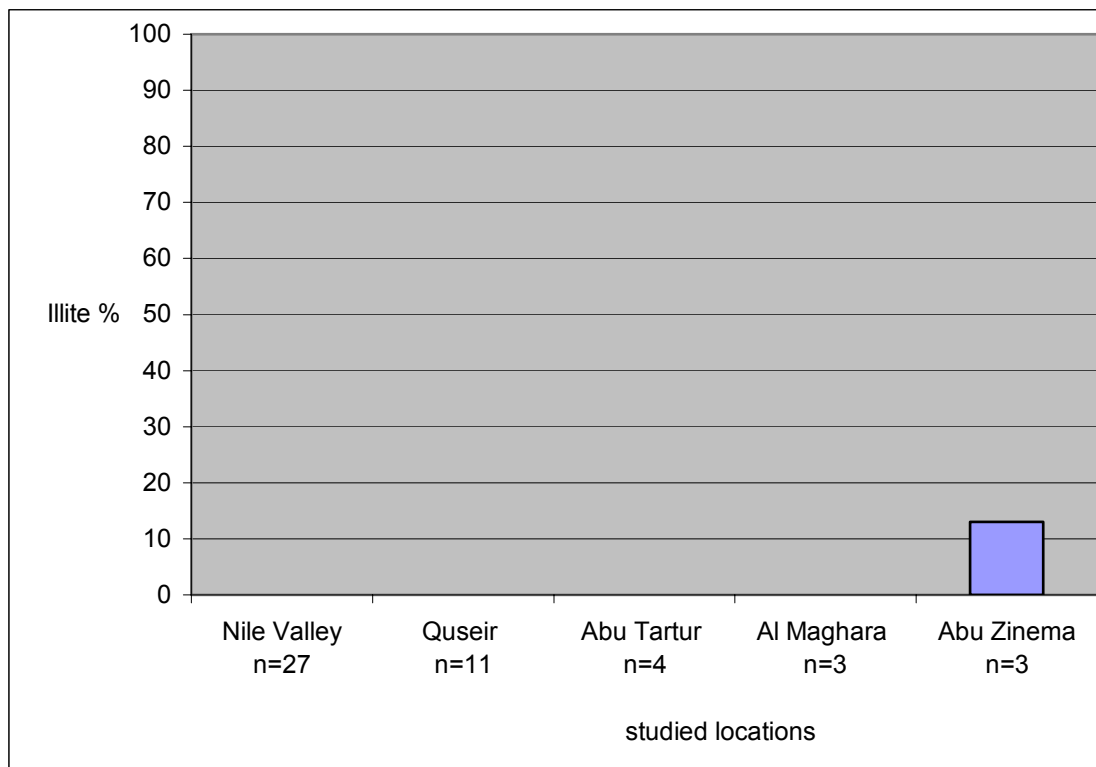


Fig. 9: Illite average at the studied locations.

Illite typically forms under conditions completely different from those under which kaolinite and smectite are formed. Illite forms in soils with little chemical weathering, in cold and/or dry climates and in areas of high relief where physical erosion is predominant (Ghandour et al. 2003).

In the present study the presence of illite in the Ataqa Formation of Carboniferous age (South Sinai) suggests the presence of mica in the source area. Mica have originated from felsic rocks from south of Sinai.

4.3 Whole rock samples

The peak height of the identified minerals in bulk samples are measured from x-ray diffractograms. The identified non-clay minerals are as follows:

4.3.1 Quartz

Quartz was found as an important non-clay mineral in all samples. Quartz varies from zero in samples N59, N35 and Q6 to 86% in sample AZ1 in Appendix (Table 3).

4.3.2 Carbonates

The carbonate minerals detected by XRD are calcite and dolomite. Calcite was found in most Nile Valley samples. It ranges from 0.0 % in black shale of Abu Tartur phosphate mine, Al-Maghara coal mine and Abu Zinema samples to about 88 % in the Tarawan Chalk in Nile Valley, sample N49. On the other hand dolomite was detected in a number of samples. It reaches up to 81% sample N59. The presence of calcite and dolomite in the studied samples from Duwi Formation, Dakhla and Esna Shale at both Quseir phosphate mines and Esna-Idfu at Nile Valley in addition to the presence of foraminifers' fossils may indicate the deposition of these formations in a marine environment.

4.3.3 Sulphates

Anhydrite was found in most samples of the Nile valley section. It is absent in the samples of Quseir phosphate mines, Abu Tartur phosphate mine, Al Maghara coal mine and Abu Zinema area. The anhydrite content reaches up to 94% on sample N52. It was identified in the XRD diffractograms by its characteristic lines at 3.50 Å and 2.85 Å.

Gypsum was identified in a number of samples by its characteristic lines at 7.56 Å, 3.06 Å and 4.27 Å. It reaches a maximum value of 47% in sample Q6.

The evaporites form from saline-rich fluids—brines. Brines may be generated by concentration of sea water, by evaporation or freezing, or as residual connate fluids in the subsurface (Selley 1988). Secondary brines can form where meteoric groundwater dissolves previously formed evaporites.

Anhydrite and gypsum in the studied shales were probably precipitated primarily as metal sulphides under reducing conditions when the shales were deposited. After the compaction of shales and oxidation of sulphides to sulphates as a result, at least in part, of the biological activity, the produced sulfates react with the calcic cement produced by weathering of carbonate to form gypsum. These dissolved sulfates will be expelled by solution due to the compaction of clays and concentrate along bedding planes as gypsiferous bands or streaks which can be easily seen in the field.

4.3.4 Pyrite

Pyrite was only detected in the black shales of the Duwi Formation in Abu Tartur phosphate mine. It reaches up to 6% in sample Tw.4. It was identified in the diffractograms by its characteristic lines at 1.63 Å, 2.71 Å and 2.42 Å.

The presence of pyrite spheres and framboids as seen by the SEM (6.3) in Duwi Formation indicate the prevalence of a reducing environment during the deposition. The presence of pyrite spheres may be an indicator of shallow water, such as found on submarine swells or in areas of nutrient upwelling in shelf settings (Schieber and Baird 2001). Pyrite forms in sediments as a consequence of the bacterial reduction of sea water sulphate (Berner 1982). Thus, the highly pyritic shales must have formed under euxinic conditions where H_2S exists above or at least at the sediment-water interface. The presence of H_2S in turn will react with Fe^{2+} which was probably delivered into the basin as colloidal material adsorbed on clay minerals to form iron sulphide. By increasing activity of the hydrogen sulphide in presence of iron and organic matter, a hydrophobic sulphide gel might have been formed (El-Dahhar 1987).

4.3.5 Carbonate fluorapatite

The phosphate minerals encountered in Quseir Safaga area, Abu Tartur mine and Nile valley section are carbonate fluorapatite, which are traditionally called francolite. This mineral is always the sole constituent of phosphorites in unweathered or only slightly weathered sedimentary deposits, whatever their age or location (Prevot et al. 1989). The peak area under the 2.79 Å is taken as the relative abundance of francolite. The amount of francolite ranges from very high (about 78 % sample N.20) to low in others (about 14 % sample Q.4).

The Upper Cretaceous–Lower Tertiary boundary in Egypt, like in many other countries, is a good example of the sedimentary association black shale – phosphate – chert – dolostone. The contacts between these facies are either gradual or abrupt. This sedimentary succession is believed to be deposited during the Late Cretaceous transgression of North Africa (Issawi 1972; Ward and McDonald 1979; Richardson 1982).

The presence of francolite, calcite and dolomite in the shales at Nile Valley, Quseir phosphate mines and Abu Tartur phosphate mine indicate their deposition in a marine environment.

The precipitation of phosphorites relates to the upwelling of nutrient-rich water (Selley 1988). Germann et al. (1987) concluded that the origin of the Egyptian phosphorites can be attributed to four distinct genetic phases, namely: primary enrichment, secondary concentration, lithification and weathering. The primary enrichment phase under suboxic to anoxic oxygen facies, during transgression produces phosphatic black shales. The secondary concentration phase under oxic facies, but during regression produces phosphatic sands and black shales. The lithification phase in an oxic/anoxic facies controlled by permeability, chemistry of the host rocks and pore fluids, is producing calcareous, siliceous, clayey, phosphatic phosphorites, and organic-rich clay-and siltstone. The weathering phase controlled by oxic, warm-humid climate and produce limonitic, gypsiferous phosphorites with Fe-phosphates and organic-poor clay-and siltstone.

The apatite formed under euxinic conditions at very low sedimentation rates that enabled anaerobic microorganisms, present in pore water, to attack the organic matter and thus to release PO_4^{3-} . This acidic medium, in turn, will dissolve the enclosing sediments and as a result, the soluble cations (e.g. Ca^{2+} , Mg^{2+} ...etc) will be concentrated within the pore waters. The presence of PO_4^{3-} , in turn, will react with Ca^{2+} and Mg^{2+} to form primarily the less stable mineral Staruvite ($\text{PO}_4(\text{Mg})\text{NH}_4$). This transitory mineral is unstable under such conditions and, thus, the produced solutions are normally rich in Mg. The Mg ions will participate in the formation of more stable phases such as dolomite or high magnesian clays. The conditions will thus become favourable for the formation of apatite in the low magnesium pore waters (Prevot et al. 1989).

5 Geochemistry

The geochemistry is concerned primarily with quantitative analysis, which measures the concentration of elements, compounds, isotopes or chemical species (e.g. Fe^{2+} as distinct from Fe^{3+}). In dealing with rocks, sediments and minerals, it is useful to distinguish between major elements (those present at concentrations exceeding 1 % by mass, making up the main minerals of the rock), minor elements (concentrations between 0.1 % and 1.0 %) and trace elements (concentrations less than 0.1 %). In drawing these distinctions, one should recognise that the same element may be a major element in one type of sample, e.g. sulphur in an ore concentrate, but a trace element in another, e.g. sulphur in fresh basalt (Gill 1997).

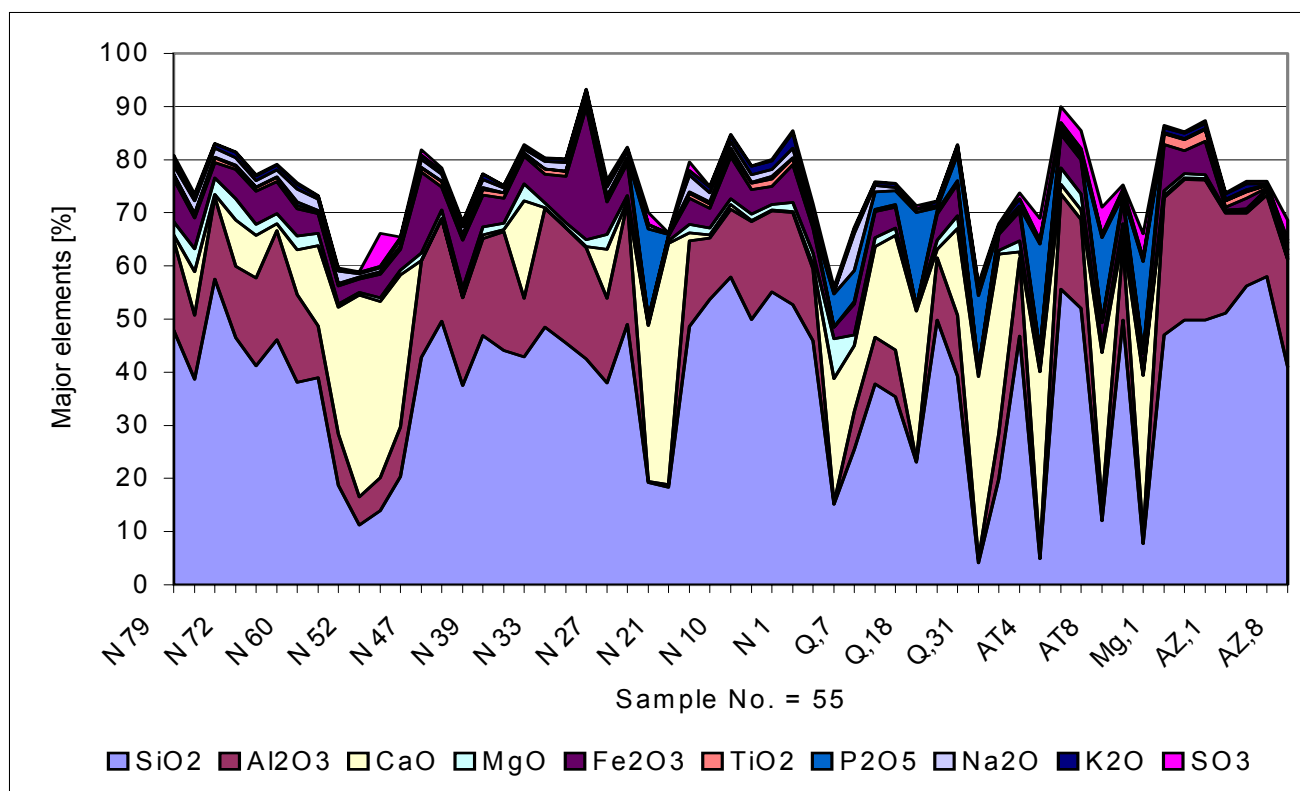
The occurrence of characteristic fossils and gross lithologic aspects of a sediment have been and still are the principal methods of environmental interpretation. However, the geochemical distribution of certain major, minor and trace elements may provide direct information on the depositional environment of the host sediments. It is emphasized, however, that it may be misleading to attempt to use the absolute abundance values of a single element as an indicator of the environment (Degens et al. 1957). Indications of the depositional environment can be revealed by elements adsorbed on organic or inorganic materials from the surrounding waters. The indicators can be incorporated into primary minerals or into organic substances forming in these waters, or they can be incorporated into authigenic minerals growing within the sediments during or shortly after their deposition (Cody 1971).

According to Degens et al. (1957) a good environmental indicator for marine or non-marine sediments should be: 1) markedly affected by salinity changes; 2) relatively widespread; 3) abundant enough to be detected and measured with a reasonable degree of precision; 4) formed or concentrated in the rock in which it is formed; and 5) relatively unaffected by post-depositional changes. There is an abundance of literature with respect to trace elements, whole rock composition, isotope ratios, exchangeable cations and other methods used in determining the environment of deposition. So far no technique has proved to be an “ideal” indicator of paleosalinity (Walters et al. 1987).

The studied samples consists mainly of carbonaceous shale and associated phosphate, limestone and marl sediments. The geochemical investigations were performed to investigate mainly shale samples. Other associated sediments are represented in small numbers.

5.1 Major and trace elements

Major and trace elements on whole rock of 48 carbonaceous shale samples and seven samples of the associated phosphate from the studied five locations were analysed by XRF. The results of the XRF analysis of the samples are presented in Appendix (Table 4 & 5). The abundance of major elements for all analysed samples is presented graphically in figure10.



The major constituents are SiO₂, Al₂O₃, Fe₂O₃, CaO, MgO, TiO₂, P₂O₅, Na₂O, K₂O, and SO₃.

AZ = Abu Zinema area (Carboniferous).

Mg = Al Maghara coal mine (Jurassic).

AT = Abu Tartur phosphate mine (Cretaceous).

Q = Quseir phosphate mines (Cretaceous).

N = Nile Valley section (Cretaceous –Eocene).

Fig. 10: Major elements variation of the studied samples including 7 phosphate samples.

The major and trace elements composition of the carbonaceous shales in this study is compared to published average shales in Table 2. In general, the bulk compositions of the carbonaceous shales in the present study compares quite closely with the published average shale compositions.

Table 2: Comparison of chemical composition of the studied shales with published average shales (1 to 4) and regional average composition (5 to 8).

	present study n =48	1	2	3	4	5	6	7	8
SiO ₂ %	45.80	64.82	58.10	58.50	n.a.	8.50	6.92	35.44	52.50
Al ₂ O ₃ %	16.80	17.05	15.40	15.00	13.22	2.90	1.98	9.82	15.41
TiO ₂ %	1.04	0.80	n.a.	0.77	0.33	0.10	0.15	0.43	0.71
Fe ₂ O %	4.80	5.70	4.02	4.72	2.86	1.20	1.12	3.97	7.04
MgO %	1.40.	2.83	2.44	2.50	1.77	0.60	0.99	3.56	3.99
CaO %	5.12	3.51	3.11	3.10	2.10	32.30	40.70	18.30	4.36
Na ₂ O %	0.75	1.13	1.30	1.30	0.94	n.a.	0.04	0.66	1.48
K ₂ O %	0.84	3.97	3.24	3.10	2.41	n.a.	0.04	0.70	0.15
P ₂ O ₅ %	0.62	0.15	n.a.	0.16	n.a.	1.80	1.89	3.34	1.48
Sr ppm	252	142	n.a.	300	200	940	1117	466	333
Ba ppm	99	636	n.a.	580	300	99	n.a.	143	116
V ppm	155	130	n.a.	130	150	78	78	639	205
Ni ppm	47	58	n.a.	68	50	136	594	124	57
Cr ppm	148	125	n.a.	90	100	256	305	277	136
Zn ppm	84	n.a.	n.a.	95	300	271	322	578	169
Cu ppm	25	n.a.	n.a.	45	70	83	60	56	42
Zr ppm	167	200	n.a.	160	n.a.	n.a.	n.a.	47	126

1= NASC (Gromet et al. 1984); 2= Average shale (Pettijohn 1975); 3= Average shales (Turekian and Wedepohl 1961); 4= Average black shales (Vine and Tourtelot 1970); 5= Average Israelian black shales (Ahmed 1997); 6= Average Jordanian black (oil) shales (Abed and Amireh 1983); 7= Average Quseir and Safaga (Eastern Desert, Egypt) black shales (Ismael 1996); 8= Average Abu Tartur (Western Desert, Egypt) black shales (Ahmed 1997).
n.a. = not available

The average of major and trace elements for the studied formations is shown in Table 3. The major constituents are SiO₂, Al₂O₃, Fe₂O₃, CaO, MgO, TiO₂, P₂O₅, Na₂O, K₂O and SO₃. The trace elements measured are Sr, Ba, V, Ni, Cr, Zn, Cu, Zr, Rb, Cl and F.

The Dakhla Shale in Quseir mines shows the highest values for the trace elements V, Ni, Cr, Zn and Cu (1357, 71, 344, 757 and 116 ppm respectively) due to oxidation of the organic matter in the in the Quseir mines (see chapter 5.2).

Table 3: The major and trace elements average of formations at the studied locations

Location	Nile Valley Section					Quseir Mines	Abu Tartur Mine	Al Maghara Mine	Abu Zinema area
	Esna Shale	Tarawan Chalk	Dakhla Shale	Duwi Fm.	Varigated Shale	Dakhla Shale	Duwi Fm.	Safa Fm.	Ataqa Fm.
SiO ₂ %	41.52	12.53	42.29	44.70	52.53	36.20	51.10	48.86	51.58
Al ₂ O ₃ %	14.51	5.77	18.20	10.20	17.00	10.00	15.83	26.21	17.03
CaO %	8.35	35.61	4.86	12.10	0.18	14.80	1.62	0.35	0.42
MgO %	2.61	0.63	1.54	1.10	1.32	1.70	2.70	0.78	0.30
Fe ₂ O ₃ %	5.18	3.43	8.32	4.35	5.02	4.77	5.61	6.42	0.79
TiO ₂ %	0.66	0.30	0.82	0.70	1.29	0.50	0.80	2.12	0.95
P ₂ O ₅ %	0.18	0.17	0.13	0.42	0.24	2.52	0.62	0.09	0.05
Na ₂ O %	1.85	0.71	1.33	1.56	1.52	1.55	0.10	0.11	0.50
K ₂ O %	0.82	0.26	0.61	0.80	2.03	0.70	1.10	0.93	0.69
SO ₃ %	0.26	3.15	0.34	0.50	0.26	0.50	2.10	0.47	1.21
Sr ppm	353	846	211	344	781	479	257	109	47
Ba ppm	145	53	81	201	163	90	84	87	108
V ppm	168	80	187	101	136	1357	175	158	128
Ni ppm	57	34	49	27	24	71	33	71	15
Cr ppm	171	149	183	100	105	344	115	196	75
Zn ppm	142	41	102	71	48	757	51	91	76
Cu ppm	22	12	21	26	31	116	23	25	25
Zr ppm	97	42	96	193	275	105	121	561	243
Rb ppm	44	12	25	26	61	30	27	40	27
Cl ppm	3006	720	2458	3123	2234	7217	63	109	2886
F ppm	1076	800	426	881	858	3292	472	36	800

On the following a discription and detailed discussion of the important and affective major and trace elements in the geochemistry of the studied carbonaceous shale and associated phosphate samples.

5.1.1 Silica (SiO₂)

Silica is the dominant constituent of all studied shale samples. The average content of silica in the samples is 45.80%. With exception of carbonate and phosphate samples, the silica averages are 51.58%, 48.86 %, 51.10 %, 36.20 % and 45.30 % in Abu Zinema, Al Maghara, Abu Tartur, Quseir and Nile Valley samples respectively.

Considerably higher average SiO₂ contents exist in NASC and average shales of Pettijohn (1975) is 64.82% and 58.50% respectively. The black shales of the neighbouring countries contain much less SiO₂ compared to the studied shales. In the Jordanian black shales the average SiO₂ is 6.92% (Abed and Amireh 1983) and 8.5% in the Israelian oil shales. Both Jordanian and Israelian oil shales are also markedly depleted in Al₂O₃ and TiO₂. This may indicate a black argillaceous limestone rather than a proper black shale (Ahmed 1997). The lower content of SiO₂ in the studied shales from Quseir confirms the previous study by Ismael (1996). This may be attributed to their enrichment in carbonate minerals. Silica tends to decrease with the increase of carbonates. Therefore, a positive relation between silica and argillaceous sediments on the one hand, a negative relation on the other hand can be expected denoting the different environmental conditions of siliceous and calcareous sediments (Abdou 1989).

According to the Pearsons correlation coefficient (r) Appendix (Table 6a), the SiO₂ is positively correlated with Al₂O₃, TiO₂ and K₂O (r=0.59, 0.57 and 0.52 respectively). Therefore SiO₂ is considered to be dominantly terrigenous in origin which is shown in a scatterplot of SiO₂ with Al₂O₃, TiO₂, Zr and K₂O (Fig. 11). A part of the silica may be attributed to a biogenic origin by silica secreting organisms, such as radiolaria or diatoms, thus the SiO₂ contents in Nile Valley and Quseir samples should be based on a biogenic origin. Silica may also be precipitated as cement filling cavities. The SiO₂ may occur as quartz disseminated with kaolinite, or deposited with the tiny flakes of the clay minerals (Bain and Smith 1987; Moore and Reynolds 1997).

Pettijohn (1975) stated that silica is present in shales as a part of the clay minerals, as undecomposed detrital silicates and as free silica, both detrital quartz and biochemically precipitated silica such as opal of radiolarians, diatoms, and spicules. The SiO₂ content in the studied shales correlates positively with Al₂O₃. This indicates that SiO₂ is mainly present in the studied shales as a part of the clay minerals and detrital silicates.

The $\text{SiO}_2/\text{Al}_2\text{O}_3$ ratio of the studied samples is listed in Appendix (Table 4). Felix (1977) reported that the $\text{SiO}_2/\text{Al}_2\text{O}_3$ ratio for pure montmorillonite ranges from 2.80 to 3.31 while for pure kaolinite it is about 1.18. With exception of the Al Maghara shale samples which recorded $\text{SiO}_2/\text{Al}_2\text{O}_3$ ratios somewhat similar to that of kaolinite (1.82, 1.88 and 1.89 for sample Mg1, Mg3, and Mg5 respectively), this is confirmed by the XRD results. The $\text{SiO}_2/\text{Al}_2\text{O}_3$ ratio for samples from other locations varies between (1.93 and 5.33) higher than that for pure kaolinite and also higher than that for pure montmorillonite. This may be indicate that the clay mineralogy of these locations (Abu Tartur, Nile Valley and Quseir) consists mainly of smectite and/or a mixture of smectite and kaolinite or chlorite. This has also been confirmed by XRD. The abundance of Si, Al, Ti and K in shales may be perturbed from parent material by weathering, transport and depositional processes (Nesbitt et al. 1980).

5.1.2 Alumina (Al_2O_3)

High alumina contents are recorded in the argillaceous and clayey sediments. The average content of alumina in the studied shales of the different localities (16.80%) is similar to that of average shales of Pettijohn (1975) and NASC (15.40% and 17.05 % respectively), slightly higher than that of the average black shales (13.22%) of Vine and Tourtelot (1970) but much higher than the argillaceous black sediments of Jordanian (1.98%) and Israelian shales (2.90 %) (Ahmed 1997). With the exception of carbonate and phosphate samples, its averages are 17.03%, 26.21%, 15.83%, 10.00% and 15.00 % in Abu Zinema, Al Maghara, Abu Tartur, and Quseir and Nile Valley samples respectively.

The Al_2O_3 concentration is thought to be a good measure of detrital influx. The positive correlation between Al_2O_3 and both SiO_2 , TiO_2 , and Zr ($r=0.59$, 0.79 and 0.54 respectively) and the positive trend in scatterplot of Al_2O_3 with both SiO_2 and TiO_2 (Fig.11) can be explained by a terrigenous origin. This may be due to the presence of a considerable amount of detrital clays. Generally the studied shales show coherence between silica and alumina Appendix (Table 4) indicating that both molecules are carried mainly in the clay minerals.

5.1.3 Calcium (CaO)

The average content of CaO in the studied mere shale samples is 5.12 %. With the exception of carbonate and phosphate samples, its averages are 0.42%, 0.35%, 1.61%, 14.80 % and 6.38 % in Abu Zinema, Al Maghara, Abu Tartur, Quseir and Nile Valley respectively.

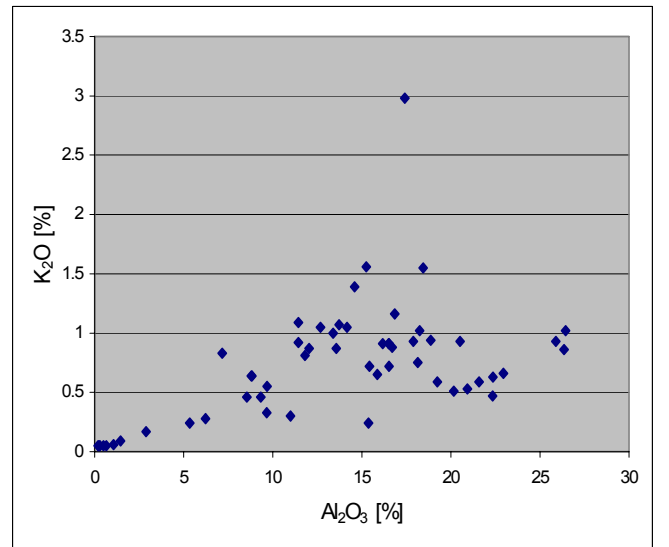
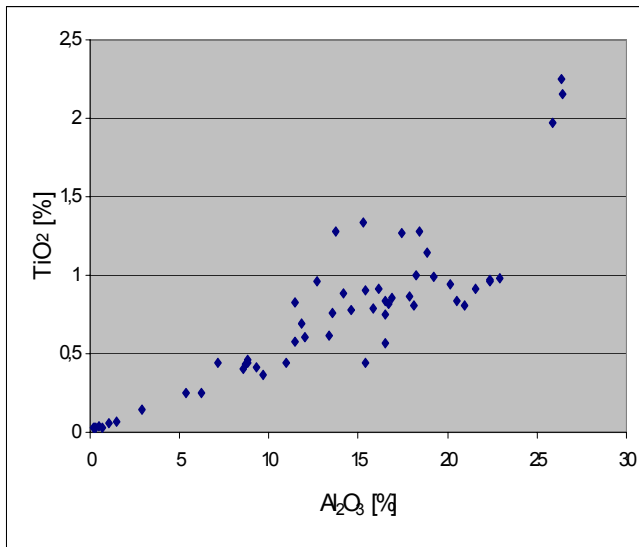
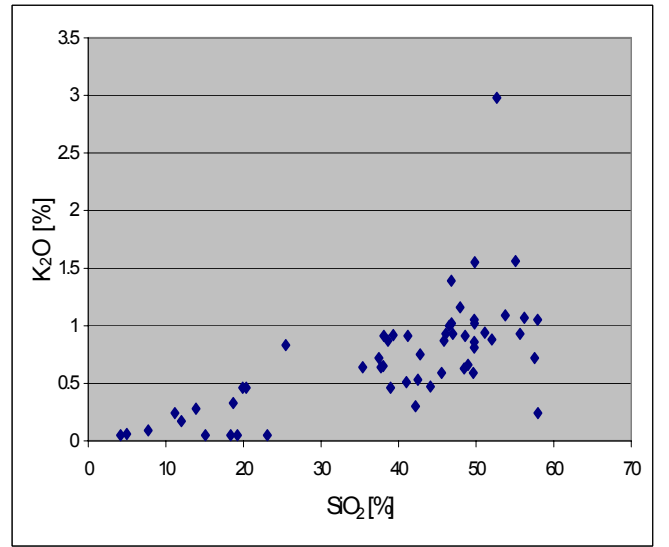
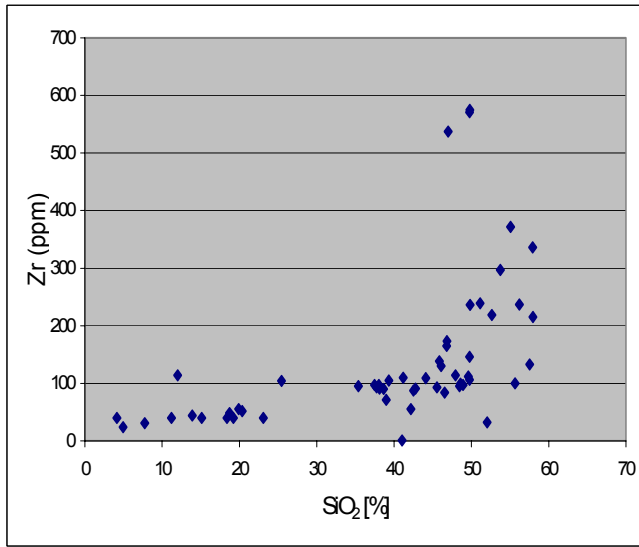
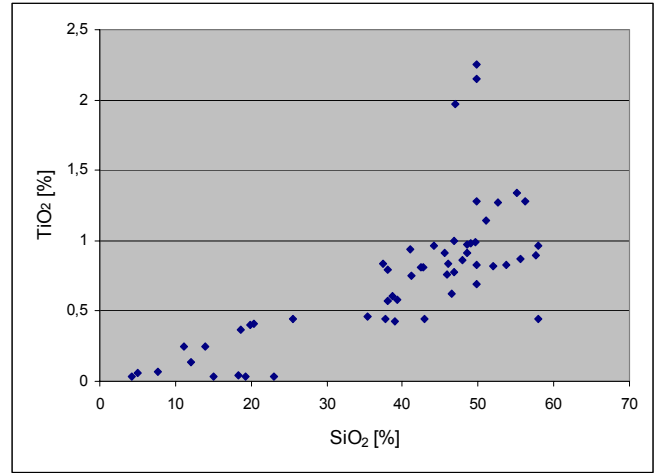
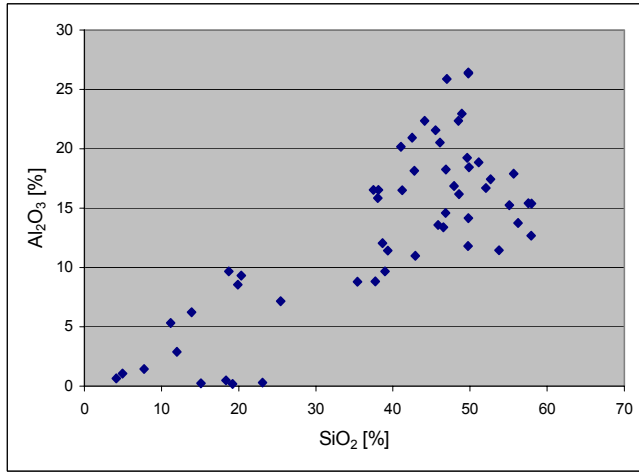


Fig. 11: The relationships between SiO_2 with Al_2O_3 , TiO_2 , Zr & K_2O and Al_2O_3 with TiO_2 & K_2O for the studied samples

The mean value of CaO in the studied shales at Abu Zinema, Al Maghara and Abu Tartur is relatively lower than that of average black shales 2.1 % of Vine and Tourtelot (1970) and average shales 3.15 % of Pettijohn (1975), while the mean value of Nile Valley samples being closely similar to NASC (3.56 %). The average content of CaO in Quseir shale samples in the present study is 14.80 %, slightly similar to a value of 18.3 % by (Ismael 1996) in Quseir.

Jordanian and Israelian oil shales are more calcareous (40.7 % and 32.3 % CaO respectively, Ahmed 1997). CaO shows a negative correlation with SiO₂, Al₂O₃, TiO₂ and K₂O ($r = -0.89$, -0.77 , -0.63 and -0.50 respectively) (Fig.12). This reflects a different source of CaO and these elements. CaO is considered to be dominantly of biochemical origin, while SiO₂, Al₂O₃, TiO₂ and K₂O are of terrigenous origin. CaO may be used as marine indicator because, marine shales often have considerably more calcium than non-marine ones (Refaat 1993). The obtained data show that the shales at Abu Zinema, Al Maghara and the lower part of Nile Valley section, which are considered as non-marine shales, have an average CaO lower than those of the shales which are considered as the marine shales of Abu Tartur, Quseir and Nile Valley Appendix (Table 4).

5.1.4 Magnesium (MgO)

The average content of MgO in the studied shales samples is 1.40 %. Its averages are 0.30 %, 0.78 %, 2.70 %, 1.70 % and 1.70 % in Abu Zinema, Al Maghara, Abu Tartur, Quseir and Nile Valley respectively. It is closely similar to those of average black shales Vine and Tourtelot (1970), average shales of Pettijohn (1975), NASC shales, shales of Jordanian and Israelian oil shales (1.17%, 2.5%, 2.85 %, 0.99 % and 0.6 % respectively).

MgO may be present as:

- 1- Octahedral and interlayer cation in the clay lattices. Mg²⁺ and Ca²⁺ substitute Al³⁺ in the octahedral sites of smectite or illite for not more than 2.7 % (Weaver and Pollard 1973). Na⁺ and Mg²⁺ ions are the major exchange cations in marine smectite.
- 2- Mg²⁺ may substitute Ca²⁺ in early formed calcite in the form of dolomite and ferroan dolomite. MgO shows a weak negative correlation with CaO ($r = -0.15$; see Fig.12) and Appendix (Table 6a). This reflects a different source of both of the elements. The study of thin sections indicates that Ca is of biogenic source and Mg of diagenetic origin by dolomitization.

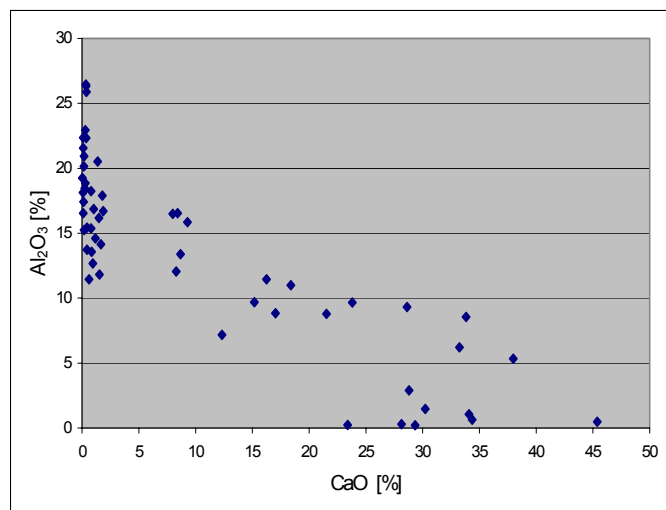
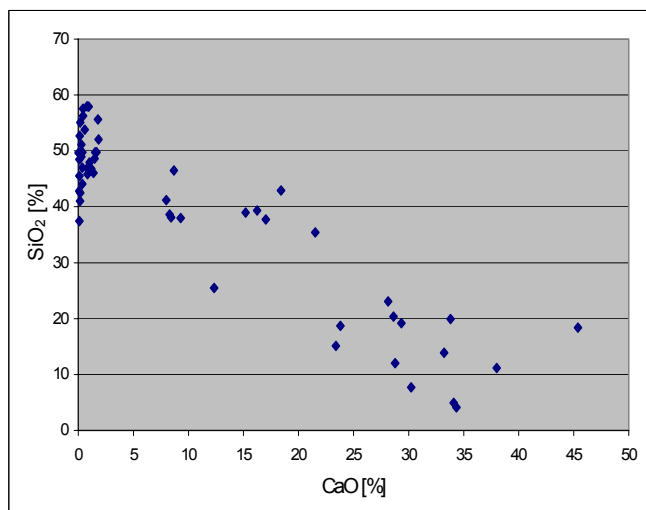
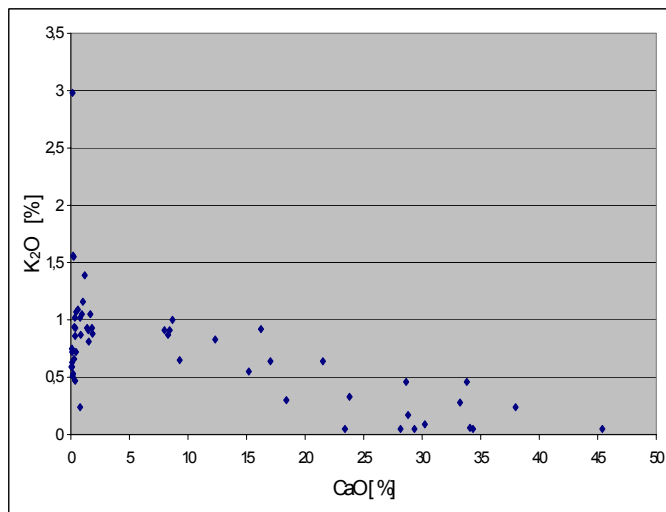
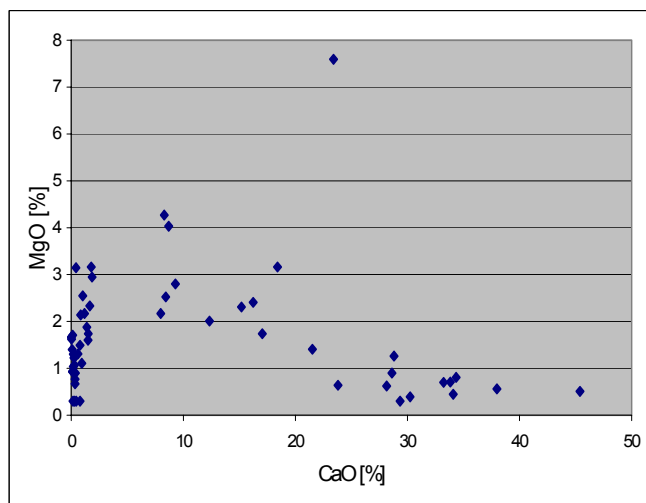
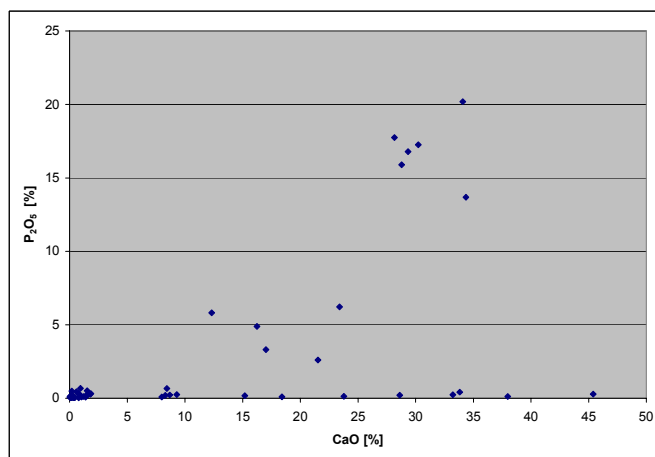
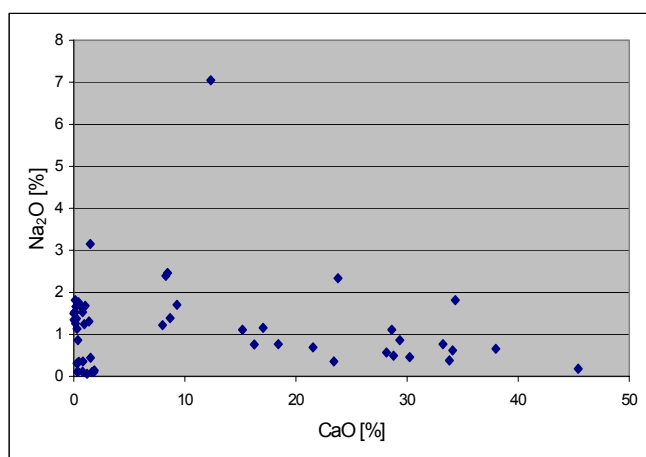


Fig. 12: The relationship between CaO with Na_2O , P_2O_5 , MgO , K_2O , SiO_2 & Al_2O_3 for the studied samples.

5.1.5 Iron Oxide (Fe₂O₃)

The average content of Fe₂O₃ in the studied shales samples is 4.80 %. Its averages are 0.79 %, 6.42 %, 5.61 %, 4.77 % and 5.72 % in Abu Zinema, Al Maghara, Abu Tartur, Quseir and Nile valley respectively. With the exception of Abu Zenima shales, the recorded averages are higher than those of average black shales of Vine and Tourtelot (1970), average shales of Pettijohn (1975), Jordanian and Israelian oil shales (2.86 %, 4.72 %, 1.12 % and 1.20 % respectively), and close to that of NASC (5.70 %).

Iron is present either in the structure of clay minerals and/or as an independent Fe-mineral such as goethite. Sharma (1979) stated that in the marine environment, the hydroxides of iron are carried as particles and colloids in suspension and therefore, tend to aggregate in the fine fraction of sediments. The enrichment of Fe₂O₃ in the studied shales may be attributed to their formation under more reducing conditions with a high input of non-reactive iron to the basin (Ahmed 1997). There is a weak positive correlation between Fe₂O₃ and the SiO₂, Al₂O₃, MgO, TiO₂, Na₂O Appendix (Table 6a) and positive correlation between Fe₂O₃ and Ni. This may be due to the association of Fe³⁺ with clay minerals.

5.1.6 Titanium (TiO₂)

The average titanium oxide content of the studied shale samples is 1.04 %, slightly higher than that of average crustal shales of Turekian and Wedepohl (1961) and NASC (0.77 % and 0.78 %) and higher than the average black shales of Vine and Tourtelot (1970) (0.33 %). The TiO₂ content of the studied samples is much higher than those of Jordanian and Israelian oil shales (0.15 % and 0.1 % respectively).

The strong positive correlation of TiO₂ with Al₂O₃ and Zr (r=0.79 and 0.87) Appendix (Table 6a) and (Fig.13). This may suggest that Ti is essentially associated with clays and reflecting its terrigenous origin. TiO₂ is usually disseminated within the clays as discrete minerals, e.g. rutile and anatase (Degens 1965). TiO₂ shows a strong negative correlation with the marine indicators or constituents e.g CaO and P₂O₅ (-0.63, -0.20) and weak negative correlation with MgO and SO₃ Appendix (Table 6a). This reflects the different sources of TiO₂ and these elements, and is indicating the detrital origin of TiO₂.

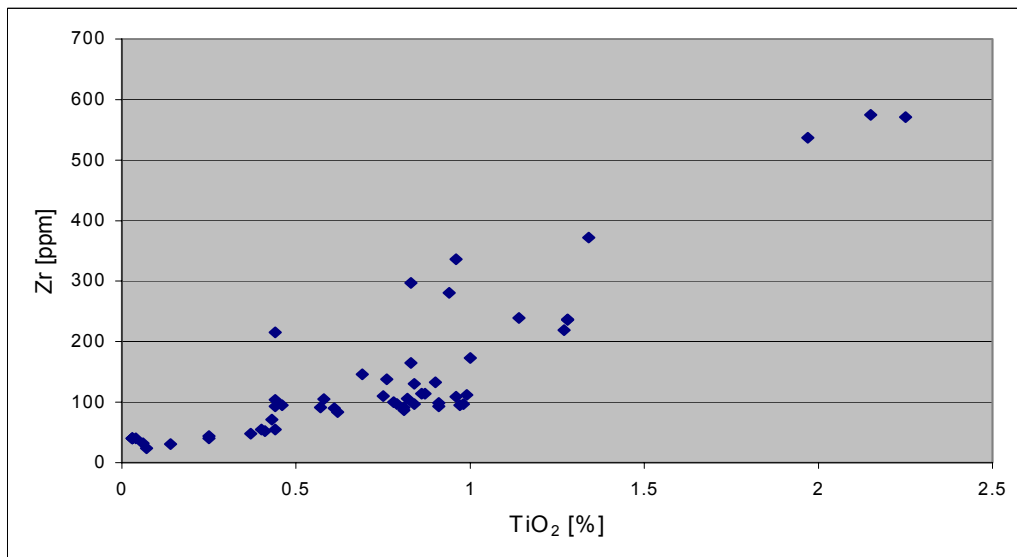
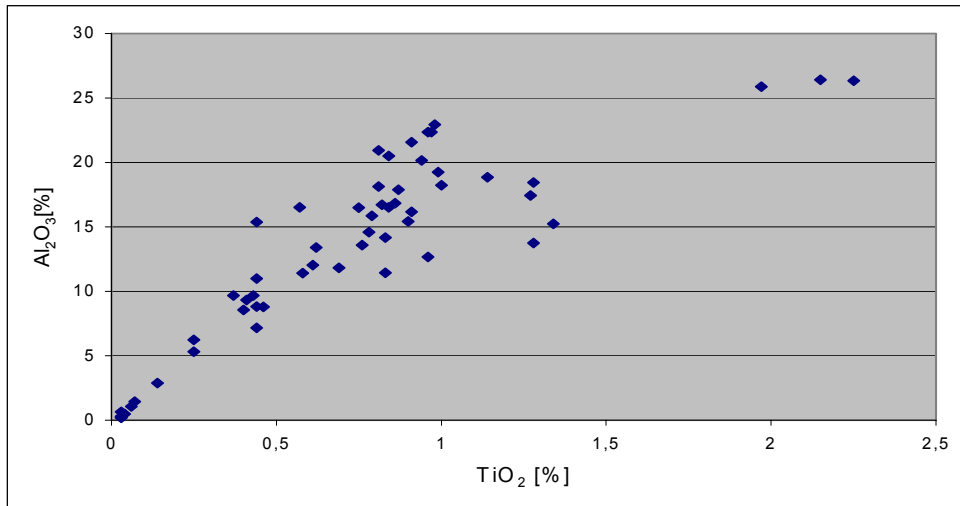


Fig. 13: The relationship between TiO_2 with Al_2O_3 , and Zr for the studied samples.

5.1.7 Phosphorus (P_2O_5)

The studied shales show a wide range of phosphorus content. High amounts of phosphorus are due to the presence of apatite or collophane. The mean value of P_2O_5 in the studied shales is 0.62 %. This is higher than those of the average shales of Turekian and Wedepohl (1961) and NASC (0.16 % and 0.11%) and lower than those of the Jordanian and Israelian oil shale (1.89 % and 1.80 %). Shales samples collected from the phosphate mines have higher P_2O_5 content than those collected from the other locations.

5.1.8 Sodium (Na_2O)

The mean value of Na_2O (0.75%) is slightly similar to that of average black shales 0.94 % of Vine and Tourtelot (1970) and lower than those of average shales of Turekian and Wedepohl (1961) and NASC (1.30 % and 1.15 % respectively), while it is higher than those of Jordanian and Israelian oil shales (0.043 %). Na_2O shows a negative correlation with SiO_2 , Al_2O_3 , and CaO . This may be due to the presence of Na_2O in the form of water soluble salts (mainly halite). Halite was detected by XRD analysis in some of the studied shale samples.

5.1.9 Potassium (K_2O)

The average content of potassium in the studied shales (0.84 %) is lower than those of the average black shales of Vine and Tourtelot (1970), the average shales of Turekian and Wedepohl (1961) and the NASC shales (2.41 %, 3.10 % and 3.99 % respectively). This may be due to the enrichment of clays in those shales mixed-layer, different to the studied shales, where smectite clays dominate. The mean value of K_2O is higher than those of Jordanian and Israelian oil shales (0.042 % and 0.04 %). K_2O shows a positive correlation with SiO_2 , Al_2O_3 , TiO_2 , Zr, Cu and Rb ($r = 0.52, 0.28, 0.48, 0.35, 0.57$ and 0.82 respectively). This indicates the association of K_2O with aluminosilicate phases.

The K_2O content is in agreement with the results of the clay mineral investigations, because the low content reflects the absence of or the low content of illite minerals (see chapter 4). The weak negative correlation of K_2O with SO_3 ($r = -0.11$) in samples with less illite content can be interpreted that potassium is preferentially adsorbed by clays (Milot 1970).

5.10 Sulphate (SO_3)

The average content of SO_3 in the studied shales (0.62 %) is higher than the content in average shales (0.60 %) of Turekian and Wedepohl (1961). The high value of SO_3 in the black shale of Abu Tartur Phosphate mine may be due to the fact that SO_3 primarily occurs in pyrite and also may occur in gypsum. This corresponds to the results of the XRD and SEM analyses. XRD shows pyrite in the Duwi Formation in Abu Tartur and gypsum in Dakhla and Esna Shale. SEM study shows pyrite framboids in the Duwi Formation in Abu Tartur.

5.2 Distribution of significant trace elements

5.2.1 Vanadium

In the studied shales, vanadium attains an average concentration of 155 ppm and varies from 20 ppm to 3151 ppm. The average vanadium content in the studied samples is higher than those of average shale (130 ppm) of Turekian and Wedepohl (1961) and also higher than vanadium in average black shale (150 ppm) of Vine and Tourtelot (1970). It has been suggested that some V may be complexed within the kerogene molecule. The high concentrations of V in the inorganic fraction may be the result of oxidation and weathering of the organic matter and the subsequent mobilization and concentration in host rocks (Riley and Saxby 1983).

Vanadium shows a positive correlation with some of the other trace elements, such as Ni, and Cr ($r=0.46$ and 0.52) Appendix (Table 6a) and (Fig.14). This association is considered to be typically of organic matter (Krauskopf 1956; Gulbrandsen 1966; Cook 1972). Vanadium shows positive correlation with Al_2O_3 , TiO_2 , the clay fraction and also a positive correlation with TOC (Fig.14). This indicates that vanadium is considered to be typically of organic matter association rather hosted by detrital silicate minerals (Stow and Atkin1987).

In the calcitic samples, the vanadium content is lower than in the dolomitic ones. This is mainly attributed to differences in the clay mineral content and not to the type of carbonates. The highest value of vanadium in the present study was recorded in the calcareous shale samples of Quseir mines at 3150 ppm. This is due to the oxidation and weathering of organic matter in these samples and subsequent mobilization and concentration of vandium.

5.2.2 Nickel

The average Ni content in the studied samples is 47 ppm, lower than Ni in average shale 68 ppm of Turekian and Wedepohl (1961) and also slightly lower than Ni in average black shale (50 ppm) of Vine and Tourtelot (1970). Nickel shows strong positive correlation with Cr and Zn ($r = 0.61$ and 0.64) Appendix (Table 6a). Nickel shows also positive correlation with TOC and slightly positive correlation with Al_2O_3 , TiO_2 and clay fraction (Fig.14). This indicates an association of these elements mainly with the organic matter and clay.

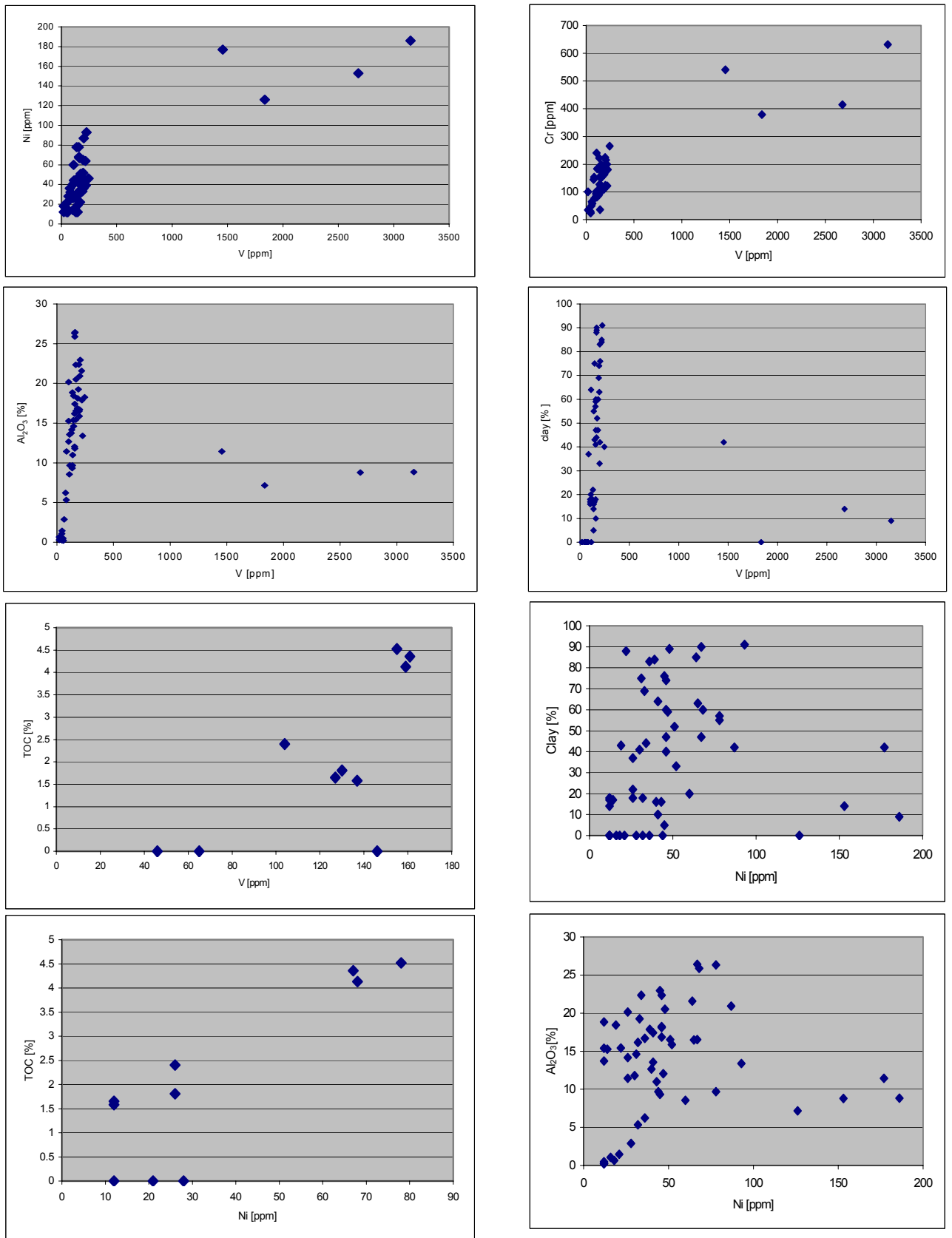


Fig. 14: The relationships between V with Ni, Cr, Al_2O_3 , clay & TOC and Ni with clay, TOC & Al_2O_3 for the studied samples.

Nickel, when present in significant quantities, originates from ultrabasic and basic rocks (Shapiro and Breger 1968). Weathering of such rocks and mobilization by humic acids may contribute to the high concentration of Ni in seawater. Turekian (1978) stated that, Ni is abundant in deep marine sediments (up to 300 ppm) but much less so in coastal sediments (39 ppm). Average contents of Ni are also less than 100 ppm in shales, 50 ppm in the black shales of the United States, 41 ppm in marine clays, 13 ppm in oil and only a few ppm in limestones. Phosphate rocks have an average content of 50 ppm similar to those of black shales, but a higher content than those of most other types of sediment. Nevertheless, Ni concentration in sea water is the order of 0.5 to 2 ppm, follows the trend of that of the nutrients P and Si and like the concentration of Zn, generally the Ni content is higher in reduced sulphidic areas compared to oxygenated areas. Moreover, Ni is concentrated in trace amounts in all organisms.

Brumsack (1980) found that the elements Ni, Cu, Zn and Fe are almost always associated with sulphides and hence concluded that normal seawater is sufficient to account for the high metal concentration in black shales: he further considered that despite of a definite correlation of the metal organic carbon, the organic matter is not regarded to be responsible for heavy metal concentrations. In the present study the low Ni content indicate that it associated with organic matter.

5.2.3 Chromium

The average chromium content of the studied samples is 148 ppm. This is higher than the Cr content in average shale (90 ppm) of Turekian and Wedepohl (1961) and also higher than Cr in average black shale (100 ppm) of Vine and Tourtelot (1970). Cr shows a weak positive correlation with Al_2O_3 , which may be due to the adsorption of Cr on the surface of clays or due to the replacement of Al_2O_3 by Cr in clays. However, Cr may be adsorbed on iron and manganese oxides, clays, apatites and organic matter (Prevot 1990).

Cr, V, Zn and Cu are always strongly intercorrelated (Fig. 15). There is a positive correlation between Cr, V and Ni ($r = 0.52$, and 0.61) Appendix (Table 6a). This association indicate that these elements are incorporated in organic matter and clay minerals. Cr shows also a positive correlation with TOC and a slightly positive correlation with Al_2O_3 and the clay fraction (Fig.15). This indicates an association of these elements mainly with the organic matter and the incorporation into the clays fraction. Cr was presumably derived from a source dominated

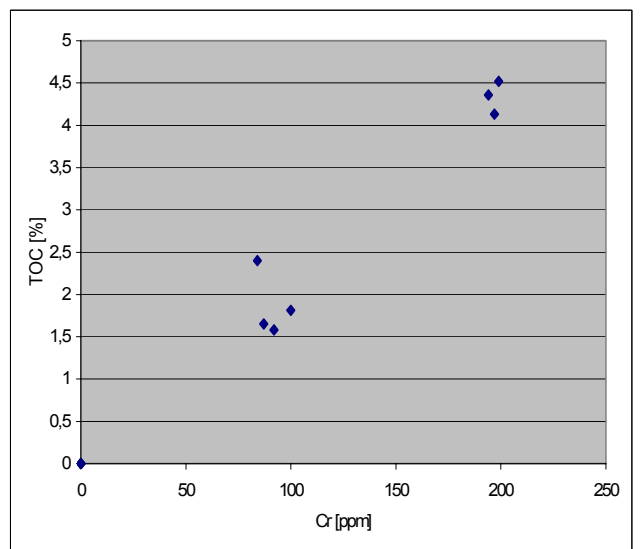
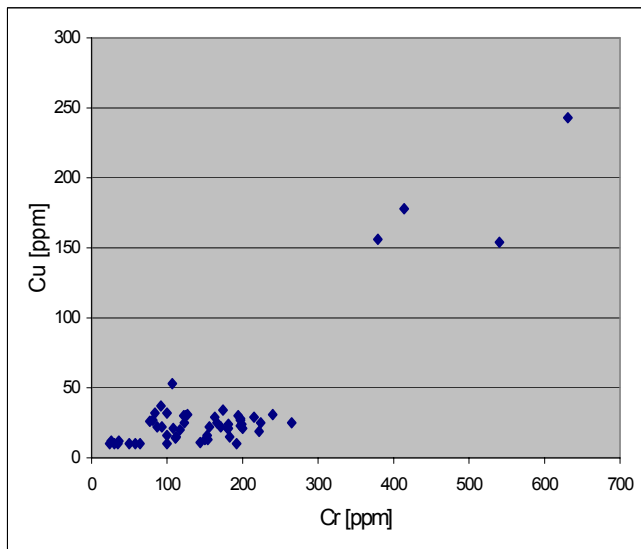
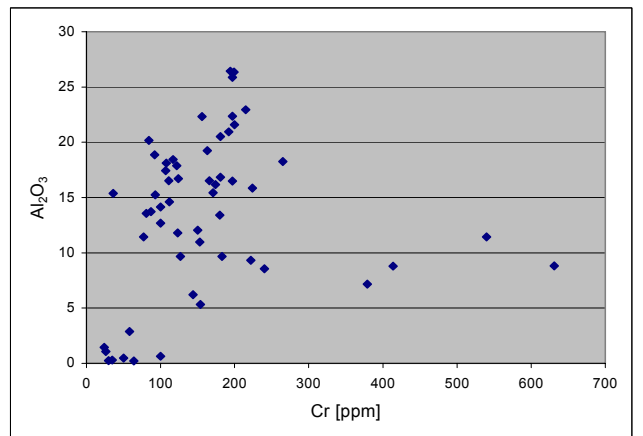
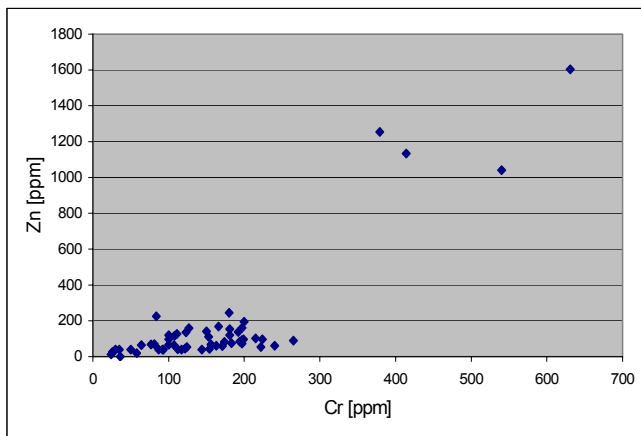
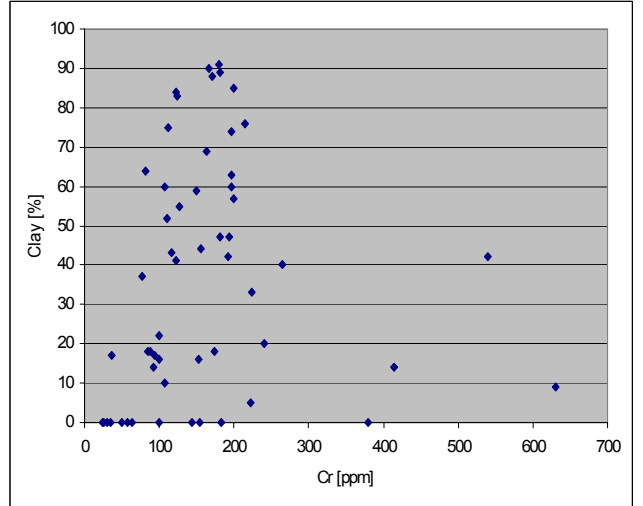
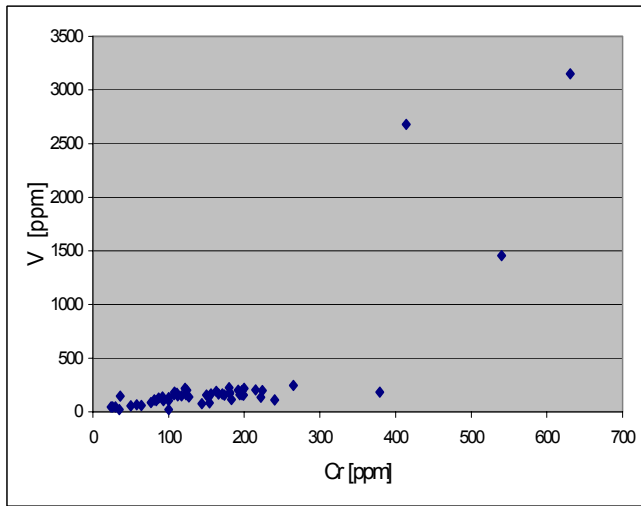


Fig. 15: The relationship between Cr with Zn, Al_2O_3 , V, clay, Cu and TOC for the studied samples.

by mafic volcanic rocks (Gill 1981). High Cr and Ni concentrations and the positive correlation between the two elements have been used as an indicator of mafic and ultramafic provenance for the sedimentary origin. The concentration of Cr and Ni in shales further reflects the incorporation of Cr and Ni ions into clay particles during the weathering of ultramafic rocks containing chromite and other Cr and Ni-bearing minerals (Garver et al 1994). The enrichment in Cr and Ni in the studied shales may indicate that mafic to ultramafic components were among the basement complex, the sediments were derived from.

5.2.4 Cobalt

The studied samples show Co contents less than 10 ppm, with the exception of Al Maghara samples which recorded high values of Co (sample No. mg1, mg3 and mg5 with 29, 25 and 36 ppm respectively) and also a few samples from the Nile Valley section. The cobalt content in the studied samples is lower than Co in average black shale (10 ppm) of Vine and Tourtelot (1970). This indicates that cobalt is not significantly adsorbed nor incorporated into the clay minerals or the organic matter admixed with the samples (Ismael 1996).

5.2.5 Strontium

Strontium is abundant in the studied shale samples. It ranges between 17 ppm and 1703 ppm with an average of 252 ppm. This average is higher than the Sr content in the average black shale (200 ppm) of Vine and Tourtelot (1970) and lower than the Sr content in both the average shale (300 ppm) of Turekian and Wedepohl (1961) and the average Israelian black shales (940 ppm) of Ahmed (1997) and the average Jordanian black shale (1117 ppm) of Abed and Amireh (1983). Sr may be concentrated by non-calcareous plankton (Knauer and Martin 1973), and especially aragonitic materials and shells, as well as by primary apatite in bones and teeth of vertebrates. In the present study, with the exception of black shale of Carboniferous and Jurassic age from Abu Zinema and Al Maghara, the studied shales show high strontium values. This related to the association of Sr with CaO and organic matter.

5.2.6 Zinc

The average zinc content in the studied samples is 84 ppm. This average is lower than Zn in average shale (95 ppm) of Turekian and Wedepohl (1961) and lowers than Zn in average black shale (300 ppm) of Vine and Tourtelot (1970).

Like chromium, zinc shows a positive correlation with the Ni element ($r = 0.64$) which may be explained as related to organic matter. With its ionic radius of 0.83 Å, Zn is liable to replace bivalent cations, such as Ca, Mg and Fe. Zn is reported to induce aragonite formation (Angus et al. 1979), but 20 to 140 ppm of Zn could also coprecipitate with calcite (Pomerol 1984). Zn is adsorbed on clay minerals and iron manganese oxides.

5.2.7 Copper

Copper is one of the elements which is indispensable to living organisms, however it becomes very highly toxic at high concentrations. This explains its association with organic matter in organic sediments but always in very moderate amounts. Black shales and bituminous clays are rich in Cu with a content of about 90 ppm (Prevot 1990). The black shale of Abu Tartur area contains moderate contents of Cu (23 ppm). This value is intermediate between those reported for bituminous clays and shallow marine sediments (Ahmed 1997). Ismael (1996) indicates that copper is somewhat enriched in the $<2\mu\text{m}$ fraction of Quseir shales, thus revealing its adsorption or incorporation into the clay minerals.

In the present study the average copper content is 25 ppm. This is lower than copper in the average shale (45 ppm) of Turekian and Wedepohl (1961) and in the average black shale (100 ppm) of Vine and Tourtelot (1970). Copper shows a positive correlation with Rb ($r = 0.52$). This indicates that copper is associated with organic matter and clay minerals..

5.2.8 Zirconium

Zirconium in the studied shale samples shows an average of 97 ppm. This average is lower than the zirconium content in the average shale (160 ppm) of Turekian and Wedepohl (1961) and higher than Zr in the average black shale (70 ppm) of Vine and Tourtelot (1970). It shows high values in Abu Zinema, Al Maghara and Abu Tartur black shale samples (243 ppm, 561 ppm and 121 ppm respectively). This indicates that Zr may be incorporated into organic matter or adsorbed by clay minerals. Zirconium shows positive correlation with Al_2O_3 and TiO_2 ($r = 0.54$ and 0.87 respectively). This is the result of the close association between these elements and clays, and therefore reflects their terrigenous origin.

5.3 Discussion of chemical effects

Elemental concentrations in sediments result from the competing influences of provenance, weathering, sorting, and sediment diagenesis (Quinby-Hunt et al., 1991). When comparing the chemical composition of the classic shale composites, the studied shales show generally enrichment of elements that are chemically immobile and are associated with terrigenous influx, such as Al, Ti and Zr. Al and Ti which can survive throughout intensive chemical weathering and diagenesis (Cullers 2000). Their concentration in sediments is used as a measure of detrital input. The major constituents of the studied shale samples do not vary greatly from one location to another. The SiO_2 , Al_2O_3 and TiO_2 tend to form together the main constituents of the studied shales and are normally related to clays. SiO_2 , Al_2O_3 and TiO_2 are well correlated in all samples. This indicates that the major constituents SiO_2 , Al_2O_3 and TiO_2 of the studied shale samples are dominantly terrigenous in origin.

In the Gulf of Mexico, shales have K_2O contents that increase systematically with depth from 2 to 4 wt % in the Paleocene-Eocene Wilcox Formation and from 2 to 5 wt% in the Oligocene–Miocene Frio Anahuac succession (Bloch et al. 1998). Potter et al. (1980) has shown the geochemical properties of shales change with time. Abdul Almanan (2002) stated a significantly higher content of K_2O in early Paleozoic shales, than in younger shales.

In the present study K_2O varies only slightly from Paleozoic shales to Eocene shales, e.g. between 0.26 for Tarawan Chalk to 2.03 for the Variegated Shale in Nile Valley. This is due to the enrichment of smectite and kaolinite in the studied shales and therefore strictly related to the mineralogy of the samples. Further it is noticed that K_2O decreases with increasing of carbonate content.

The black shales at Abu Zinema area of Carboniferous age and at Al Maghara coal mine of Jurassic age are enriched in SiO_2 , Al_2O_3 , TiO_2 , and Zr and depleted in the marine indicators CaO and MgO. This seems to indicate that the shales at Abu Zinema area and Al Maghara coal mine have been deposited under reducing conditions with non-calcareous planktons input or under continental conditions. This is confirmed by their association with coal and detrital kaolinite.

In the contrary the shales from the Abu Tartur phosphate mine, the Quseir phosphate mines and the Nile Valley section were deposited in a marine environment, as given evidence for by

foraminifera, smectite, pyrite and their association with phosphate. The Abu Tartur and the lower part of the Nile Valley samples are more argillaceous and depleted in CaO than those of Quseir and Dakhla and Esna Shale at the Nile Valley, which might have been deposited in a shallow marine environment with a high productivity of calcareous organic matter.

Numerous of investigators have used several trace elements, including B, Ga, V, Li, Ni, Rb, as paleosalinity indicators for sediments especially of shales (Goldschmidt and Peters 1932; Potter et al. 1963; Ohrdorf 1968; Dominik 1985; Schreier 1988). These studies showed that Ba, Rb, Mg, Fe, and Ca are higher in marine shales, whereas Zr, Ti, Al, Ga, Li and Cr are terrestrial indicators. Schultz et al. (1980) observed that Cr, Ni, Zn, Fe and P are significantly more abundant in marine strata of Pierre Shale (Cretaceous) of the northern Great Plains. Walters et al. (1987) observed a pattern of trace elements in the shale of the Dakota Sandstone similar to pattern of terrestrial indicators described above.

In the present study the shale samples at Abu Tartur phosphate mine, Quseir phosphate mines and Nile Valley section show higher contents of the trace elements Sr, Ba, V, Ni, Cr, Zn, Rb than shale samples at Abu Zinema and Al Maghara. This indicates that the shale samples at Abu Tartur phosphate mine, Quseir phosphate mines and Nile Valley section were deposited in a marine environment.

5.4 Weathering effects

The chemical index of alteration (CIA) defined as $CIA = 100 \times Al_2O_3 / (Al_2O_3 + CaO + Na_2O + K_2O)$ have been established as a general indicator of the degree of weathering in any provenance regions (Nesbitt and Young 1982). High values (i.e, 76-100) indicate intensive chemical weathering in the source area whereas low values (i.e., 50 or less) indicate unweathered source areas.

The CIA values for the studied shales Appendix (Table 4) indicate that the shale samples of Ataq Formation of the Carboniferous in Abu Zinema and of Safa Formation in Al Maghara have experienced strong chemical weathering ($CIA > 90$) at the source area. Further, the depletion of Na and Ca reflects an intense chemical weathering of the source rocks. As Al_2O_3 , CaO, Na_2O and K_2O are related with (CIA) they exhibit variations between the investigated samples reflecting variable climatic zones or rates of tectonic uplift in source areas. This corresponds with the results of Ghandour et al. (2003) in Safa Formation and also with the

observations of Nyakairu and Koeberl (2001) who recorded high CIA values (87 to 96) and low contents of alkali elements from kaolinitic rich sediments in Central Uganda.

For the calcite-enriched samples the CIA was not applied. The calcite-free samples of the Duwi Formation, the Dakhla Shale and the Esna Shale in Abu Tartur, the Nile Valley and Quseir show high CIA values (>76). This indicates moderate to intensive chemical weathering in the source area. This is also confirmed by the dominance of smectite in these formations. This proves the assumption that the area was located near the palaeoequator and had experienced warm, wet, and tropical to subtropical conditions characterized by low seasonality contrasts and predominantly chemical weathering, as also described by Tantawy et al. (2001).

Also Rb/Sr ratios of sediments are a monitor of the degree of source-rock weathering (McLennan et al. 1993). The studied shale samples of Upper Cretaceous-Lower Tertiary in Quseir, Abu Tartur and Nile Valley have an average Rb/Sr ratio of 0.16. This value is lower than that of the average upper continental crust of 0.32 and the average post-Achean Australian shale of 0.8 (McLennan et al. 1983). This suggests that the degree of source area weathering was moderate. On the other hand the studied shales of Carboniferous and Jurassic age in Abu Zinema and Al Maghara have average Rb/Sr ratios of 0.49, indicate that the degree of source area weathering was more intense compared to the younger sediments of Cretaceous and Tertiary age.

5.5 Provenance analysis for sedimentary rocks

Cr and Ni High levels of Cr and Ni and strong positive correlations between the two elements have been used by various authors (e.g., Hiscott 1984; Wrafter and Graham 1989 and Garver et al. 1994, 1996) to infer a mafic to ultramafic provenance of the sedimentary rocks. The concentration of Cr and Ni in shales is further reflecting the incorporation of Cr and Ni ions to clay particles during the weathering of ultramafic rocks containing chromite and other Cr and Ni-bearing minerals (Garver et al. 1996). The level of Cr enrichment in the studied shales (weight average 148 ppm), its strong positive correlation with Ni ($r = 0.61$) and the high Cr/Ni ratios of about 3.7 indicate that mafic to ultramafic components were the main components among the basement complex source rocks.

Vanadium Stow and Atkin (1987) stated that V is enriched in organic rich shales deposited under reducing conditions and might also be hosted by detrital silicate minerals.

The V/Cr ratio has been used as a paleo-oxygenation indicator in a number of studies. Values of V/Cr >2 are thought to represent anoxic depositional conditions, whereas values below 2 are indicative of more oxidizing conditions (Dill et al. 1988). The studied shales of Egypt have V/Cr values below 2 Appendix (Table 5), which may indicate that all of the studied sediments were deposited under relatively oxidizing conditions with exception of the Duwi Formation in Abu Tartur, which was deposited in a reducing environment.

TiO₂/Al₂O₃ Brooks (1973, Spears and Kanaris (1976) found that the Carboniferous sediments in England have high TiO₂/Al₂O₃ ratios reflecting a strong correlation to the ratios in the parent basalt. Amajor (1987) utilized the TiO₂ versus Al₂O₃ binary plot to distinguish between granitic and basaltic source rocks. In figure 16 the TiO₂ versus Al₂O₃ binary diagram for the studied samples, it is demonstrated that the provenance material varies from predominantly granitic to mixed granitic basaltic rocks.

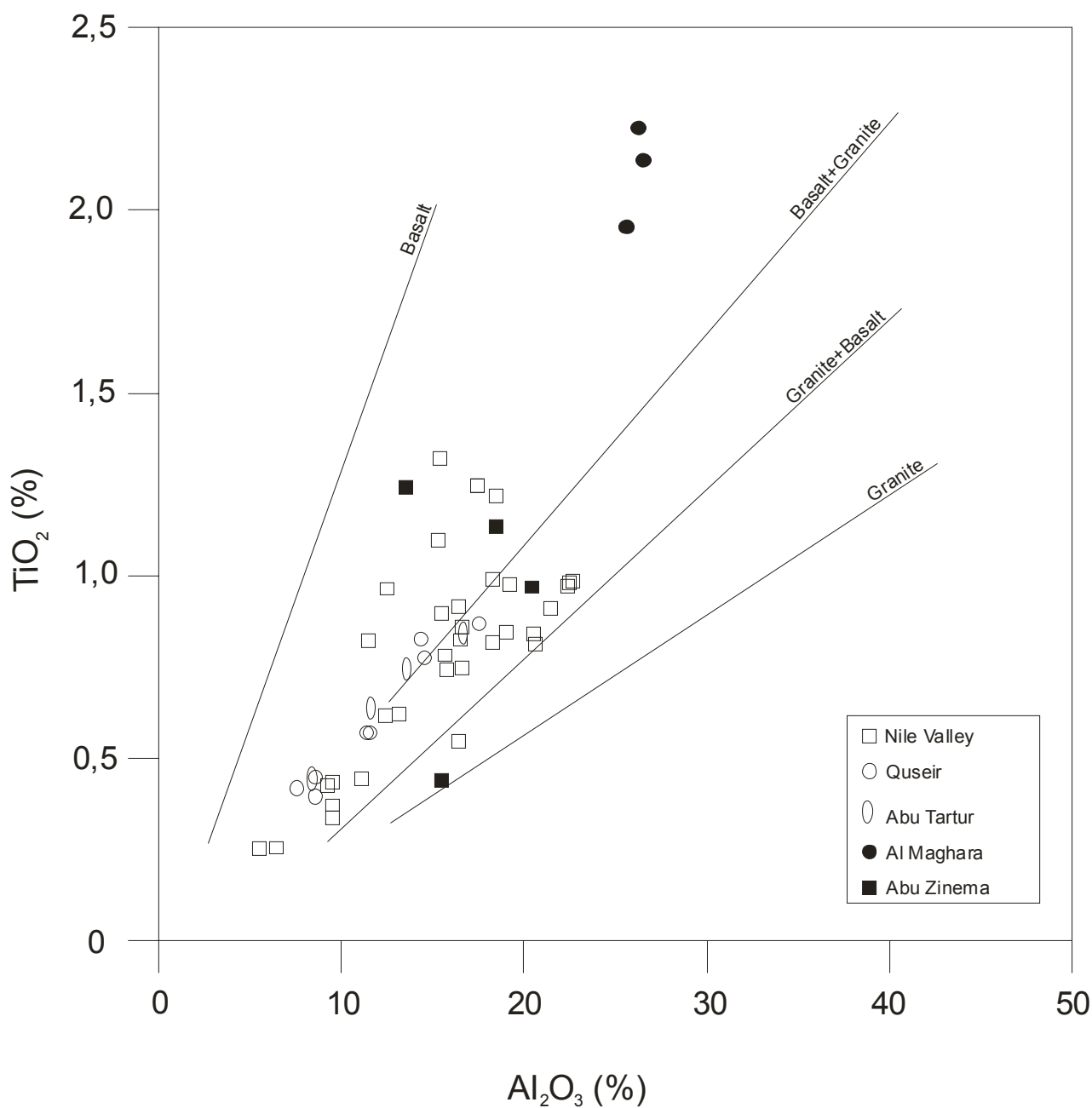


Fig. 16: $\text{TiO}_2 / \text{Al}_2\text{O}_3$ binary plot of the studied shale samples.
(provenance field from Amajor, 1987)

5.6 Distribution of major and trace elements in phosphate rocks

The studied phosphate samples show P_2O_5 values ranging between 6.20 % in the cherty phosphate in Quseir mine to 20 % in Abu Tartur mine and average 15.40 % (Fig. 17). In Egypt, phosphate bearing strata of economic importance and associated shales of the Duwi Formation are stretching from the Red Sea coast in Quseir over the Nile Valley into the Western Desert in Abu Tartur. They belong to a marine transgressive sequence which started on the top of predominantly fluvial Nubia Sandstone and grades into a sequence of an open marine environment (Germann et al. 1987). The Campanian to Maastrichtian Duwi Formation of a shallow marine origin (El-Ayyat and Kassab 2004) is overlain by shales, marls and limestones of the Maastrichtian to Paleocene Dakhla Formation, the sediments reflecting deposition under inner neritic to outer shelf conditions and repeated sea level changes (Hendriks 1985; Tantawy et al. 2001).

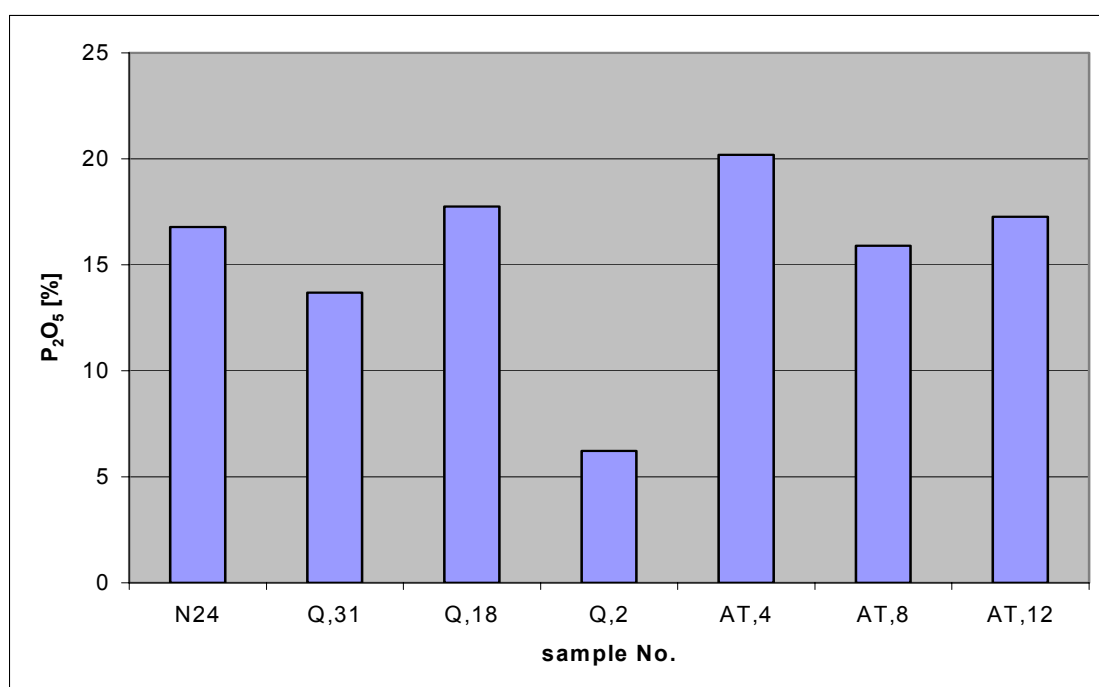


Fig 17: Distribution of P_2O_5 in the studied phosphate samples.

Phosphorus in sediments exists mainly in three forms, authigenic minerals (Ruttenberg and Berner 1993; Schuffert et al. 1994, 1998), in an organic form (Filipek and Owen 1981) and adsorbed on sediment particles (Sundby et al. 1992; Jensen et al. 1995). Inorganic phosphorus, which is synthesized authigenically in pore water, generally accounts for around 70 % of the total reactive phosphorus in marine sediments (Filippelli, 1997). Phosphorus in

organic matter accounts for 10-40 % of total phosphorus in coastal marine sediment (Kamatani and Maeda 1989) but is preferentially released during decomposition of the organic matter (Ingall and Van Cappellen 1990). Dissolved reactive phosphate which is released to pore water can be adsorbed on sediment particles; it is easily desorbed and dissolved into pore water under anoxic conditions (Watanabe and Tsunogai 1984). Thus, authigenic phosphorus minerals in sediments are the main sinks for phosphorus from the ocean (Filippelli, 1997; Louchouart et al. 1997).

Marine phosphatogenesis and its characteristically P-C-Si-enriched sedimentary products are intimately related to upwelling phenomena (Cook 1984; Slansky 1986). Upwelling of nutrient-rich waters stimulates biomass productivity, and thus, biological preconcentration of phosphorus, silica and carbon is affected. Analysis of regional and stratigraphical distribution of phosphate and black-shale facies, and their sedimentological and geochemical properties has led to the general description of a phosphatogenetic model based mainly on an upwelling conception (Ganz 1984; Schröter 1986). The periods of particularly intensive and world-wide phosphate enrichment, as e.g. the Upper Cretaceous-Lower Tertiary Span, coincide with periods of warm-humid climatic conditions and related intensive chemical weathering (Valeton 1983; Prasad 1983; Riggs 1984).

The strong positive correlation of P_2O_5 with CaO, Sr and F ($r = 0.66, 0.93$ and 0.95 respectively Appendix (Table 6b) and (Fig. 18) is interpreted to be due to the substitution of both, the Sr and CaO within the carbonate-fluorapatite phase (Gulbrandsen 1966, 1970; Bliskovsky et al. 1967; Tooms et al. 1969; McConnell 1973)

The high silica content in the cherty phosphate samples from both of Quseir and Nile Valley, with average 14.11 % and 19.21% is indicating of biogenic origin, by diatoms (Germann et al. 1987). The vertebrate fauna of the Egyptian phosphorites (Dominik & Schaal 1984) is characterized by the simultaneous occurrence of marine (mainly sharks and mosasaurs) and freshwater inhabitants (e.g. Ceratodontids and other fish species). Germann et al. (1987) stated that, from the paleoecological point of view, the depositional situation of the Late Cretaceous phosphorites in Egypt is characterized by marginal marine conditions more or less influenced by freshwater influx.

The trace elements V, Ni, Cr, Zn and Rb in the phosphate show averages of 43, 17, 48, 46 and 8 ppm lower than these of the overlain black shales. This indicates leaching processes

outgoing from the overlain black shales. The low average content of detrital terrigenous influx Al_2O_3 , TiO_2 and Rb (Fig.18) and the association of the phosphate bed with oyster limestone and diatom enrichment in Quseir and in the Nile Valley is indicating the marine origin of the phosphates in the Eastern part of Egypt.

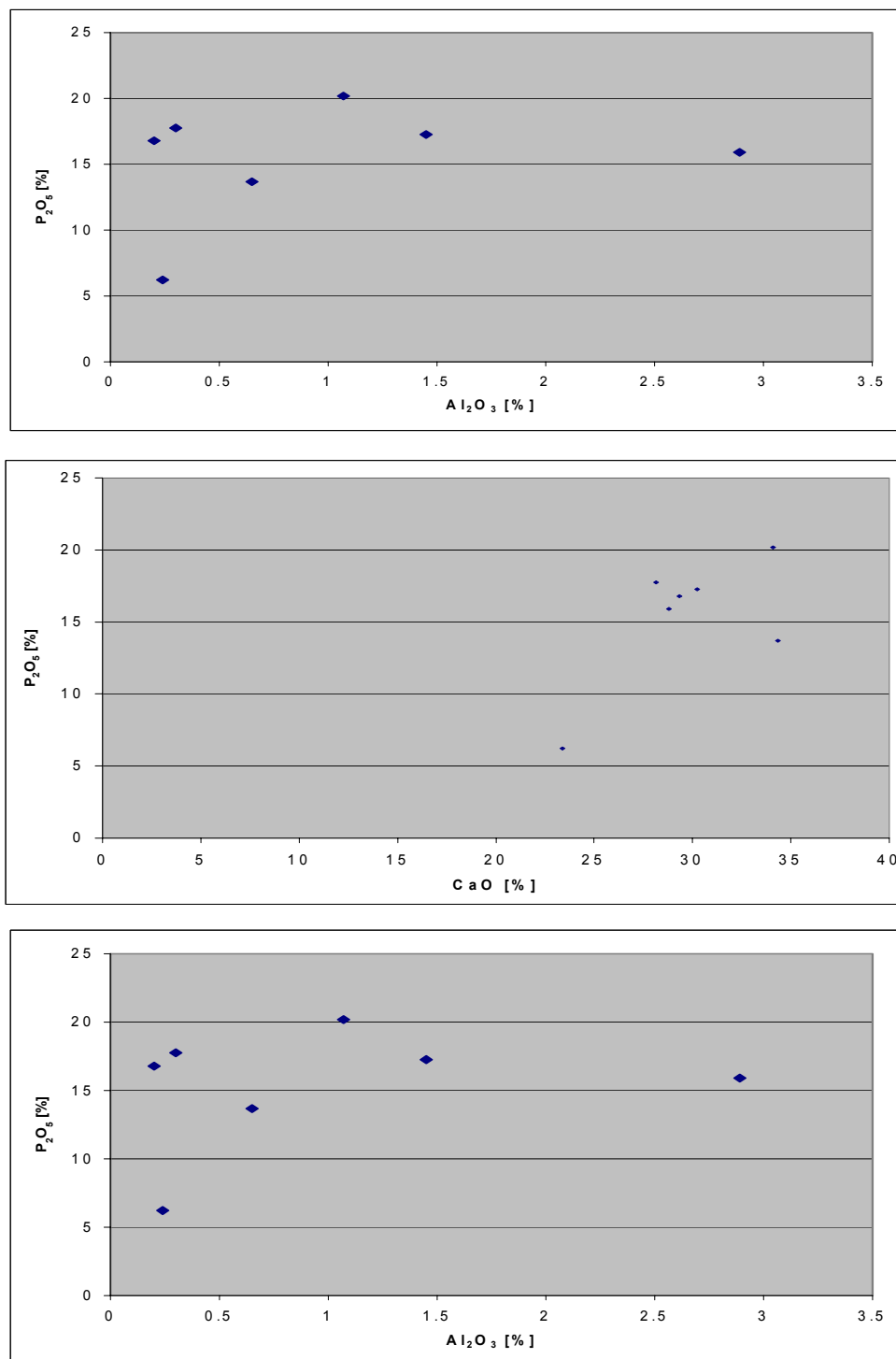


Fig. 18: The relationship between P_2O_5 with TiO_2 , CaO & Al_2O_3

6- Petrography and SEM investigations

Mudrocks are fine-grained sedimentary rocks consisting mostly of silt and clay. Mudrocks sometimes called argillite. Because of their small grain size, mudrocks are difficult to study, even with the petrographic microscope. The importance of the mudrocks is based on their abundance, making up over 65% of all sedimentary rocks; further mudrocks are the source rocks for petroleum and natural gas, and are sometimes valuable ore deposits.

Classification of mudrocks is mainly based on observations in the field or at the level of hand specimen. The classification of mudrocks depends on the mudrock texture which includes, the fissility or the lack of fissility, and laminations mainly based on the grain size of the minerals making up the rock. The fissility of mudrock is depending on several factors, including the abundance, the degree of preferred orientation, and the recrystallization of clay minerals. Fissility is caused by the tendency of clay minerals to be deposited with their sheet structures [(001) crystallographic planes] parallel to the depositional surface. A fissile rock tends to break along sheet-like planes that are nearly parallel to the bedding planes.

The more clay minerals contained in the rock, the more likely the rock is to be fissile. Small clay minerals tend to adhere to one another if they collide during transport. This tendency is promoted by increased salinity of the water and the presence of organic matter in the water. Adhesion of small mineral grains is referred to as flocculation. If the clay minerals flocculate, then they are less likely to have a preferred orientation, and thus less likely to form rocks with fissility. If the clay minerals recrystallize during diagenesis, they will tend to do so with a preferred orientation with their (001) crystal planes oriented perpendicular to the maximum principal stress direction. This process also results in slaty cleavage and foliation in metamorphic rocks. If diagenesis occurs shortly after deposition, then it is likely that the maximum principal stress direction will also be oriented perpendicular to the bedding planes. The bioturbation of organisms within or on the surface of the sediment can disturb the preferred orientation of clay minerals, and thus lead to a non-fissile rock.

Laminations are parallel layers less than 1 cm thick. Such laminations can represent differences in grain size of the clastics in different laminae due to changes in current velocity of the depositing medium, or could be due to changes in the organic content and oxidation conditions at the site or time of deposition of the different layers.

Most mudstones fall into two classes in terms of their color. Gray to black color usually indicates the presence of more than 1% organic matter in the form of carbon or some carbon compound. Red, brown, yellow, and green colorations of mudrocks are a reflection of the oxidation state of Fe in the sediments. Under oxidizing conditions most of the Fe will be Fe^{+3} and give the sediment a red coloration as in hematite.

The petrographical investigation in the present work is mainly concerned with defining the mineralogical composition, texture, matrix and diagenesis which can be described and observed under the polarizing microscope. Most of the studied shales are exceedingly uniform in composition, relatively fissile and don't show bioturbation (burrows etc.). The Abu Zinema samples of Carboniferous age, Al Maghara coal mine samples of Jurassic age and both Abu Tartur phosphate mine and the lower part of Nile valley samples of Maastrichtian age are almost completely lacking fossils, while Quseir phosphate mines and the upper part of the Nile Valley section samples of Late Maastrichtian to Early Eocene age are rich in foraminiferal tests. The petrographical investigations of the studied carbonaceous shales and associated sediments reveal the following lithofacies:

6.1 Organic matter-rich black shale facies

This facies shows a dark gray to black colour. It is dominant in the black shale of Ataqa Formation of Carboniferous age at Abu Zinema, Safa Formation of Jurassic age at Al Maghara coal mine and Duwi Formation of Upper Cretaceous age at Abu Tartur phosphate mine. In thin sections, Ataqa Formation samples are composed of silty to sandy claystone, brownish in colour, carbonaceous, nonfissile, bioturbated, and nonfossiliferous. The quartz grains are of silt size grading into fine sand, angular to subangular, and are poorly sorted Appendix (Plate 1 A). This may reveal a rapid burial of the sediments during the time of deposition in lakes or lagoons with prevailing reducing conditions which leads to preservation of carbon and carbon compounds in rocks. The angular quartz grain shape in this facies indicates a near source area. Safa Formation samples are composed mainly of brown claystone, ferruginous, non fossiliferous, wisps of kerogen and dark organic matter filled burrows, wavy laminae and bioturbation Appendix (Plate 1 B). The oriented texture and disrupted shale lamination indicate bioturbation as the dominant fabric forming process during the deposition of this facies (Neal et al. 1998). This may indicate that Safa Formation was deposited in lagoons adjacent to the coastline. The black shale of Carboniferous and Jurassic age of Ataqa Formation at Abu Zinema and of Safa Formation at Al Maghara coal

mine may have been deposited in reducing conditions. Reducing conditions usually occur in stagnant water where little circulation takes place. This can occur in restricted aquatic environments, like swamps, lakes or lagoons.

The SEM investigations show that kaolinite is the dominant clay mineral in the studied shales of Ataqa Formation at Abu Zinema and of Safa Formation at Al Maghara coal mine as it was also identified by XRD. The SEM observations show swirly textures with face to face arrangement of coarse detrital kaolinite Appendix (Plate 2 A), suggesting a detrital origin (Keller 1978; Manju et al 2001). Furthermore, kaolinite occurs as discrete, poorly crystallized clasts with angular or irregular geometry, an indication that reworking has taken place Appendix (Plate 2 B). The characteristic vermicular and booklet shape of authigenic kaolinite, as well as the blocky crystals of diagenetic kaolinite, are completely absent.

In diagenesis, the morphology of kaolinite changes from vermicular or aggregates of books to individual blockier crystals (Ehrenberg et al. 1993). In the studied shales there is no evidence for the role of diagenesis in the formation of clay minerals.

In thin section it is shown that the Duwi Formation is composed of brownish, ferruginous, nonfissil, nonfossiliferous, and massive claystone Appendix (Plate 3 A). The SEM observations show that smectite is the dominant clay mineral in the studied shales of Abu Tartur phosphate mine samples, Quseir phosphate mine samples and the Nile Valley section. Generally, all the smectite group minerals are characterized by extremely fine-grained, poorly defined particles, with diffuse outlines and curled edges. The montmorillonite particles can be regarded as aggregates a foliated and lamellar aggregate structure also addressed as (papery structure) (Plate 3 B). This may be the result of the expulsion of water and gas during the compaction and oxidation of organic matter see also (Keller et al. 1986).

Pyrite is very dominant in the black shales of Abu Tartur phosphate mine samples. The pyrite is found as disseminated particles, crystals, clusters globular framboids, irregular masses, bands and small nodules. The most common forms of pyrite observed under the SEM are framboidal and euhedral crystals or masses Appendix (Plate 4 A&B). These two textural forms are related to the availability of iron within the sediment, which control the trace element composition of these sediments. The formation of framboids can only be related to the abundance of carbonaceous matter intimately mixed with the detrital iron and preserved under the strongly anoxic stratified water column which is necessary for sulphide formation. Moreover, the dominant occurrence of the framboids, particularly the clustered forms, in

organic-rich shales tends to indicate a biogenic origin as a consequence of the bacterial reduction of seawater sulphate (Berner 1982). This process cannot take place in the presence of dissolved oxygen, because the bacteria that accomplish it are obligate anaerobes. In most pelagic sediments either dissolved oxygen is present, or there is so little reactive organic matter that sulphate reduction does not take place and consequently, no pyrite forms (Berner 1981).

Thus, the studied highly pyritic shales from Abu Tartur must have formed under euxinic conditions at which H_2S exists above or at least at the sediment water interface. The presence of H_2S in turn, will react with Fe^{2+} which was probably delivered into the basin as colloidal material adsorbed on clay minerals to form iron sulphide. By increasing activity of the hydrogen sulphide in presence of iron and organic matter, a hydrophobic sulphide might have been formed (El-Dahhar 1987). As a result of the biological activity, precipitation of sulphide around bacteria in the gel will promote the development of pyrite globules rather than other forms. Preservation of the framboids from further deformation is accomplished partly by precipitation of an inorganic sheath-like envelope due to a slight increase of acidity (McBain 1954).

6.2 Foraminifera-rich shale facies

This facies is characterized by the presence of foraminifer's shells (Appendix, Plate 5 A&B). This facies rarely shows any sedimentary structure other than bioturbation, and sometimes microlamination; the latter is usually flexed around foraminiferal tests. This may reveal that these foraminiferal tests were deposited in situ, in calm water conditions. The foraminifer's shells are scattered throughout the matrix. The matrix is composed of clay (mainly smectite and traces of kaolinite) and organic matter. Detrital quartz is relatively uncommon and iron oxides may be present within the foraminifer's tests and as pore fillings. This facies characterises the Dakhla Shale samples at Quseir phosphate mines and both Dakhla and Esna Shale at the Nile Valley section. The abundance of planktonic foraminifera in this facies gives evidence of a marine environment of deposition.

6.3 Carbonate facies

The carbonate lithofacies can be subdivided into bioclastic limestone and chalky limestone. Bioclastic limestone usually caps the underlying shales and phosphatic rocks at Quseir phosphate mines and Esna-Idfu at Nile valley. It consists mainly of oyster shell fragments,

and few foraminiferal tests embedded in a micritic, microsparitic or sparitic matrix (Appendix, Plate 6 A) in Particular oyster limestone bed in Quseir is very rich in oyster fossils. The depositional regime in the bioclastic subfacies is revealed by the presence of micritic carbonate pellets and fossil fragments. This association may reflect a high energy marine environment (Longmann1980).

The chalky limestone subfacies is mainly represented by the Tarawan Chalk which overlies Dakhla Shale and underlies Esna Shale at the Nile Valley section. It is composed mainly of chalky, fossiliferous limestones, of micritic, microsparitic or sparitic texture (Appendix, Plate 6 B). Foraminiferal tests are embedded in the micritic matrix and sometimes filled with iron oxide (hematite).The presence of sparite in micritic ground mass in this subfacies reflects a marine environment with normal salinity, low energy and a considerable distance from the land mass (Dunham 1962).

6.4 Phosphatic facies

The term phosphorite is applied to rocks containing more than 18 % P_2O_5 (Kolodny1981; Slansky 1986). The petrography of phosphate is based on three categories: grains (coated and uncoated), biophases (bone fragments and fish teeth), and matrix. Apatite is the main constituent in the phosphorite beds in Abu Tartur phosphate mine, Quseir phosphate mines and in the Duwi Formation at the Nile Valley section. The apatite is represented by peloids (coated and non-coated grains), microfossils, microsphere aggregates and sometimes as megafossils, bone fragments and fish remnants (Appendix, Plate 7 A, B&C). Uncoated grains are predominant and represent about 80% of the phosphatic grains. The grains are oval, elongated or irregular shaped.

The coated grains represent about 10 % of the phosphatic grains. They are characterised by inorganic or biogenic nuclei surrounded by a cortex, various layers of phosphatic coatings. The biophases concentric mainly of bone fragments of different forms. The matrix consists of carbonate, silica or carbonate - silica matrix. Selley (1988) stated that the bulk of the world's bedded phosphates occur in the famous phosphate belt which stretches from Syria through the Levant, Sinai, Egypt, Morocco and into Mauritania. These phosphates resulted from the upwelling of oceanic currents from the Tethys onto the broad continental shelves along its southern shore. The optimum depth for phosphate formation is 30–200m. Based on morphological arguments, apatite particles in both modern and ancient phosphorite have been

interpreted as phosphatized bacteria. It is established that microorganisms participate in the precipitation of a spectrum of minerals in aquatic environments (Simkiss and Wilbur 1989; Mclean and Beveridge 1990). The studied phosphate samples show that the phosphatic beds vary in composition from one area to the other. This may indicate a basically shallow water depositional environment, which was influenced periodically by both marine conditions and terrigenous influx.

7 Organic Geochemistry

7.1 Total organic carbon (TOC) content

High primary production of coastal waters, a stratified water column, anoxic bottom waters, low influx of clastic material (low dilution), and high supply of terrestrial organic matter may promote the formation of organic carbon-rich sediments (Calvert and Petersen 1992; Meyers 1997). Favorable conditions for the formation of argillaceous, organic carbon-rich sedimentary rocks, so-called black shales, are best known from the mid-Cretaceous where most of our present-day petroleum reserves were generated (Larson 1991; Langrock et al. 2003). Geological evidence indicated that organic-rich sediments could be deposited even in an open shelf until the early Paleozoic period, but they could be deposited only in a hydrologically isolated basin afterwards (Klemme and Ulmishek 1991). This change in the history of geological age is attributed to the evolution of benthic animals and bacteria (Klemme and Ulmishek 1991) and/or the increase of dissolved oxygen in the ocean (Berner and Canfield 1989).

The higher enrichment of organic matter in sediments is also one of the criteria for the identification of oil and gas source rocks. Various recent reviews have been published on preservation of organic-rich source beds (e.g. Brooks 1981; Daly and Edman 1989; Heydari et al. 1997; Tissot and Welte 1984). Preservation of the organic matter is controlled by conditions such as bottom water circulation rates, degree of oxygenation of bottom water, deposition rates, supply rate of terrestrial organic matter from the continents, and productivity in the surface water. Change in these factors creates highly variable quantities of organic carbon.

The organic carbon analyses in the study consist of 27 shale samples from the five areas. The total organic carbon (TOC) data for the analysed samples are given in figure 19.

The amount of organic matter is variable from location to location according to the type of shale and their characteristic attributes. The black shale samples from Ataqa Formation of Carboniferous age recorded TOC values of 1.58 %, 1.65 % and 2.4 %. The Safa Formation black shale samples of Jurassic age gave the highest values: 4.13 %, 4.36 % and 4.52 %. These high TOC values of both formations may be related to the association of this black shale with coal beds. On the other hand the black shale of Duwi Formation of Cretaceous age which is associated with phosphate beds in Abu Tartur and Quseir show variable values ranging from 0.41% to 1.84 % TOC in Abu Tartur and 2.29 % to 2.92 % TOC in Quseir.

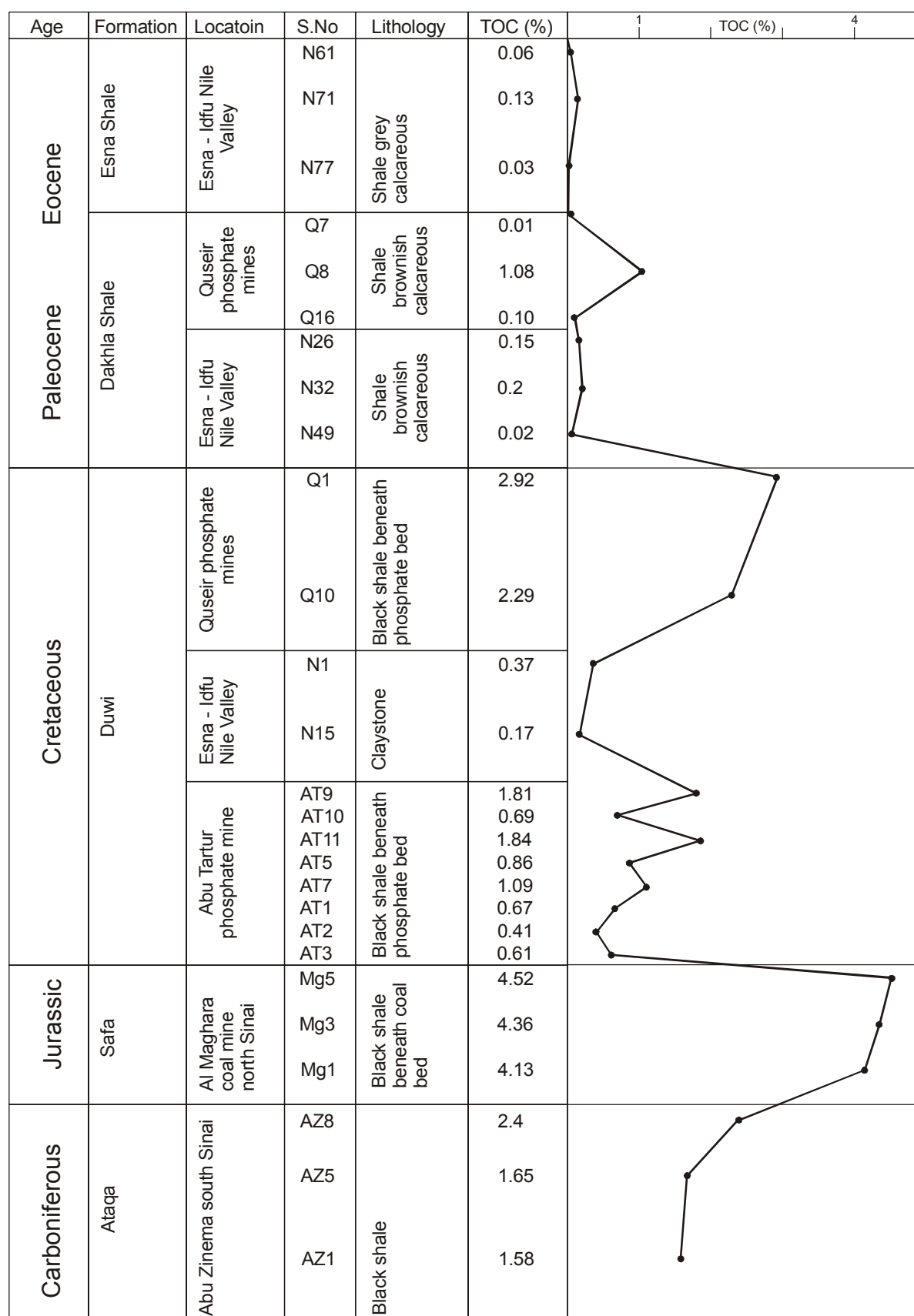


Fig. 19: Stratigraphic position of the studied shales and composite TOC (%) profile (vertically not to be scaled)

The obtained values in Dakhla Shale and Esna Shale from the Nile Valley show very low values of less than 0.5%. This indicates the oxydization of organic matter in these formations in the outcrops.

7.2 Rock-Eval pyrolysis

Rock-Eval pyrolysis provides information on the quantity, type and thermal maturity of the associated organic matter as well as its hydrocarbon potential. Details of the analytical methods have been reported by Espitalie (1977), Tissot and Welte (1984) and Peters (1986). In Table 4 Rock-Eval pyrolysis results for 10 bulk rock samples are listed.

Table 4: The TOC and Rock-Eval results of the studied shales

	Location	APT ID	S1 (mg/g)	S2 (mg/g)	S3 (mg/g)	Tmax (°C)	PP (mg/g)	PI (wt ratio)	HI (mg HC/ g TOC)	OI (mg CO ₂ / g TOC)	TOC (%)
AT10	Abu Tartur	23580	0.01	0.18	0.49	418	0.19	0.06	25	68	0.72
AT11		23581	0.03	0.91	1.41	431	0.94	0.03	44	68	2.06
AT7		23582	0.02	0.84	0.42	425	0.86	0.02	75	38	1.12
AT1		23583	0.03	0.25	0.43	424	0.28	0.10	37	64	0.67
AT3		23584	0.01	0.09	0.35	418	0.10	0.09	15	57	0.61
Q1	Quseir	23585	0.05	1.12	1.56	425	1.16	0.04	41	57	2.72
Q10		23586	0.03	1.10	0.21	412	1.13	0.03	98	19	1.12
Mg1	Al Maghara	23587	0.10	6.23	0.45	427	6.33	0.02	113	8	5.51
Mg3		23588	0.18	10.21	1.36	432	10.38	0.02	195	26	5.24
Mg5		23589	0.15	7.73	2.60	432	7.88	0.02	161	54	4.79

The hydrogen index (HI) vs. oxygen index (OI) diagram is shown in Figure 20 indicating the main types of organic matter of the different formations. These indices can often be directly related to the atomic can H/C and O/C ratios, and interpreted in the same way as a van Krevelen diagram (Espitalie 1977; Tissot and Welte 1984). Most of the samples are scattered in type III kerogen. Very low HI of 25 to 98 mg HC/g TOC and relatively low to medium OI of 19 to 68 mg CO₂/g TOC are observed for the Duwi Formation samples of Abu Tartur and Quseir phosphate mines. On the other hand samples of Safa Formation of Al Maghara coal

mine show low HI of 113 to 195 mg HC/g TOC and very low OI of 8 to 54 mg CO₂/g TOC. These low HI values of less than 195 mg HC/g TOC is due to bad preservation of organic matter.

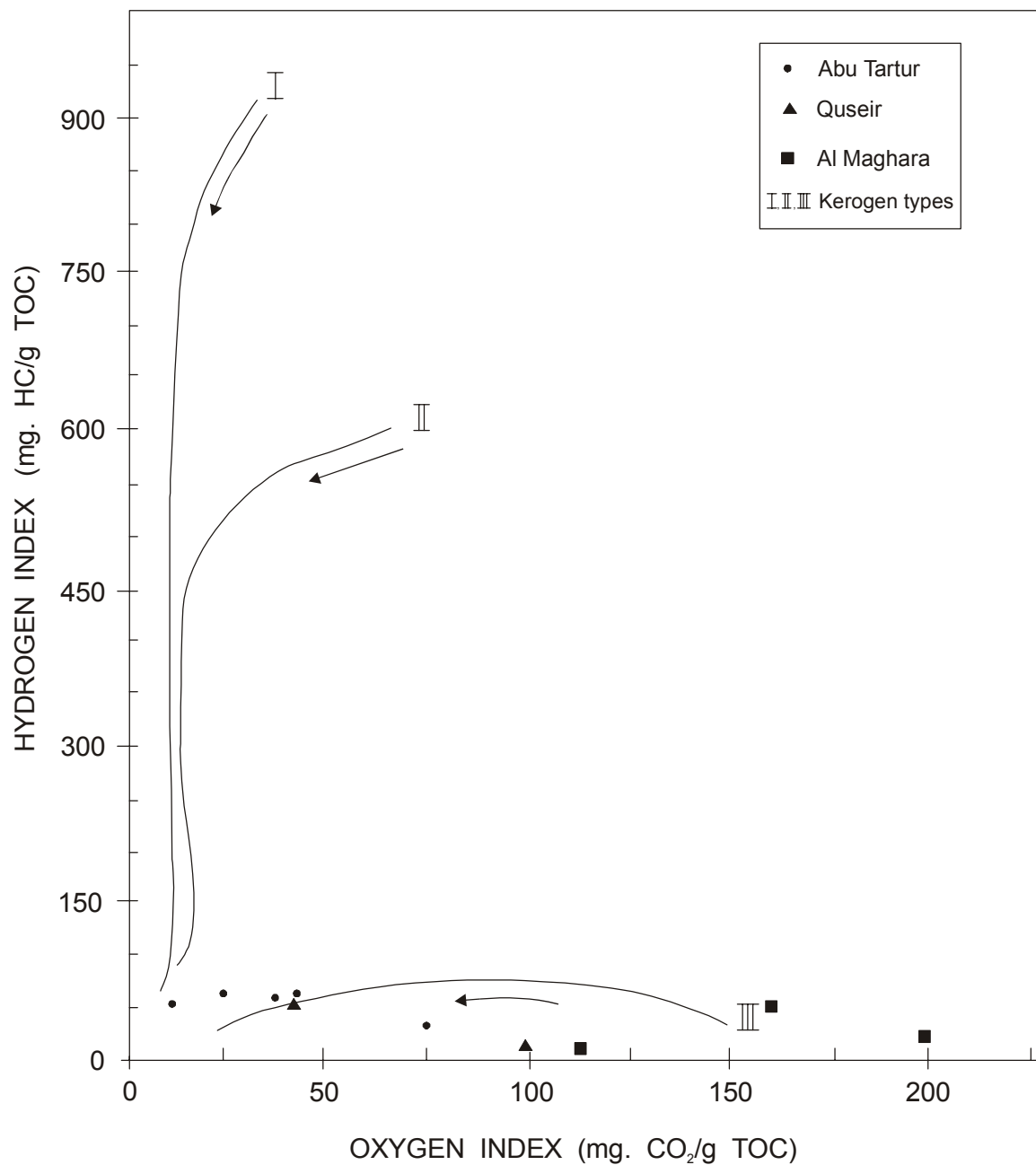


Fig. 20: Van Krevelen-type plot of Rock-Eval data for the studied bulk samples.

7.2.1 Hydrocarbon source potentials

The hydrocarbon genetic potential (PP) in mg/g is determined from the sum of (S_1+S_2) peaks. The PP values of the Duwi Formation in Abu Tartur range from 0.1 to 0.94 mg/g and 1.13 to 1.16 mg/g in Quseir. The Duwi Formation therefore displays values below typical average hydrocarbon yields of source rocks >2.5 mg HC/g rock (Tissot and Welte 1984). Whereas the samples of Safa Formation in Al Maghara coal mine show values in hydrocarbon yields of 6.33 to 10.88 mg/g rock.

7.2.2 Determination of thermal maturity (T_{max})

The determination of the degree of maturity of the sedimentary organic matter is an essential parameter in order to characterise a petroleum source rock. It is the main cause of hydrocarbon generation and transformation. The T_{max} is the temperature at the maximum point of the S_2 peak, used in Rock-Eval pyrolysis. The studied samples of Duwi Formation in Abu Tartur and Quseir phosphate mines, as well as samples of Safa Formation in Al Maghara coal mine are immature with T_{max} values between 412-432 °C. This low T_{max} value indicates that the organic matter has not generated a substantial amount of hydrocarbon. This result is in correspondence with the T_{max} value of 428 °C obtained by Mostafa and Younes (2001) for the Safa Formation in the Al Maghara coal mine.

8 Summary and Conclusions

The present investigation comprises insights in the mineralogical and geochemical composition of carbonaceous shales from the different geological ages and areas of Egypt.

The study is concerned mainly with:

- 1- the black shale of Ataqa Formation of Carboniferous age in Abu Zinema southwest Sinai,
- 2- the black shale of Safa Formation of Jurassic age in Al Maghara coal mine North Sinai,
- 3- the black shale of Duwi Formation of Upper Cretaceous age in Abu Tartur phosphate mine, Western Desert,
- 4- the carbonaceous and black shales of Duwi Formation, Dakhla Shale and Esna Shale in the Nile Valley area,
- 5- and the black and carbonaceous shales of Duwi Formation and Dakhla Shale in Quseir phosphate mine at Red Sea coast

Mineralogically, the clay minerals of the Ataqa Formation are consisting predominantly of kaolinite with a minor part of illite while the Safa Formation clays consist mainly of detrital kaolinite. The clay minerals of the Duwi Formation in Abu Tartur consist mainly of smectite in addition to different proportions of kaolinite in Quseir and Nile Valley. The Dakhla and Esna shales in Nile Valley consist predominately of smectite in addition to different proportions of kaolinite and chlorite.

The chemical composition of the studied shales shows generally enrichment of elements that are chemically immobile and associated with terrigenous influx, such as SiO_2 , Al_2O_3 , and TiO_2 . The Ataqa and Safa formations show enrichment of zirconium and depletion in CaO which reveals the proximity to the land. On the other hand the studied shales in Abu Tartur, Nile Valley and Quseir show enrichment of CaO.

The studied phosphate samples show enrichment in P_2O_5 , CaO and fluor, which reveal that fluor apatite is the main phosphate mineral in Egyptian phosphate. The low content of detrital terrigenous influx SiO_2 , Al_2O_3 , TiO_2 and Rb, and the association of the phosphate beds with oyster limestone and diatom enrichment in Quseir and in the Nile Valley is indicating the deeper marine origin of the phosphates in the Eastern part of Egypt. The deposition of the phosphatic beds associated with black shales clearly demonstrates a diachronous transgression from the east to the west, starting in the Eastern desert during Lower campanian and culminating in Upper Campanian and Lower Maastrichtian, covering both, the East and the West, from Quseir, via the Nile Valley towards the Abu Tartur depositional centre.

The distribution of many trace elements has been affected by weathering. The studied shales in Abu Tartur, Quseir and Nile Valley show higher contents of the trace elements Sr, Ba, V, Ni, Cr, Zn, and Rb than shale samples from Abu Zinema and Al Maghara. The Dakhla Shale in Quseir mine shows the highest enrichment of V, Ni, Cr, Zn, and Cu due to the oxidation and weathering of organic matter and subsequent mobilization and concentration of these trace elements. The low trace elements enrichment in the studied phosphate samples indicates leaching processes outgoing from the overlain black shales.

Petrographically the study samples reveal the presence of four lithofacies namely;

- 1- Organic matter-rich black shale facies,
- 2- Foraminifera-rich shales facies,
- 3- Carbonate facies,
- 4- and phosphate facies.

The depletion of Ataqa Formation of Carboniferous age, Safa Formation of Jurassic age and Duwi Formation, in foraminifera and their dark colour as well as the presence of pyrite framboids in Duwi Formation reveal reducing environment of deposition.

The abundance of foraminifera in Dakhla Shale and Esna Shale in Quseir and the Nile Valley give evidence for an oxidation environment of deposition in middle to inner shelf positions.

The phosphate samples in Abu Tartur show pelloids of P_2O_5 cemented by carbonate, while the phosphates in the Nile Valley are cemented by silica, an indication for more open marine conditions to the East.

The SEM micrographs show that the kaolinite in Ataqa and Safa formation is of swirly textures with face to face arrangement of coarse detrital kaolinite.

The smectite in Duwi Formation in Abu Tartur show papery structure. The most common forms of pyrite are framboidal and euhedral or masses. There are indications that the trace elements composition of these sediments is influenced by pyrite.

The total organic carbon (TOC) analysis shows high values in the black shales of Safa Formation of Jurassic in Al-Maghara, Ataqa Formation of Carboniferous in Abu Zinema and Duwi Formation of Cretaceous in Abu Tartur and Quseir. The obtained values in Dakhla Shale and Esna Shale show very low values indicating the oxidation of organic matter in outcrop.

The Rock-Eval pyrolysis of the studied shales show that, most of the studied samples are of type III kerogen with low hydrogen index HI due to bad preservation of organic matter. The thermal maturity T_{max} values of the studied shales indicate immature organic matter for hydrocarbon generation.

9 References

- Abdallah, A. M. and A. Adindani (1963):** Stratigraphy of upper Paleozoic rocks, western side of Gulf of Suez. Geol. Surv. Egypt, Paper 25, 18pp.
- Abd El-Hameed, A.T. (1997):** Sedimentology and geochemistry of the subsurface Jurassic Rocks in the North Western Desert, Egypt. Egyptian J. Geol. 41, 225-252.
- Abdel Razik, T.M. (1967):** Stratigraphy of the sedimentary cover of Anz Atshan South Duwi District. Bull. Fac. Sci., Cairo Univ., No. 41, pp 153-179.
- Abdel Razik, T.M. (1970):** Geological microfacies studies on the Upper Cretaceous-Lower Eocene Formation in East Qena area, Eastern Desert, U.A.R.: Ph.D. Thesis, Cairo Uni., 422 pp.
- Abdel Razik, T.M. (1972):** Comparative studies on the Upper Cretaceous Early Paleocene sediments on the Red Sea Coast, Nile Valley and Western Desert, 8th Arab Petrol. Cong. Algiers. Paper 71 (B-3), 23pp.
- Abdou, N.M.F. (1989):** Petrology and Geochemistry of some subsurface Cretaceous Rocks in the Northern part of the Western Desert, Egypt. - M.Sc. Thesis, Al-Azhar Univ. Cairo, Egypt.
- Abdul Mannan (2002):** Stratigraphic evolution and geochemistry of the Neogene Surma Group, Surma Basin, Sylhet, Bangladesh. Ph.D. Thesis University of Oulu.Oulu Finland 2002
- Abed, A.M. and Amireh, B.S. (1983):** Petrology and geochemistry of some Jordanian oil shales from north Jordan. J. Petrol. Geol., 3, 261 – 274.
- Ahmed H. A. (1997):** Mineralogical and geochemical studies of the black shales intercalated with phosphorite deposits at Abu Tartur area Western Desert, Egypt, M.Sc. thesis, Ain Shams Uni. Cairo, Egypt, 284p.
- Al Far, D.M. (1966):** Geology and coal deposits of Gebel Maghara, north Sinai. Geol. Surv. Egypt. Paper 37, 59pp.
- Amajor, L.C. (1987):** Major and trace elements geochemistry of Albin and Turonian shales from the Southern Benue trough, Nigeria J. Afr. Earth Sci., 6, pp 633 – 461.
- Angus, J.C., Raynor, J.B. and Robson, M. (1979):** Reliability of experimental partition coefficients in carbonate systems: evidence for inhomogeneous distribution of impurity cations. Chem. Geol., Amsterdam, 27, 181-205.
- Arkell, W.J. (1956):** Jurassic geology of the world. Oliver & Boyd, London, 806pp.
- Awad, G.H. and Ghobrial, M.G. (1965):** Zonal stratigraphy of the Kharga Oasis, Geol. Surv., U.A.R., paper No. 34, 77 pp.

- Bain, D.C. and Smith, B.F.L. (1987):** Chemical Analysis; In: A Handbook of Determinative Methods in Clay Mineralogy, WILSON, M.J. (Ed). pp 248-274.
- Ball, J. (1913):** A brief note on the phosphate deposits of Egypt. Geol. Surv. Rep., Cairo.
- Ball, J. (1916):** The geography and geology of west central Sinai, Egypt. Survey Dept., Cairo, 219 p.
- Barakat, M.G. (1970):** A stratigraphic review of the Jurassic formations in Egypt and their oil potentialities. 7th Arabian Petroleum Congress, Kuwait.
- Barron, T. and Hume, W.F. (1902):** Notes on geology of the Eastern Desert of Egypt, Dulau and Co., London, 42 pp.
- Barthoux, J.C. & H. Douville (1913):** Le Jurassique dans le desert a l'isthme de Suez. C.R. Soc. Geol. France 157: 265-268.
- Beadnell, H.J.L. (1905):** The relation of the Eocene and Cretaceous systems in the Esna-Aswan stretch of the Nile Valley. - Quart. J. Geol. Soc. London, V. 61, pp 667-676.
- Berner, R.A. (1981):** Authigenic mineral formation resulting from organic matter decomposition in modern sediments. - Fortschr. Mineralogie, 59, 117 – 135.
- Berner, R.A. (1982):** Burial of organic carbon and pyrite sulfur in the modern ocean: its geochemical and environmental significance. *Am. J. Sci.*, 282, 451 – 473.
- Berner, R.A. and Canfield, D.E. (1989):** A new model for atmospheric oxygen over Phanerozoic time. *Am. Jour. Sci.* **289**, 333-361.
- Bliskovsky, V.Z., Yefimova, V.A. and Romanova, L.V. (1967):** The strontium content of phosphorites. *Geochem. Int.*, 4, 1186-1190.
- Bloch, J., Hutcheon, I.E., and Carital, P.D. (1998):** Tertiary volcanic rocks and the potassium content of Gulf Coast shales- The smoking gun. *Geol.* **26**: 527-530.
- Brooks, C.K. (1973):** Rifting and doming in Southern East Greenland, *Nature (London)*, **V.** 244, pp 23-24.
- Brooks, J. (1981):** Organic maturation of sedimentary organic matter and petroleum exploration: a review. In: Brooks, J. (ed.), Organic maturation studies and fossil fuel exploration, 1-37, London and New York (Academic Press).
- Brumsack, H.J. (1980):** Geochemistry of Cretaceous black shales from the Atlantic Ocean (DSDP Legs 11, 14, 36 and 41). *Chem. Geol.*, 31, 1-25.
- Calvert, S.E., and T.F. Petersen (1992):** Organic carbon accumulation and preservation in marine sediments: How important is anoxia?, in *Organic Matter: Productivity, Accumulation, and Preservation in Recent and Ancient Sediments*, edited by J. K. whelan and J.W. Farrington, 533 pp., Columbia Univ. Press, New York.
- Chamley, H. (1989):** Clay Sedimentology. Heidelberg, Springer – Verlag, 623 p.

- Cody, R.D. (1971):** Adsorption and the reliability of trace elements as environment indicators for shales. - J. Sed. Petrol., **41**, 461-471, Tulsa.
- Cook, P.J. (1972):** Petrology and geochemistry of the phosphate deposits of northwest Queensland, Australia. - Econ. Geol., **67**, 1193-1213.
- Cook, P.J. (1984):** Spatial and temporal controls on the formation of phosphate deposits - a review – In: NRIAGU, J.O. and MOORE, P.B. (eds.): Phosphate Minerals. - 242-274, Berlin-Heidelberg-New York (Springer).
- Cullers, R.L. (2000):** The geochemistry of shales, siltstones and sandstones of Pennsylvanian-Permian age, Colorado, USA: implications for provenance and metamorphic studies. Lithos, **51**, 181-203.
- Daly, A.R. and Edman, J.D. (1989):** Loss of organic carbon from source rocks during thermal maturation. AAPG Bull., 71, 546, Tulsa.
- Darwish, M. (1984):** Optimistic hydrocarbon potentialities of the oil shales in the Quseir-Safaga land stretch, Egypt. Bull. Fac. Sci., Zagazig Univ., Zagazig, **5**, 409-419.
- Degens, E.T. (1965):** Geochemistry of sediments: A brief survey Prentice-hall, New Jersey.
- Degens, E.T., Williams, E.G. and Keith, M.L. (1957):** Environmental studies of Carboniferous sediments, Part I. Geochemical criteria for differentiating marine from fresh-water shales. - Am. Ass. Petrol. Geol. Bull., **41**, 2427-2455, Tulsa.
- Dill, H., Teschner, M. and Wehner, H. (1988):** Petrography, inorganic and organic geochemistry of Lower Permian carbonaceous fansequences ("Brandschiefer Series") Federal Republic of Germany: constraints to their paleogeography and assessment of their source rock potential. Chem. Geol. **67**, 307-325.
- Dominic, E. and Andrew, R. (1993):** Inorganic Geochemistry, Application to Petroleum Geology – Text book
- Dominik, W. (1985):** Stratigraphie und Sedimentologie (Geochemie, Schwermineralanalyse) der Oberkreide von Bahariya und ihre Korrelation zum Dakhla Becken (Western Desert, Ägypten).- Berliner Geowiss. Abh. (A), **62**, 173pp, Berlin.
- Dominik, W. and Schaal, S. (1984):** Notes on the stratigraphy of Cretaceous phosphorites (Campanian) of the Western Desert, Egypt, Berl. Geowiss. Abh. (A), V 50, pp 153-175.
- Dunham, R. J. (1962):** Classification of carbonate rocks according to depositional texture. In: Ham (ed.) Classification of carbonate rocks. AAPG. Mem., 1 p. 108-121, Tulsa.
- Ehrenberg, S.N., Aagaard, P., Wilson, M. J., Fraser, A.R. and Duthie, D. M.. L. (1993):** Depth-dependent transformation of kaolinite to Dickite in sandstones of the Norwegian continental shelf. - Clay Minerals 28, 325- 352.

- Ehrmann, W.U., Melles, M., Kuhn, G., and Grobe, H. (1992):** Significance of clay mineral assemblages in the Antarctic Ocean: marine Geology, V. 107, p. 249-273.
- El Akkad, S. and Dardir, A (1966):** Geology and phosphate deposits of Wasif, Safaga area. - Geol. Surv. and Min. Res. Egypt., Cairo. Paper No. 36, 35 pp.
- El Kammar, A.M., Darwish, M., Phillip, G. and El Kammar, M.M. (1990):** Composition and origin of black shales from Quseir area, Red Sea coast, Egypt. J. Univ. Kuwait (Science), 17, 177-190.
- El Kammar, M.M. (1987):** Stratigraphical and mineralogical studies on the black shale at Quseir area, Red Sea Coast, Egypt. - M.Sc. Thesis, Cairo Univ., Cairo.
- El Kammar, M.M. (1993):** Organic and Inorganic Components of the Upper Cretaceous-Lower Tertiary Black Shales from Egypt and Their Hydrocarbon Potentialities. - Ph.D. Thesis, Cairo Univ., Egypt.
- El Nagggar, Z.R. and Ashor, M.M. (1983):** Microstratigraphical analyses of the Late Cretaceous Early Paleocene succession in Egypt, typified by Dakhla Nile Valley and Red Sea Coast section. - Proceeding of the first Jordanian Geological conf. pp 112-180.
- El-Anbaawy, M. and Youssef, M.H.M. (1989):** Recognition of diagenetic clay mineral composition in Jurassic rocks of Gebel El-Maghara area, North Sinai, Egypt. - Proc. 5th Phanerozoic Development Egypt Sympos.; pp 35-52, Al-Azhar Univ. Cairo, Egypt.
- El-Ayyat M.A. and Kassab, S.A. (2004):** Biostratigraphy and facies analysis of the Upper Cretaceous oyster strom shell beds of the Duwi Formation, Qusseir District, Red Sea Region, Egypt. J. Afric., Earth Sci., 2004. 07. 024.
- El-Dahhar, M.A. (1987):** Diagenetic pyrite framboids in the phosphate deposits of Abu Tartur area, Western Desert, Egypt. J. Afric., Earth Sci., 6, 807 –811.
- Espitalie, J. Laporte, J.L., Madec, M., Marquis, F., Lelplat, P., Paulet, J. and Boutefeu, A. (1977):** Methode rapide de caracterisation des roches meres de leur potentiel petrolier et de leur degre d, evolution-Inst. Fr. Petr. 32, 23-42, Paris.
- Faris, M.I. and Hassan, M.Y. (1959):** Report on the stratigraphy and fauna of the Upper Cretaceous-Paleocene rocks of Um-El Huetat, Safaga area, Ain Shams Sci. Bull. No. 4, pp 191-207.
- Felix, N.S. (1977):** Physico-chemical studies on bentonites with special reference to Fayoum Deposits, Ph.D. Thesis, Fac. of Sci., Cairo, Univ. Egypt.
- Filipek, L.H. and Owen, R.M. (1981):** Diagenetic controls of phosphorus in outer continental-shelf sediments from the Gulf of Mexico. *Chem. Geol.* **33**, 181-204.

- Filippelli, G.M. (1997):** Controls on phosphorus concentration and accumulation in oceanic sediments. *Mar. Geol.* 139, 231-240.
- Ganz, H. (1984):** Organic geochemical and palynological studies of Dakhla Shale profile, Southeast Egypt. Part B, Origin of the organic matter and its relation to phosphorite formation. *Berliner Geowiss. Abh (A)*, 50, 363-374.
- Ganz, H. (1987):** Geochemical evaluation of hydrocarbon source-rock characteristics and facies analysis. Methods and applications. - *Berliner Geowiss. Abh. (A)*, 75.3, 669-690.
- Garver, J.I., Royce, P.R. and Scott, T.J. (1994):** The presence of ophiolites in tectonic highlands as determined by chromium and nickel anomalies in synorogenic shales: two examples from North America. *Russian Geol. Geophys.* 35, 1-8.
- Garver, J.I., Royce, P.R. and Smick, T.A. (1996):** Chromium and nickel in shale of the Taconic Foreland: A case study for the provenience of fine-grained sediments with an ultramafic source. *J. Sedim. Res.*, **66**, 100-106.
- Germann, K., Bock, W.D., Ganz, H., Schröter, T. and Tröger, U. (1987):** depositional conditions of Late Cretaceous phosphorites and black-shales in Egypt. - *Berl. Geowiss. Abh. (A)*, 75. 3, 629-668.
- Ghandour, I.M., Harue, M. and Wataru, M. (2003):** Mineralogical and chemical characteristics of Bajocian-Bathonian shales, G. Al-Maghara, North Sinai, Egypt: Climatic and environmental significance. *Geochemical Journal*, Vol. 37. pp.87-108, 2003.
- Ghorab, M.A. (1956):** A summary of proposed rock, stratigraphic classification for the Upper Cretaceous rocks in Egypt. Read before the Geol. Soc. of Egypt. April 9th.
- Gibbs, R.J. (1965):** Error due to segregation in quantitative clay mineral X-ray diffraction mounting techniques.- *Amer. Mineral.*, 50, 741- 751, Washington.
- Gill, J. (1981):** Organic Andesites and Plate Tectonics. Springer-Verlag, Berlin, 390 pp.
- Gill, R. (1997):** Modern analytical geochemistry. Wesley Longman, 329p.
- Gindy, A.R. (1983):** Factors controlling the clay mineralogy of Egyptian Phanerozoic mudrocks and marls. *Geol. Jb., B*, 49, 3-25, Hannover.
- Glenn, C.R. (1980):** Stratigraphy, petrology and sedimentology of Duwi Formation Eastern Desert, Egypt, M.Sc. Thesis, California, Santa Cruz.
- Glenn, C.R. and Mansour, S.E.A. (1979):** Reconstruction of the depositional and diagenetic history of phosphorites and associated rocks of Duwi Formation (Late Cretaceous) Eastern Desert, Egypt, *Geol. Surv.*, VIX pp 388-407.

- Goldschmidt, V.M. and Peters, O. (1932):** Zur Geochemie des Bors, Teil I und II.- Nachr. Ges. Wiss. Math. Physik, 402-407, 528-545, Gottingen.
- Gromet, L.P., Dymek, R.F., Haskin, L.A. and Korotev, R.L. (1984):** The "North American Shale Composite": Its compilations, major and trace element characteristics.- Geochim. Cosmochim. Acta, **48**, 2469-2482, London.
- Gulbrandsen, R.A. (1966):** Chemical composition of phosphorites of the Phosphoria Formation. - Geochim. Cosmochim. Acta, **30**, 769-778.
- Gulbrandsen, R.A. (1970):** Relation of carbon dioxide content of Apatite of the Phosphoria Formation to regional facies. - U.S.G.S. Prof. Pap., 700-B, B9 - B13.
- Hallam, A., Grose, J.A. and Ruffell, A.H. (1991):** Paleoclimatic significance of changes in clay mineralogy across the Jurassic-Cretaceous boundary in England and France. - Palaeogeog. Palaeoclimat. Palaeoecol., **81**, 173-187.
- Hassaan, M.M., El Kady, H.H. and Hassan, M.M. (1979):** Geochemical characteristics of Esna Shale and Thebes limestone, Gebel El Gurnah, Egypt. - Abst. In; 5th Conf. African Geol. Surv. Egypt, Cairo.
- Hassan, A.A. (1967):** A new Carboniferous occurrence in Abu Durba, Sinai, Egypt. 6th Arab Petrol. Congr., Baghdad.
- Hendriks, F. (1985):** Upper Cretaceous to Lower Tertiary sedimentary environments and clay mineral associations in the Kharga Oasis area (Egypt). N.Jb. Geol. Palaont. Mh. **10**, 579-591 (Stuttgart).
- Hendriks, F. (1988):** Die Kreide und das Alttertiär in Südostägypten: Sedimentologie und Tonmineralogie eines intrakratonalen Ablagerungsraumes - Berl. Geowiss. Abh. (A), **104**, 129 p. Berlin.
- Hendriks, F., Luger, P. and Strouhal, A. (1990):** Early Tertiary Marine Palygorskite and Sepiolite Neof ormation in SE Egypt. - Z. dt geol. Ges., **141**, 87-97.
- Hendriks, F., Luger, P., Bowitz, J. and Kallenback, H. (1987):** Evolution of depositional environments of SE-Egypt during the Cretaceous and Lower Tertiary. - Berl. Geowiss. Abh., (A), **75**, 49 –82, Berlin.
- Hermine, M.H., Ghobrial, M.G. and Issawi, B. (1961):** The geology of the Dakhla Area. - Geol. Surv. Egypt., 33 p., Cairo.
- Heydari, E., Wade, W. J. and Anderson, L.C.(1997):** Depositional environments, organic carbon accumulation, and solar-forcing cyclicity in Smackover Formation lime mudstones, Northern Gulf Coast. - AAPG Bull, **81**, 760-774, Tulsa.
- Higazy, R. and Hussein, A. (1955):** Remarks on the uranium content of some black shales and phosphates from Quseir and Safaga. - Proc. Egypt. Acad. Sci., **11**, 63 –66.

- Hiscott, R.N. (1984):** Ophiolitic source rocks for Taconic-age flysch: Trace element evidence. *Geol. Soc. Amer. Bull.* **95**, 1261-1267.
- Horowitz, A. (1973):** *Noeggerathia dickeri* n sp. from the Carboniferous of Sinai. - *Rev. Paleobot. and Palyn.* 15: 51-56.
- Hume, W.F. (1927):** The phosphate deposits in Egypt. - *Surv. Dept., Egypt*, paper no. 41, 20p.
- Ibrahim, D.M., Abdel Aziz, D.A., Awad, S.A. and Abdel Monem, A.M. (2004):** Utilization of black shales in earthenware recipes. - *Ceramics International*. V. 30, Issue 6, 2004, P 829-835.
- Ibrahim, H.I. (1992):** Geochemistry and Mineralogy of some Dakhla and Esna Shales South of Egypt. - M.Sc. Thesis, Al-Azhar Univ. Cairo.
- Ingall, E. D. and Van Cappellen, P. (1990):** Relation between sedimentation rate and burial of organic phosphorus and organic carbon in marine sediments. - *Geochim. Cosmochim. Acta*, **54**, 373-386.
- Ismael, S.I. (1996):** Mineralogical and geochemical studies of the black shales intercalated with the phosphate deposits along the Red Sea coast, Egypt. - Ph.D. Thesis Ain Shams Uni. Cairo, Egypt.
- Issawi, B. (1972):** Review of Upper Cretaceous-Lower Tertiary Stratigraphy in central and southern Egypt. - *Am. Assoc. Petrol. Geol. Bull.*, V. 56, No.8, pp 1448-1463.
- Issawi, B. and U. Jux (1982):** Contribution to the stratigraphy of the Paleozoic rocks in Egypt. *Geol. Surv. Egypt*, Paper 64, 28pp
- Issawi, B., El Hinnawi, M., Francis, M. and El Deftar, T. (1971):** Geology of Safaga-Quseir Coastal plain and Mohammed Rabah area. - *Ann. Geol. Surv., Egypt*, V. I., pp 1-19.
- Issawi, B., El Hinnawi, M., Francis, M. and Mehanna, A. (1968):** Contribution to the structure and Phosphate deposits of Quseir area, Egypt, *Geol. Surv.*, paper 50, pp 1-35.
- Jenkins, D., J.C. Harms and T.W. Oesleby (1982):** Mesozoic sediments of Gebel Maghara, north Sinai, ARE. - *6th Petrol. Explor. Seminar, EGPC*, Cairo.
- Jensen, H.S., Mortensen, P. B., Andersen, F.O., Rasmussen, E. and Jensen, A. (1995):** Phosphorus in a coastal marine sediments, Aarhus Bay, Denmark. - *Limnol. Oceanogr.* **40**, 908-917.
- Jeong, G.Y. and Yoon, H.I. (2001):** The origin of clay minerals in soils of King George Island, South Shetland Islands, West Antarctica, and its implications for the clay-mineral compositions of marine sediments. *Journal of Sedimentary Research*, Vol. 71, No. 5, September, 2001, p. 833-842.

- Johns, W.D., Grim, R.E. and Bradley, W.F. (1954):** Quantitative estimation of clay minerals by diffraction methods. - *J.Sed. Petrol.*, 24, 242-251, Tulsa.
- Kamatani, A. and maeda, M. (1989):** Distribution and budget of phosphorus in Tokyo Bay. *Chikyukagaku (Geochemistry)* **23**, 85-95.
- Keller, W.D. (1978):** Classification of kaolins exemplified by their texture in Scan Electron Micrographs. *Clays and Clay Minerals* 26, 161-172.
- Keller, W.D., Reynolds, R.C., JR., and Inoue, A. (1986):** Morphology of clay minerals in the smectite- to -illite conversion series by scanning electron microscopy. - *Clays and Clay Miner.*, 34, 187 –197.
- Khaled, K.A., Abdel Ghany, A.R. and El-Fadly, A. (1987):** Lateral variation of the geochemical characteristics of some oil shale beds in Quseir-Safaga Environs, Eastern Desert, Egypt. The Fourth Symposium on phanerozoic and Development in Egypt. Al-Azhar University, Cairo, Egypt (Abstract).
- Klemme, H.D. and Ulmishek, G.F. (1991):** Effective Petroleum source rocks of the world: stratigraphic distribution and controlling depositional factors. *Amer. Assoc. Petrol. Geol. Bull.* **75**, 1809-1851.
- Klitzsch, E. (1980):** Neue stratigraphische und paläogeographische Ergebnisse aus dem Nordwest-Sudan.-*Berl.geowiss. Abh.*, A. 20, 217-222, Berlin.
- Klitzsch, E. (1983a):** Paleozoic formations and a Carboniferous glaciation from the Gifl Kebir-Abu Ras Area in south-western Egypt. - *J. Afri. Earth Sci.*, 1, 1, 17-19, Oxford.
- Klitzsch, E. (1983b):** Geological Research In and Around Nubia. – *Episodes*, 3, 15- 19, Ottawa, Ontario.
- Klitzsch, E. (1984):** Northwestern Sudan and bordering areas: geological development since Cambrian time. - *Berl. Geowiss. Abh.*, (A) 50, 23-45, Berlin.
- Knauer, G.A. and Martin, J.H.(1973):** Seasonal variation of Cd, Co, Mn, Pb ad Zn in water and phytoplankton in Monterey bay, California.- *Limnol. Oceanogr.*, Milwaukee, 18, 597- 604.
- Kolodny, Y. (1981):** Carbon isotopes ad depositional environment of high productivity sedimentary sequence. The case of the Mishash - Ghareb Formation. - *Israel Isr. J. Earth. Sci.* V. 29, pp 147-156.
- Krauskopf, K.B. (1956):** Factors controlling the concentration of the thirteen rare metals in sea water. - *Geochim. Cosmochim. Acta*, **9**, 1-3, London.
- Langrock, U.R. Stein, M. Lipinski, and H.J. Brumsack (2003):** Paleoenvironment and sea-level change in the Early Cretaceous Barents Sea- Implications from near shore marine sapropels. - *Geo. Mar. Lett.*

- Larson, R. L. (1991):** Geological consequence of superplumes, *Geology*, 19, 963-966.
- Lindgreen, H. and Surlyk, F. (2000):** Upper Permian-Lower Cretaceous clay mineralogy of East Greenland: provenance, paleoclimate and volcanicity. *Clay Minerals* **35**, 791-806.
- Longmann, M.W. (1980):** Carbonate diagenetic textures from surface diagenetic environments. - AAPG. Bull., vol. 64, p. 461- 487.
- Louchouart, P., Lucotte, M., Duchemin, E. and deVernal, A. (1997):** Early diagenetic processes in recent sediments of the Gulf of St-Lawrence: phosphorus, carbon and iron burial rates. *Mar. Geol.* **139**, 181-2000.
- Malak, E.K., Philobos, A. and Ashry, M.M. (1977):** Some petrographical, mineralogical and organic geochemical characteristics of black shales from Quseir and Safaga, Red Sea Area, Egypt. *Desert Inst. Bull. ARE*, 27, 1 - 15.
- Manju, C.S., Narayanan Nair, V. Lalithambika, M. (2001):** Mineralogy, geochemistry and utilization study of the Madayi kaolin deposits, North Kerala, India. - *Clays and Clay Minerals* **49**, 355- 369.
- McBain, J.W. (1954):** Colloidal Science. D. C.
- McConnell, D. (1973):** Apatite, its crystal chemistry, mineralogy, utilization, and geologic and biologic occurrences. Springer – Verlag, Wien –New York, p. 111.
- Mclean, R.J.C. and Beveridge, T.G. (1990):** Metal-binding capacity of bacterial surfaces and their ability to form mineralized aggregates. In: *Microbial Mineral Recovery* (Ed. by H.HRLICH and C.L. BRIERLY), McGraw-Hill, New York, 185-222.
- McLennan, S.M. (1993):** Weathering and global denudation. *J.Geol.* **101**, 295-303.
- Meyers, P.A. (1997):** Organic geochemical proxies of paleoceanographic, paleolimnologic, and paleoclimatic processes, *Organic Geochem*, **27**, 213-250.
- Millot, G. (1970):** *Geology of Clays - Weathering in Sedimentology. – Geochemistry.* Springer, Heidelberg-Berlin – Masson, Paris – Chapman and Hall, London.
- Mohammed, H.M. (1982):** Lithostratigraphy, petrology and geochemistry of the Thebes Formation in the Eastern Desert, Egypt. Ph.D. Thesis, Al Azhar Univ., 322pp.
- Moore, D.M. and Reynolds, R.C. (1989):** X-Ray diffraction and the Identification and Analysis of Clay Minerals. – 332 pp., Oxford (Oxford University Press).
- Moore, D.M. and Reynolds, R.C., Jr. (1997):** X-Ray diffraction and the Identification and Analysis of Clay Minerals. Oxford University Press, New York, 378 pp.
- Mostafa, A.R. and Younes, M.A. (2001):** Significance of organic matter in recording paleoenvironmental conditions of the Safa Formation coal sequence, Maghara area, North Sinai, Egypt. - *Intern. J. Coal Geol.* **47**, 9-21.

- Mustafa, A. and Ghaly, El. (1964):** Survey of Quseir shales and other carbonaceous shales in Egypt. *J. Chem. Eng. Data*, 9, 557 – 563, Cairo.
- Neal R. O' Brien, Calton E. Brett and Martin J. (1998):** Shale Fabric as a Clue to Sedimentary Processes – Example from the Williamson –Willowvale Shales (Silurian), New York. *Shale and Mudstone*, V.II.- Schieber/ Zimmerle /Sethi Stuttgart.
- Nesbitt, H.W. and Young, G.M. (1982):** Early Proterozoic climates and plate motions inferred from major element chemistry of lutites. - *Nature*, *V.* 299, pp715-717.
- Nesbitt, H.W., Markovics, G. and Price, R.C. (1980):** Chemical processes affecting alkalies and alkaline earths during continental weathering. *Geochim. Cosmochim. Acta*, **44**, p 1695 –1766, London.
- Nyakairu, G. W.A. and Koeberl, C. (2001):** Mineralogical and chemical composition and distribution of rare earth elements in clay-rich sediments from central Uganda, *Geochem. J.***35**, 13-28.
- Ohrdorf, R. (1968):** Ein Beitrag zur Geochemie des Lithium im Sedimentgestein.- *Geochim. Cosmochim. Acta*, **32**, p 191-208, London.
- Peters, K.E. (1986):** Guidelines for evaluating petroleum source rock using programmed pyrolysis.- *AAPG Bull.*, 70, 318-329 source rock using programmed pyrolysis.- *AAPG Bull.*, 70, 318-329, Tulsa., Tulsa.
- Pettijohn, F.J. (1975):** *Sedimentary Rocks*. - 3rd Ed., 628 pp., New York (Harper & Row).
- Philobos, E.R., Mansour, H.H. and El Haaddad, A. (1985):** Petrology and origin of the Quseir-Safaga evaporites, Red Sea Coastal area. - *Appl. Sci. Bull. Fac. Sci., Egypt*.
- Pomerol, B. (1984):** *Geochemie des craies du bassin de Paris. Utilisation des elements traces et des isotopes stables du carbone et de l'oxygene en sedimentologie et en paleoceanographie*. - These Sci., Paris 6, 531p.
- Potter, P.E., Maynard, J.B. and Pryor, W.A. (1980):** *Sedimentology of Shale*- 310 pp., New York (Springer).
- Potter, P.E., Shimp, N.F. and Witters, J. (1963):** Trace elements in marine and freshwater argillaceous sediments. - *Geochim. Cosmochim. Acta*, **27**, p 669-694, London.
- Prasad, G. (1983):** A review of the early Tertiary bauxite event in South America, Africa and Indian. - *J. Afri. Earth Sci.*, 1, ³/₄, 305 – 313, London.
- Prevot, L. (1990):** *Geochemistry, Petrography, Genesis of Cretaceous-Eocene Phosphorites. The Ganntour Deposit (Morocco): a type example*. Ph.D. Thesis, University Louis Pasteur, Strasbourg.

- Prevot, L., El Faleh, E.M. and Lucas, J. (1989):** Details on synthetic apatites formed through bacterial mediation: Mineralogy and chemistry of the products. In: Apatite and Phosphorites (Ed. by J.Lucas, P.J. Cook and L. Prevot). Sci. Geol. Bull., Strasbourg, 42, 237-254.
- Quinby-Hunt, M.S., wilde, P. and Berry, W.B.N.(1991):** The provenance of low-calcic black shales. Mineralium Deposita **26**, 113-121.
- Ramadan, F.S. (1992):** Petrological and geochemical studies of Upper Cretaceous-Lower Tertiary sediments in Safage Umm-Gheigh area Red Sea, Coast, Egypt, Ph. D. Thesis, Fac. of Sci. Zagazig Univ.
- Refaat, A.A. (1993):** Facies Development of the Coniacian-Santonian Sediments along the Gulf of Suez, Egypt. Ph.D.Thesis TU. Berlin, Germany.
- Richerdson, M. (1982):** A depositional Model for the Cretaceous Duwi (phosphate) Formation, South of Quseir, Red Sea Coast, Egypt. - M.Sc. Thesis, University of South Carolina.
- Riggs, S.R. (1984):** Paleooceanographic model of Neogene phosphorite deposition, U.S. Atlantic continental margin. - Science, 223,123-131, Washington D.C.
- Riley, K.W. and Saxby, J.H. (1983):** Association of organic matter and vanadium in oil shale from the Toolebuc Formation of the Eromanga Basin, Australia. Chem. Geol., 37.
- Robison, V.D. and Tröger, U. (1983):** Geology and organic geochemistry of Dakhla Shale, Egypt (Abstract). - AAPG Bull., 67, No. 3, p 542, Tulsa.
- Russegger, J.R. (1937):** Kriede and Sanstein; Einfluss Van Granit auh Letuztern Neues Jahrb. Mineral., V.1, pp 665-669.
- Russell, C.A. (1970):** Geochemistry and halmyrolysis of clay minerals, Rio Ameca, Mexico: Geochim. Cosmochim. Acta, V. 34, p. 893-907.
- Ruttenberg, K.C. and Berner, R. A. (1993):** Authigenic apatite formation and burial in sediments from non-upwelling continental margin environments. - Geochim. Cosmochim. Acta, **57**, 991-1007.
- Saad, M.H. (1983):** Aeromagnetic and gravity interpretation of Safage area, Red Sea, Egypt, M.Sc. Thesis Cairo Univ., 127pp.
- Said, R. (1960):** Planktonic foraminifera from the Thebes Formation Luxor, Egypt: Micropaleontology, V. 6, pp277-286.
- Said, R. (1961):** Tectonic frame work of Egypt and its influence on the distribution of foraminifera. Am. Assoc. Petrol. Geol. Bull ., V. 45, pp198-218.
- Said, R. (1962):** The Geology of Egypt. Elsevier, New York, 377 p.

- Said, R. (1980):** The Paleozoic of the Gulf of Suez. Internal Report, Conoco, Egypt.
- Said, R. (1990):** The Geology of Egypt. A.A. Balkema, Rotterdam, Netherlands 734 p.
- Said, R. and Sabry, H. (1964):** Planktonic foraminifera from the typical locality of the Esna Shale in Egypt. - Micropaleontological, V. 10, pp 375-395.
- Schandelmeier, H., Klitzsch, E., Hendriks, F. and Wycisk, P. (1987):** Structural development of North-East Africa since Precambrian Times. - Berl. Geowiss. Abh., (A), 75, 5-24, Berlin.
- Schieber, J. and Baird, G. (2001):** On the origin and significance of pyrite spheres in Devonian black shale of North America. - J. of Sedimentary Research, Vol. 71, No. 1., 2001, p.155-166.
- Schieber, J. and Zimmerle, W. (1998):** Petrography of Shales: A Survey of Technics. Shales and Mudstones II. - E. Schweizerbartsche Verlagsbuchhandlung (Nägele u. Obermiller), Stuttgart.
- Schrank, E. and Ganz, H. (1984):** Organic geochemical and palynological studies of Dakhla Shale profile (Late Cretaceous) in Southeast Egypt. Part A: Succession of microflora and depositional environment. - Berliner Geowiss Abh (50).
- Schreier, C. (1988):** Geochemie und Mineralogie Oberkretazischer und alttertiärer Pelite Der östlichen Wüste Ägyptens und ihre geologische Interpretation.- Berliner Geowiss. Abh. (A), 97, 124pp., Berlin.
- Schröter, T. (1986):** Die lithofazielle Entwicklung der oberkretazischen Phosphatgesteine Ägyptens – Ein Beitrag zur Genese der Tethys-Phosphorite der Ostsahara.- Berliner Geowiss. Abh. (A), 67, 105 pp., Berlin.
- Schuffert, J.D., Janke, R.A., Kastner, M., Leather, J., Sturz, A. and Wing, M.R. (1994):** Rate of formation of modern phosphorite of western Mexico. - Geochem. Cosmochim. Acta **58**, 5001-5010.
- Schuffert, J.D., Kastner, M. and Janke, R.A. (1998):** Carbon and phosphorus burial associated with modern phosphorite formation. Mar. Geol. **146**, 21-31.
- Schultz, L.G., Tourtelot, H.A., Gill, J.R. and Boerngen, J.G. (1980):** Composition and properties of the Pierre Shale and equivalent rocks, northern Great Plains region. - U.S. Geol. Surv. Prof. Pap., **1064-B**, 114 pp., Washington.
- Sediek, K.N. and Amer, A.M. (2001):** Sedimentological and technological studies of Abu Tartur black shales, Western Desert, Egypt. *Physicochemical Problems of Mineral Processing*, 35 (2001), 141-152.
- Selley, R.C. (1988):** Applied Sedimentology. - Textbook. 446pp.

- Seward, A.C. (1935):** Leaves of dicotyledons from Nubian sandstone of Egypt, Geol., Surv., Egypt, Cairo, 21pp.
- Shackleton, R.M., A.C. Ries, R.H. Graham and W.R. Fitches (1980):** Late Precambrian ophiolite melange in the Eastern Desert of Egypt. *Nature* 285: 472-474.
- Shahin, A.N., Shehab, M. and Mansour, H. (1986):** Organic geochemistry of Mohammed Rabah mining area with special emphasis on potential flammable gas accumulations, Geol. Soc. of Egypt annual convention, Cairo. Egypt.
- Shapiro, L. and Breger, I.A. (Translators and Editors)(1968):** Geochemistry of organic substances by S.M. Manskaya and T.V. Drozdova. Pergamon Press, Oxford.
- Sharma, G.D. (1979):** The Alaskan Shelf. Springer-Verlag, New York.
- Shata, A. (1951):** The Jurassic of Egypt. *Bull. Inst. Desert Egypte* 1(2): 68-73.
- Simkiss, K. and Wilbur, K.M. (1989):** Biomineralization: Cell Biology and Mineral Deposition. Academic Press, San Diego.
- Slansky, M. (1986):** Geology of sedimentary phosphates. – 210pp, New York, Amsterdam, Oxford (Elsevier).
- Snively, P.D., Garrison, R.E. and Megvid, A.A. (1979):** Stratigraphy and regional depositional history of the Thebes Formation (Lower Eocene), Egypt. *Ann. Geol. Surv., Egypt.* V. 9, pp 244-362.
- Spears, D.A. & Kanaris – Sotirious, R. (1976):** Titanium in some Carboniferous sediments from Great Britain. - *Geochim. Cosmochim., Acta*, V. 40, pp345-351.
- Stow, D.A. V. and Atkin, B. P. (1987):** Sediment facies and geochemistry of Upper Jurassic mudrocks in the central North Sea area. - *Petroleum Geology of North West Europe* (Brooks J and Glennie K., eds.), 797-808, Graham and Trotman, London.
- Strougo, A. and Abu Nasr, R. (1981):** On the age of the Thebes Formation of Gebel Duwi, Quseir area, Egypt, *N. Jv. Geol. Palaont. Min., Stuttgart*, pp 45-53.
- Sundby, B., Gobeil, C., Silverberg, N. and Mucci, A. (1992):** The phosphorus cycle in coastal marine sediments. - *Limnol. Oceanogr.* **37**, 1129-1145.
- Surdam, R.C. and Stanley, K.O. (1979):** Lacustrine sedimentation during the culminating phase of Eocene Lake Gosiute, Wyoming (GreenRiver Formation). *Geological Society of American Bulletin*, 90, 93-110.
- Tantawy, A.A., Keller, G., Adatte, T., Stinnesbeck, W., Kassab, A. and Schulte, P. (2001):** Maastrichtian to Paleocene depositional environment of the Dakhla Formation, Western Desert, Egypt: sedimentology, mineralogy, and integrated micro- and macrofossil biostratigraphies. *Cretaceous Research*, V. 22, Issue 6, 795-827.

- Thiry, M. and Jaquin, T. (1993):** Clay mineral distribution related to rift activity, sea-level changes and paleoceanography in the Cretaceous of the Atlantic Ocean. *Clay Minerals*, 28, 61-84.
- Tissot, B. P. and Welte, D.H. (1984):** Petroleum formation and occurrence- 699 pp., Second Edition Berlin (Springer Verlag).
- Tooms, J.S., Summerhayes, C.P. and Cronan, D.B. (1969):** Geochemistry of marine phosphate and manganese deposits. - *Oceanogr. Mar. Biol. Annu. Rev.* 7, 49 – 100.
- Tröger, U. (1984):** The oil shale potential of Egypt. *Berliner Geowiss. Abh.*, (A), 50, 375-380.
- Turekian, K.K. (1968):** Nickel. In: K.H. Wedepohl (Ed.), *Handbook of Geochemistry*. Springer, Berlin, Vol. II/3, pp. 28-K-1-28-L-3.
- Turekian, K.K. and Wedepohl, K.H. (1961):** Distribution of the elements in some major units of the earth's crust.- *Bull. Geol. Soc. Amer.*, **72**, 175-192, Baltimore.
- Valeton, I. (1993):** Klimaperioden lateritischer Verwitterung und ihr Abbild in den synchronen Sedimentationsräumen.– *Zt.Dtsch. Geol. Gesell.*, 134, 413-452, Hannover.
- Van Houten, F.B., Bhattacharyya, D.P. and Mansour, S.E.I. (1984):** Cretaceous Nubia formation and Correlative deposits, East Egypt., Major regressive transgressive complex *Bull. Geol. Soc. Am.*, V. 95, pp 397-405.
- Velde, B. (1992):** Introduction to Clay Minerals. – 198 p., London (Chapman & Hall)
- Velde, B. (1995):** Origin and Mineralogy of Clays. – 334 p., Berlin (Springer).
- Vine, J.D. and Tourtelot, E.B. (1970):** Geochemistry of black shales a summary report. *Econ. Geol.*, V. 65, pp 253 – 273.
- Walker, J.R. (1993):** Chlorite polytype geothermometry: Clays and Clay minerals, **41**, 260-67.
- Walters, L.J., Owen, D.E., Henley, A.L., Winsten, M.S. and Valek, K.W. (1987):** Depositional environments of the Dakota Sandstone and adjacent units in the San Juan basin utilizing discriminant analysis of trace elements in shales.- *J. Sed. Petrol.*, **57**, 265-277, Tulsa.
- Ward, C., Mc Donald, K.C. & Mansour, S.E.I. (1979):** The Nubia Formation of the Quseir Safaga area- Egypt, *Geol., Surv., Egypt V. IX* pp 420-431.
- Watanabe, Y. and Tsunogai, S. (1984):** Adsorption-desorption control of phosphate in anoxic sediment of a coastal sea, Funka Bay, Japan. *Mar.Chem.* **15**, 71-83.
- Weaver, C.E. (1958):** The effects and geologic significance of potassium fixation; by expandable clay minerals derived from muscovite, biotite, chlorite, and volcanic material-*Am. Mineral.*, 43, 839-861, Washington.

- Weaver, C.E. (1989):** Clays, Mud, and Shales: Amsterdam, Elsevier, 819 p.
- Weaver, C.E. and Pollard, L.D. (1973):** The Chemistry of Clay Minerals. Elsevier, Amsterdam.
- Weber, J. (1991):** Untersuchungen zur Tonmineralführung der Messel-Formation in der Fundstätte Messel (Mittel-Eozä). Forsch.-Inst. Senckenberg, 139, 71-81.
- Weissbrod, T. (1969):** The Paleozoic of Israel and adjacent countries: Part II, The Paleozoic outcrops in southwestern Sinai and their correlation with those of southern Israel. Bull. Geol. Surv. Isr. 48: 1-32.
- Welton, J.E. (1984):** SEM Petrology Atlas.- AAPG Methods in Exploration Series, **4**, 237 pp, Tulsa.
- Wrafter, J.P. and Graham, J. R. (1989):** Ophiolitic detritus in the Ordovician sediments of South Mayo. Ireland. J. Geol. Soc. London **146**, 213-215.
- Youssef, M. I. (1949):** Stratigraphical studies in Quseir area Ph.D. Thesis, Alexandria, Univ., U.A.R.
- Youssef, M. I. (1957):** Upper Cretaceous rocks in Kosseir area. Bull. Inst.Desert Egypt. V., 7. pp 35-54.
- Yuretich, R., Melles, M., Sarata, B. and Grobe, H. (1999):** Clay minerals in the sediments of Lake Baikal: A useful climate proxy. Journal of Sedimentary Research, 69(3), 588-596.

10 Appendix

Appendix A = Table 1 to Table 6b

Appendix B = XRD profiles

Appendix C = Plates of petrography and SEM

Notice:

N = Nile Valley (Esna-Idfu region)

Q = Quseir phosphate mine

AT = Abu Tartur phosphate mine

Mg = Al Maghara coal mine

b.d.l. = below detection limit

< = below

Table 1: Lithological description of the studied samples.

Sample No.	Description
N80	Limestone , white, compact, fossiliferous.
N79	Limestone , as above.
N78	Marl , green to light brownish, moderately compact, fractured fossiliferous, evaporitic.
N77	Marl , as above
N76	Limestone , light yellowish, slightly argillaceous, fossiliferous, compact.
N75	Shale , , dark grey, calcareous compact, fractured with veins of evaporites.
N74	Argillaceous limestone , yellowish, compact, silty in parts, fractured.
N73	Shale , dark grey, calcareous, moderately hard, ferruginous.
N72	Marl , green to light brownish, moderately hard, ferruginous, trace fossils.
N71	Shale , dark grey, calcareous, moderately hard, silty in parts, ferruginous, with veins of evaporites.
N70	Claystone , greenish to yellowish, calcareous, compact, ferruginous spots, evaporitic.
N69	Shale , dark grey, grey to light brownish, calcareous, compact, silty in parts, veins of evaporites.
N68	Shale , as above.
N67	Shale , as above.
N66	Shale , as above.
N65	Shale , as above.
N64	Shale ,. as above.
N63	Shale , as above.
N62	Shale , as above.
N61	Shale , as above.
N60	Shale , as above.
N59	Shale, marly , grey to yellowish, soft to moderate hardness, silty in parts, lamination, ferruginous.
N58	Shale, marly , as above.
N57	Claystone , grey to light brownish, calcareous, fractured, veins of evaporites.
N56	Argillaceous limestone , moderately hard, silty in parts, fractured, evaporitic, ferruginous spots.
N55	Claystone , dark grey, calcareous, moderately hard, silty in parts, ferruginous spots, evaporitic.
N54	Claystone , grey, calcareous, moderately hard, silty in parts, ferruginous spots, veins of evaporites.
N53	Chalky limestone , white to yellowish, compact, fractured with veins of evaporites, silty in parts , fossiliferous.
N52	Chalky limestone , as above.
N51	Argillaceous limestone , grey to light grey, moderate to hard, veins of evaporites.
N50	Argillaceous limestone , as above.
N49	Marl , grey to dark grey, fossiliferous, ferruginous spots, hard, evaporitic, Pecten shells.
N48	Claystone , reddish, ferruginous, calcareous, compact, fractured evaporitic.
N47	Shale , black, dark grey, ferruginous patches and spots between fissiles and through fractures, evaporites, organic remains and traces of shells well preserved, silty in parts..
N46	Shale , as above.
N45	Shale , as above.
N44	Shale , as above.
N43	Shale , as above.
N42	Shale , dark grey, alternating with ferruginous siltstone, brownish and reddish, fractured, evaporite lamination between fissiles.
N41	Shale , as above.
N40	Shale , as above.
N39	Claystone , grey to yellowish , calcareous, moderately hard, silty, in parts with gypsum laminae.
N38	Shale , dark grey to brownish, soft hardness, alternating with gypsum lamination, fractured.
N37	Shale , black, dark grey to brownish, moderately hard, fractured filled with ferruginous, silty.
N36	Shale , as above.
N35	Claystone , grey to light brownish, moderately hard, ferruginous spots and patches, calcareous, large veins of evaporites.
N34	Shale , black to grey, compact, calcareous, veins of evaporite, patches of ferruginous through fractures and between sheets.
N33	Shale , black, moderately hard, fractured, ferruginous patches, few evaporite, calcareous.
N32	Shale , as above.
N31	Shale , grey to brownish, calcareous , moderate to soft, veins of evaporites, ferruginous .

Table 1: cont.

Sample No.	Description
N30	Shale , as above
N29	Shale , black to dark grey compact, ferruginous patches evaporite, calcareous.
N28	Shale , dark grey to brownish, moderately hard, less orites, ferruginous patches and spots embedded.
N27	Shale , as above.
N26	Shale , black to grey, medium hard, fractured, ferruginous patches, reddish to brownish veins of evaporite, salts and calcareous.
N25	Shale , grey with red hematitic siltstone as lenses and tubes, moderately hard, evaporite embedded between shale, siltstone
N24	Phosphat , yellow to light brownish, highly fossiliferous, less hardness, organic matter and bones remains, cherty nodules.
N23	Oyster limestone , greyish, very compact, fractures filled with calcite and rock fragments.
N22	Argillaceous limestone , yellow, very compact, patches of organic matter.
N21	Dolomitic limestone , grey, very compact.
N20	Phosphate , yellow to light brownish, highly fossiliferous, less hardness, organic remain, highly calcareous.
N19	Conglomerate bed , light brownish, very compact, calcareous, phosphatic.
N18	Sandstone , grey to light brownish, moderately hard, lamination of sand, silt and claystone, fractured, evaporitic
N17	Claystone , grey, medium hard, silty, fissiles, fractured, veins of evaporite.
N16	Phosphate , brownish, to yellowish, compact, fossiliferous, ferruginous, with sandy and chert nodules.
N15	Siltstone , grey, brown to yellowish, alternating with claystone, fissil, medium hard, ferruginous patches interbedded change the colour to yellowish, brownish.
N14	Sandstone , yellow, moderately hard, ferruginous.
N13	Claystone , yellowish to light brown, silty, compact, fissil fractured with black patches of organic matter and evaporites.
N12	Phosphate bodies , with conglomerate and breccia, yellow to brownish, compact, ferruginous.
N11	Siltstone , brown to reddish surrounding the phosphate nodules.
N10	Claystone/Siltstone , brownish to grey, medium hard, rare evaporites, slightly fissil.
N9	Claystone , green, moderately hard, silty in parts, slightly fissiles with evaporites interclation
N8	Siltstone , grey, yellowish, brownish lamination, moderately hard, sandy in parts, iron concretion, ferruginous, and few evaporites
N7	Claystone , green, moderately hard, fractured with rare evaporites.
N6	Siltstone , brownish, ferruginous, calcareous, moderately hard, with embedded veinlets of sandstone, cross laminated, few evaporite laminae are interbedded also
N5	Siltstone , green to brownish, moderately hard, slightly calcareous, sandy in parts, slightly fissiles.
N4	Siltstone , reddish brown, ferruginous moderately hard and with rare evaporites
N3	Claystone , green to grey, silty in parts, with rare evaporites.
N2	Siltstone , brownish, ferruginous, sandy in parts.
N1	Claystone , dark grey, silty in parts, rare evaporites and ferruginous spots.
Q1	Shale , black, subfissil, highly carbonaceous, pyritic.
Q2	Marl , yellowish brown, compact.
Q3	Phosphate , yellow to light brownish, highly fossiliferous, less hardness, organic matter and bone remains, cherty nodules.
Q4	Phosphate , silicified, yellow brownish, compact, organic matter, bone remains, cherty nodules.
Q5	Oyster limestone , greyish, very compact, fractured.
Q6	Shale , grey to yellowish, calcareous, micaceous, slightly fissiles.
Q7	Shale , brownish, micaceous, fissile, gypsiferous, slightly calcareous.
Q8	Shale , black to grey, compact, subfissile, alternated with gypsum laminae.
Q9	Shale , as above.
Q10	Shale , black, weathered.
Q11	Shale , pale brown, fossiliferous, highly calcareous, fissile.
Q12	Shale , as above.
Q13	Shale , pale brown, fossiliferous, highly calcareous, fissile, gypsiferous.
Q14	Shale , as above.
Q15	Shale , pale brown, grey, fossiliferous, highly calcareous.

Table 1: cont.

Sample No.	Description
Q16	Shale , as above.
Q17	Shale , black, weathered.
Q18	Phosphate , silicified, yellow to light brownish, organic matter and bone remains, cherty nodules.
Q19	Phosphate , yellow to light brownish, compact, organic matter and bone remains.
Q20	Marl , yellowish brown ,compact.
Q21	Oyster limestone , greyish, very compact, fractured.
Q22	Phosphate , yellow to light brownish, highly fossiliferous.
Q23	Shale , pale brown, grey, fossiliferous (pecten), highly calcareous.
Q24	Shale , as above.
Q25	Shale , as above.
Q26	Shale , as above.
Q27	Shale , black, weathered.
Q28	Shale , grey to greenish grey, fissile, gypsiferous, slightly compact.
Q29	Shale , as above.
Q30	Shale , as above.
Q31	Phosphate , yellow, brownish, compact, organic matter and bones remains, highly calcareous.
Q32	Shale , pale brown, grey, fossiliferous, highly calcareous.
Q33	Shale , as above
Q34	Shale , as above
Q35	Shale , black, weathered.
AT1	Shale , black, compact, subfissil, pyritic, slightly gypsiferous.
AT2	Shale , as above
AT3	Shale , as above
AT4	Phosphate , black, calcareous, slightly compset.
AT5	Phosphate , black, calcareous, slightly compset.
AT6	Shale , as above
AT7	Shale , as above
AT8	Phosphate , black, calcareous, slightly compset.
AT9	Phosphate , black, calcareous, slightly compset, fissile to sub fissile.
AT10	Shale , as above
AT11	Shale , as above
AT12	Phosphate , black, calcareous, slightly compset.
Mg1	Shale , black, compact, highly carbonaceous, ferruginous.
Mg2	Shale , as above
Mg3	Shale , as above
Mg4	Shale , as above
Mg5	Shale , as above
AZ1	Shale , black, gypsiferous, fissile, highly carbonaceous.
AZ2	Shale , as above
AZ3	Shale , as above
AZ4	Shale , black, gypsiferous, fissile, highly carbonaceous.
AZ5	Shale , as above
AZ6	Shale , as above
AZ7	Shale , as above
AZ8	Shale , as above
AZ9	Shale , as above
AZ10	Shale , as above
AZ11	Shale , as above
AZ12	Shale , as above

Table (2): Semiquantitative mineralogical composition of clay fraction.

Age	Formation	Location	S.No.	Smectite	Kaolinite	Chlorite	Illite
Late Maastrichtian – Early Eocene	Esna Shale	Nile Valley (Esna -Idfu) region	N79	95	5	0	0
			N78	90	0	10	0
			N75	98	2	0	0
			N73	95	0	5	0
			N72	97	0	3	0
			N71	95	5	0	0
			N69	71	0	29	0
			N66	70	0	30	0
			N64	93	7	0	0
			N60	62	Trace	38	0
			N55	100	0	0	0
			Avg.	88	2	10.	0
Late Maastrichtian-Middle Paleocene	Dakhla Shale		N47	93	7	0	0
			N43	58	0	42	0
			N41	55	0	45	0
			N37	83	17	0	0
			N35	35	0	65	0
			N33	86	14	0	0
			N31	68	Trace	32	0
			N29	88	12	0	0
			N27	78	22	Trace	0
			N26	86	14	0	0
			Avg.	73	9	18.	0
			Campanian-Maastrichtian	Variegated, Duwi	N17	92	Trace
N15	85				0	15	0
N10	90				0	10	0
N9	70				Trace	30	0
N5	65				Trace	35	0
N1	98				2	0	0
Avg.	83.				0	16.	0
Maastrichtian	Duwi and Dakhla	Quseir Mines	Q.1	98	2	0	0
			Q.7	94	6	0	0
			Q.9	33	67	0	0
			Q.11	84	16	Trace	0
			Q.14	88	12	0	0
			Q16	92	8	0	0
			Q.20	85	15	0	0
			Q.23	94	6	0	0
			Q.26	97	3	0	0
			Q.32	80	20	0	0
			Q.34	34	66	0	0
			Avg.	80	20.	0	0
Maastrichtian	Duwi	Abu Tartur Mine	AT.2	99	1	0	0
			AT.5	100	0	0	0
			AT.7	100	Trace	0	0
			AT.9	100	Trace	0	0
			Avg.	100	0	0	0
Middle Jurassic	Safa	Maghra Mine	Mg.1	0	100	0	0
			Mg.3	Trace	100	0	0
			Mg.5	0	100	0	0
			Avg.	0	100	0	0
Carboniferous	Ataqa	Abu Zenima	AZ.1	0	100	Trace	Trace
			AZ.5	0	60	0	40
			AZ.8	0	100	0	0
			Avg.	0	87	0	13

Avg =average

Table (3): Semiquantitative mineralogical composition of bulk studied samples.

Age	Formation	Location	Sample No.	Quartz	Feldspare	Calcite	Dolomite	Anhydrite	F-apatite	Iron oxides	Halite	Gypsum	Clay	
Late Paleocene – Early Eocene	Esna Shale	Nile Valley (Esna- Idfu) region	N79	13	0	5	0	35	0	0	0	0	47	
			N78	5	0	25	1	1	0	0	9	0	59	
			N77	6	0	24	54	0	0	0	0	0	16	
			N75	12	0	0	0	0	0	0	0	0	88	
			N74	10	0	68	0	14	0	0	0	0	8	
			N73	9	0	0	0	0	0	0	0	0	91	
			N72	11	0	22	0	7	0	0	0	1	59	
			N71	8	0	0	0	12	0	0	0	0	80	
			N70	7	0	27	0	19	0	0	0	0	47	
			N69	8	0	26	0	3	0	0	0	0	63	
			N68	9	0	2	0	17	0	0	0	0	72	
			N67	8	0	0	3	16	0	6	0	0	67	
			N66	6	0	5	0	0	0	0	0	0	89	
			N65	6	0	39	0	1	0	0	0	0	54	
			N64	6	0	15	50	2	0	0	0	0	27	
			N63	8	0	37	0	16	0	0	0	0	39	
			N62	6	0	5	0	26	0	0	0	0	63	
			N60	10	0	0	0	0	0	0	0	0	90	
			N59	0	0	8	81	0	0	0	0	0	11	
			N58	8	0	13	0	4	0	0	0	0	75	
			N57	6	0	29	0	24	0	0	0	0	41	
			N56	5	0	79	0	10	0	0	0	0	6	
			N55	16	0	52	0	7	0	0	0	0	25	
			Avg.	8	0	21	8	9	0	0	0	0	53	
Middle Paleocene	Shale		N52	6	0	0	0	94	0	0	0	0	0	0
			N50	3	0	56	0	41	0	0	0	0	0	0
			Avg.	4.5	0	28	0	68	0	0	0	0	0	0
			N49	7	0	88	0	0	0	0	0	0	0	5
			N47	30	0	0	0	0	0	0	10	0	0	60
			N46	23	0	0	0	7	0	0	0	0	0	70
			N45	28	3	0	0	0	0	0	0	0	0	69
			N44	17	0	0	0	29	0	0	0	13	0	41
			N43	19	0	0	0	0	0	0	29	0	0	52
			N42	22	0	0	0	0	0	0	0	0	0	78
			N41	20	5	3	0	0	0	0	0	0	0	72
			N39	47	9	0	0	4	0	0	0	0	0	40
			N37	7	0	0	0	44	0	5	0	0	0	44
			N36	17	6	6	0	16	0	7	0	0	0	48
			N35	0	0	0	0	84	0	0	0	0	0	16
			N34	19	0	0	0	0	0	7	0	0	0	74
			N33	23	3	0	0	0	0	0	0	0	0	74
			N32	21	3	0	0	0	0	0	0	0	0	76
			N31	14	1	0	0	0	0	0	0	0	0	85
			N30	24	1	0	0	0	0	0	0	0	0	75
			N29	16	3	0	0	0	0	0	39	0	0	42
			N28	10	4	0	0	0	0	0	0	0	0	86
			N27	17	0	42	3	0	0	2	0	3	33	
			N26	20	4	0	0	0	0	0	0	0	0	76
Avg.	19	2	7	0	9	0	5	0	0	60				
Late Maastrichtian- Campanian -Maastrichtian	Dakhla	N24	40	0	13	0	0	47	0	0	0	0	0	
		N21	5	0	95	0	0	0	0	0	0	0	0	
		N20	18	0	4	0	0	78	0	0	0	0	0	
		N17	4	0	0	76	0	0	0	0	2	18		
		N15	17	0	0	46	0	0	0	0	0	37		
		N13	33	4	0	0	10	0	16	0	1	36		
		N12	45	10	0	0	11	0	0	0	0	34		
		N10	53	31	0	0	0	0	0	0	0	16		
		N9	42	15	0	0	0	0	0	0	0	43		
		N7	64	5	0	0	13	0	0	0	0	18		
		N5	64	19	0	0	0	0	0	0	0	17		
		N1	75	15	0	0	0	0	0	0	0	10		
		Avg.	33	8	9	10	2	10	1	0	0	19		
		Campanian -Maastrichtian	Variegated- Duwi	N79	13	0	5	0	35	0	0	0	0	0
N78	5			0	25	1	1	0	0	9	0	59		
N77	6			0	24	54	0	0	0	0	0	16		
N75	12			0	0	0	0	0	0	0	0	88		
N74	10			0	68	0	14	0	0	0	0	8		
N73	9			0	0	0	0	0	0	0	0	91		
N72	11			0	22	0	7	0	0	0	1	59		
N71	8			0	0	0	12	0	0	0	0	80		
N70	7			0	27	0	19	0	0	0	0	47		
N69	8			0	26	0	3	0	0	0	0	63		
N68	9			0	2	0	17	0	0	0	0	72		
N67	8			0	0	3	16	0	6	0	0	67		
N66	6			0	5	0	0	0	0	0	0	89		
N65	6			0	39	0	1	0	0	0	0	54		

Avg =average

Table (3): cont.

Age	Formation	Location	Sample No.	Quartz	Feldspar	Calcite	Dolomite	Anhydrite	F-apatite	Iron oxides	Pyrite	Gypsum	Clay
Late Maastrichtian - Middle Paleocene	Duwi and Dakhla Shale	Quseir Mines	Q.1	33	0	0	0	0	0	0	2	1	64
			Q.2	19	0	0	51	0	30	0	0	0	0
			Q.4	47	0	0	12	0	14	0	0	0	0
			Q.6	0	0	0	0	0	53	0	0	47	0
			Q.9	14	0	52	0	0	0	0	0	34	0
			Q.10	43	0	0	0	0	0	0	4	4	49
			Q11	27	0	54	0	0	10	0	0	0	9
			Q.14	18	0	61	0	0	0	8	0	0	13
			Q.15	29	0	56	0	0	0	0	0	0	15
			Q.16	30	0	56	0	0	0	0	0	0	14
			Q.17	19	0	68	0	0	0	0	1	0	12
			Q.19	9	0	0	51	0	40	0	0	0	0
			Q.20	50	4	0	0	0	0	5	0	0	41
			Q.21	3	0	83	14	0	0	0	0	0	0
			Q22	6	0	54	0	0	40	0	0	0	0
			Q.23	40	0	0	0	0	32	0	0	0	28
			Q.26	20	0	38	0	0	0	0	0	0	42
			Q.27	14	0	48	0	0	21	0	3	2	12
			Q.31	8	0	40	0	0	52	0	0	0	0
			Q.32	74	0	0	0	0	0	0	0	6	20
			Avg.	25	0	31	6	0	15	1	0	5	16
Late Maastrichtian	Duwi	Abu Tartur Mine	AT.1	13	0	0	0	0	0	0	3	0	84
			AT.2	21	0	0	0	0	0	0	3	1	75
			AT.3	23	0	0	0	0	0	0	6	1	70
			AT.4	6	0	0	45	0	44	0	4	1	0
			AT.5	11	0	0	0	0	0	0	4	1	84
			AT.6	11	0	0	0	0	0	0	1	3	85
			AT.7	12	0	0	0	0	0	0	4	1	83
			AT.8	12	0	0	34	0	49	0	5	0	0
			AT.9	73	0	0	0	0	0	0	5	0	22
			AT.10	17	0	0	0	0	0	0	4	1	77
			AT.11	60	0	0	0	0	0	0	1	0	39
			AT.12	15	0	0	0	0	74	0	6	6	0
			Avg.	23	0	0	7	0	14	0	4	1	52
Middle Jurassic	Safa	Al Maghara Mine	Mg.1	35	0	0	0	0	0	4	1	0	60
			Mg.2	39	0	0	0	0	0	1	1	0	59
			Mg.3	49	0	0	0	0	0	0	4	0	47
			Mg.4	46	0	0	0	0	0	0	0	0	54
			Mg.5	43	0	0	0	0	0	0	0	0	57
			Avg.	42	0	0	0	0	0	1	1	0	55
Carboniferous	Ataqa	Abu Zinema	AZ.1	86	0	0	0	0	0	0	0	0	14
			AZ.3	75	0	0	0	0	0	0	0	0	25
			AZ.8	82	0	0	0	0	0	0	0	0	18
			AZ.9	83	0	0	0	0	0	0	0	0	17
			AZ.10	73	0	0	0	6	0	0	0	0	21
			AZ.11	80	0	0	0	0	0	0	0	0	20
			Avg.	80	0	0	0	0	0	0	0	0	20

Avg =average

Table(4): Major element composition(wt %) of the studied samples.

Location	Formation	Sample No.	SiO ₂ [%]	Al ₂ O ₃ [%]	CaO [%]	MgO [%]	Fe ₂ O ₃ [%]	TiO ₂ [%]	P ₂ O ₅ [%]	Na ₂ O [%]	K ₂ O [%]	SO ₃ [%]	LOI [%]	Total [%]	CIA	SiO ₂ /Al ₂ O ₃
Nile Valley (Esna-Idfu) region	Esna	N79	47.93	16.85	1.02	2.55	7.97	0.86	0.085	1.68	1.16	0.72	19.0	99.21	81	2,84
		N78	38.63	12.04	8.29	4.27	5.83	0.61	0.191	2.39	0.87	0.41	26.4	99.93	--	3,21
		N75	57.56	15.42	0.43	3.15	2.94	0.90	0.043	1.77	0.72	0.148	16.90	99.98	84	3,73
		N72	46.53	13.39	8.68	4.03	5.50	0.62	0.227	1.39	1.00	0.128	18.50	99.99	--	3,47
		N69	41.20	16.50	7.99	2.17	6.16	0.75	0.096	1.22	0.91	0.195	22.70	99.89	--	2,50
		N66	46.08	20.51	1.38	1.88	6.01	0.84	0.068	1.31	0.93	0.120	20.80	99.92	85	2,25
		N60	38.11	16.53	8.43	2.52	5.20	0.57	0.657	2.46	0.91	0.286	24.30	99.97	--	2,31
		N55	38.97	8.68	15.19	2.31	3.65	0.43	0.175	1.11	0.46	0.140	28.40	99.23	--	4,03
	Tarawan	N54	18.71	9.67	23.79	0.64	3.36	0.37	0.136	2.34	0.33	0.266	40.30	99.91	--	1,93
		N52	11.18	5.33	37.99	0.56	2.48	0.25	0.117	0.66	0.24	0.119	41.00	99.92	--	2,10
		N50	13.88	6.22	33.23	0.70	4.38	0.25	0.234	0.77	0.28	6.2	33.80	100	--	2,23
	Dakhla	N49	20.34	9.33	28.62	0.90	3.95	0.41	0.212	1.11	0.46	0.126	34.50	99.95	--	2,18
		N47	42.78	18.13	0.08	1.40	15.25	0.81	0.144	1.51	0.75	1.032	18.00	99.88	89	2,36
		N45	49.63	19.24	0.03	1.62	4.35	0.99	0.059	1.35	0.59	0.575	21.50	99.93	90	2,58
		N43	37.46	16.53	0.01	1.66	9.11	0.84	0.102	1.50	0.72	0.313	31.70	98.95	87	2,27
		N39	46.85	18.24	0.79	1.49	6.01	1.00	0.335	1.53	1.02	0.121	22.60	99.98	84	2,57
		N37	44.11	22.34	0.36	1.26	4.70	0.96	0.054	0.86	0.47	0.050	24.80	99.96	93	1,97
		N35	42.19	10.99	18.40	3.16	5.22	0.44	0.108	0.77	0.30	0.570	17.80	99.94	--	3,90
		N33	48.48	22.36	0.10	0.93	5.40	0.97	0.059	1.33	0.63	0.136	19.60	99.99	91	2,17
		N31	45.54	21.57	0.10	0.93	8.75	0.91	0.094	1.54	0.59	0.134	19.80	99.65	90	2,11
		N29	42.51	20.93	0.19	1.30	24.99	0.81	0.123	1.66	0.53	0.266	6.70	98.51	90	2,03
		N27	38.02	15.86	9.29	2.80	6.08	0.79	0.262	1.70	0.65	0.668	23.82	99.94	58	2,40
		N26	48.95	22.94	0.28	1.07	6.12	0.98	0.065	1.13	0.66	0.142	17.08	100	92	2,13
	Duwi	N24	19.21	0.20	29.34	0.30	1.05	0.03	16.78	0.86	0.05	2.173	30.00	99.99	--	96,05
		N21	18.37	0.49	45.39	0.51	0.86	0.04	0.290	0.18	0.05	0.050	33.77	100	--	37,49
		N17	48.59	16.17	1.48	1.60	4.93	0.91	0.244	3.15	0.91	1.544	20.47	99.77	74	3,00
		N15	53.75	11.44	0.60	1.31	3.71	0.83	0.453	1.68	1.09	0.075	25.00	99.93	77	4,70
		N10	57.94	12.67	0.94	1.11	7.88	0.96	0.673	1.24	1.05	0.296	15.24	99.99	79	4,57
		N9	49.85	18.44	0.24	1.22	4.56	1.28	0.202	1.38	1.55	0.137	21.10	99.95	85	2,70
		N5	55.09	15.25	0.19	1.04	3.42	1.34	0.494	1.38	1.56	0.266	19.95	99.98	83	3,61
		N1	52.66	17.42	0.13	1.71	7.09	1.27	0.041	1.81	2.98	0.394	14.49	99.99	78	3,02
Quseir phosphate mines	Duwi and Dakhla	Q.1	45.85	13.57	0.83	2.14	4.77	0.76	0.132	0.36	0.87	2.424	28.00	99.70	87	3,38
		Q.2	15.10	0.24	23.40	7.59	2.14	0.03	6.219	0.36	0.05	0.929	42.20	98.25	--	62,92
		Q.7	25.45	7.16	12.33	2.01	5.87	0.44	5.817	7.05	0.83	0.229	32.00	99.16	--	3,55
		Q.11	37.73	8.83	17.03	1.74	4.88	0.44	3.317	1.16	0.64	0.132	22.28	98.17	--	4,27
		Q.16	35.39	8.79	21.53	1.41	3.92	0.46	2.600	0.69	0.64	0.136	23.34	98.90	--	4,03
		Q.18	23.08	0.30	28.15	0.62	0.14	0.03	17.75	0.57	0.05	0.662	27.96	99.31	--	76,93
		Q.20	49.75	11.81	1.52	1.74	4.88	0.69	0.513	0.44	0.81	0.050	27.40	99.60	81	4,21
		Q.26	39.32	11.43	16.24	2.41	6.07	0.58	4.897	0.76	0.92	0.213	15.85	98.69	--	3,44
		Q.31	4.15	0.65	34.35	0.81	0.70	0.03	13.68	1.81	0.05	0.344	40.30	96.87	--	6,38
		Q.34	19.89	8.55	33.82	0.71	3.00	0.40	0.423	0.38	0.46	0.288	31.70	99.62	--	2,33
Abu Tartur	Duwi	AT.2	46.81	14.60	1.18	2.17	5.51	0.78	0.127	0.06	1.39	1.154	26.14	99.92	85	3,21
		AT.4	4.94	1.07	34.09	0.45	3.33	0.06	20.18	0.62	0.06	4.120	29.30	98.22	--	4,62
		AT.5	55.66	17.89	1.79	3.16	6.31	0.87	0.275	0.10	0.93	3.019	9.80	99.80	86	3,11
		AT.7	52.04	16.70	1.85	2.95	6.41	0.82	0.322	0.14	0.88	3.394	14.25	99.75	85	3,12
		AT.8	12.00	2.89	28.79	1.26	4.32	0.14	15.90	0.49	0.17	5.087	27.60	98.64	--	4,15
		AT.9	49.77	14.16	1.65	2.33	4.22	0.88	0.303	0.10	1.05	0.836	24.60	99.89	83	3,51
Al Maghra	Safa	AT.12	7.73	1.45	30.23	0.39	3.72	0.07	17.26	0.46	0.09	4.606	32.55	98.55	--	5,33
		Mg.1	47.01	25.88	0.37	0.90	8.70	1.97	0.093	0.11	0.93	0.543	13.25	99.75	95	1,82
		Mg.3	49.80	26.43	0.34	0.77	4.28	2.15	0.088	0.11	1.02	0.277	14.50	99.76	95	1,88
Abu Zinema	Ataqa	Mg.5	49.77	26.34	0.35	0.67	6.30	2.25	0.089	0.11	0.86	0.599	12.44	99.77	95	1,89
		AZ.1	51.12	18.86	0.29	0.30	0.49	1.14	0.067	0.31	0.94	0.207	26.00	99.72	92	2,71
		AZ.5	56.23	13.73	0.44	0.30	2.00	1.28	0.043	0.35	1.07	0.517	23.85	99.81	88	4,10
		AZ.7	57.98	15.37	0.79	0.30	0.23	0.44	0.028	0.11	0.24	0.414	24.20	99.90	93	3,77
		AZ.8	41.02	20.16	0.16	0.30	0.47	0.94	0.064	1.26	0.51	3.714	30.40	98.99	91	2,03

Table(5): Trace element composition(ppm) of the studied samples.

Location	Formation	Sample.No.	Sr ppm	Ba ppm	V ppm	Ni ppm	Co ppm	Cr ppm	Zn ppm	Cu ppm	Zr ppm	Mn ppm
Nile Valley	Esna	N79	289	150	180	46	10<	181	119	24	114	46<
		N78	309	100	160	47	13	150	141	13	90	289
		N75	248	150	170	22	<10	171	58	22	133	<150
		N72	362	120	226	93	<10	180	244	21	84	499
		N69	331	150	196	65	10	197	160	28	110	185
		N66	211	180	170	48	15	181	154	21	130	<150
		N60	280	288	170	67	11	166	168	25	91	266
		N55	428	95	140	78	10	127	159	31	71	131<
	Tarawan	N54	719	70	110	44	<10	183	75	15	48	<150
		N52	990	48	83	32	<10	154	43	13	<40	<150
	Dakhla	N50	703	59	77	36	<10	144	<40	11	44	<150
		N49	784	62	140	45	<10	222	54	19	52	<150
		N47	113	60	180	46	25	108	116	21	91	608
		N45	109	69	190	33	9<	163	61	29	112	<150
		N43	43	110	170	51	22	111	127	14	97	831
		N39	158	140	250	46	12	265	90	25	173	<150
		N37	263	97	170	34	<10	156	68	22	109	<150
		N35	400	73	140	43	13	153	110	16	55	<150
		N33	197	73	190	46	11	197	73	27	95	<150
		N31	54	72	218	64	18	200	195	21	93	<150
		N29	40	73	202	87	25	192	138	<10	87	1040
		N27	299	74	197	52	<10	224	96	25	97	<150
	Duwi	N26	82	77	210	45	13	215	101	29	97	<150
		N24	1203	362	58	<12	<10	64	65	<10	<40	379
		N21	208	83	55	<12	<10	50	<40	<10	<40	1770
		N17	497	120	160	32	8<	174	82	34	99	<150
		N15	250	264	86	26	<10	77	68	26	297	<150
		N10	423	339	100	40	<10	100	96	32	336	359
		N9	562	134	150	19	<10	117	<40	20	236	<150
		N5	1703	219	100	14	<10	93	<40	22	372	<150
		N1	78	140	160	41	12	107	65	53	219	<150
Quseir Phosphate mines	Duwi and Dakhla	Q.1	76	92	110	41	20	81	69	27	138	195
		Q.2	301	34	45	<12	<10	<30	<40	<10	<40	732
		Q.7	470	72	1835	126	<10	379	1250	156	104	<150
		Q.11	486	79	3151	186	<10	631	1600	243	93	<150
		Q.16	513	93	2679	153	<10	414	1130	178	95	<150
		Q.18	951	110	20	<12	<10	35	<40	<10	<40	152
		Q.20	128	110	160	30	<10	123	135	25	146	<150
		Q.26	649	98	1455	177	12	540	1040	154	105	<150
		Q.31	895	53	20	18	<10	100	119	<10	<40	<150
Abu Tartur	Duwi	Q.34	1030	87	110	60	b.d.l.	240	61	31	55	<150
		AT.2	207	110	130	26	12	100	66	16	165	<150
		AT.4	1324	61	46	21	<10	<30	<40	<10	<40	556
		AT.5	226	69	150	31	13	112	41	15	100	<150
		AT.7	300	78	65	39	14	122	44	30	114	<150
		AT.8	1398	64	44	16	10	<30	<40	12	<40	738
		AT.9	296	79	130	36	10	124	53	30	106	<150
Al Magahra	Safa	AT12	1139	58	46	28	9<	58	<40	10	<40	660
		Mg.1	110	90	160	68	29	197	92	23	537	785
		Mg.3	113	100	160	67	25	194	84	30	575	272
Abu Zinema	Ataqa	Mg.5	105	72	160	78	36	199	97	24	571	709
		AZ.1	60	140	140	<12	<10	92	<40	37	239	b.d.l.
		AZ.5	62	140	130	<12	<10	87	<40	22	237	b.d.l.
		AZ.7	17	47	150	<12	<10	36	b.d.l.	12	215	b.d.l.
		AZ.8	48	100	100	26	17	84	224	32	281	<150

Table(5): Cont.

Location	Formation	Sample No	Mo ppm,	Cd ppm	U ppm	Th ppm	Cs ppm	Pb ppm	Rb ppm	Cr/Ni	Rb/Sr	V/Cr
Nile Valley	Esna	N79	<5	b.d.l.	<5	<10	<8	<15	56	3,93	0,19	1,00
		N78	<5	<5	<5	<10	<8	<15	49	3,19	0,16	1,05
		N75	<5	<5	<5	<10	<8	<15	30	7,77	0,12	0,98
		N72	<5	<5	<5	<10	<8	<15	59	1,94	0,16	1,26
		N69	<5	<5	<5	<10	<8	<15	51	3,03	0,15	0,99
		N66	<5	<5	<5	13	<8	<15	59	3,77	0,28	0,93
		N60	<5	<5	7	<10	<8	<15	52	2,48	0,19	1,01
		N55	<5	b.d.l.	<5	<10	<8	<15	29	1,63	0,07	1,09
	Tarawan	N54	b.d.l.	<5	<5	<10	b.d.l.	<15	16	4,16	0,02	0,62
		N52	b.d.l.	b.d.l.	6	<10	b.d.l.	<15	12	4,81	0,01	0,54
	Dakhla	N50	<5	b.d.l.	<5	<10	b.d.l.	<15	12	4,00	0,02	0,53
		N49	b.d.l.	<5	<5	<10	<8	<15	19	4,93	0,02	0,61
		N47	<5	<5	<5	<10	<8	16	24	2,35	0,21	1,70
		N45	<5	b.d.l.	<5	<10	<8	<15	26	4,94	0,24	1,16
		N43	<5	<5	<5	<10	b.d.l.	<15	30	2,18	0,70	1,56
		N39	<5	<5	<5	<10	b.d.l.	<15	41	5,76	0,26	0,93
		N37	<5	<5	<5	<10	b.d.l.	16	19	4,59	0,07	1,07
		N35	b.d.l.	<5	<5	<10	b.d.l.	<15	16	3,56	0,04	0,92
		N33	<5	<5	<5	<10	<8	<15	25	4,28	0,13	0,98
		N31	<5	<5	<5	<10	b.d.l.	<15	27	3,13	0,50	1,09
		N29	b.d.l.	382	380	<10	b.d.l.	<15	27	2,21	0,68	1,05
		N27	<5	<5	<5	<10	<8	<15	25	4,31	0,08	0,88
	Duwi	N26	<5	<5	<5	11	b.d.l.	<15	28	4,78	0,34	0,95
		N24	<5	<5	51	b.d.l.	b.d.l.	<15	10	5,33	0,01	0,91
		N21	b.d.l.	<5	<5	<10	<8	<15	10	4,17	0,05	1,10
		N17	<5	b.d.l.	<5	<10	<8	<15	35	5,44	0,07	0,90
		N15	<5	<5	<5	<10	b.d.l.	<15	29	2,96	0,12	1,12
		N10	<5	b.d.l.	<5	<10	<8	66	29	2,50	0,07	1,04
		N9	<5	<5	<5	<10	<8	<15	48	6,16	0,09	1,26
		N5	b.d.l.	7	<5	<10	<8	<15	41	6,64	0,02	1,11
Quseir phosphate mines	Duwi and Dakhla	N1	<5	<5	b.d.l.	<10	<8	<15	96	2,61	1,23	1,49
		Q.1	<5	b.d.l.	<5	<10	<8	<15	28	1,98	0,37	1,38
		Q.2	9	b.d.l.	27	b.d.l.	b.d.l.	15	10	2,50	0,03	1,50
		Q.7	214	15	52	<10	<8	33	32	3,01	0,07	4,84
		Q.11	474.2	47	41	<10	<8	20	31	3,39	0,06	4,99
		Q.16	258	73	34	<10	<8	29	30	2,71	0,06	6,47
		Q.18	b.d.l.	b.d.l.	24	b.d.l.	b.d.l.	<15	10	2,92	0,01	0,57
		Q.20	<5	<5	9	<10	b.d.l.	<15	32	4,10	0,25	1,28
		Q.26	302	40	44	<10	b.d.l.	30	40	3,05	0,06	2,69
		Q.31	<5	7	27	b.d.l.	b.d.l.	<15	10	5,56	0,01	0,20
Abu Tartur	Duwi	Q.34	<5	b.d.l.	11	<10	b.d.l.	<15	19	4,00	0,02	0,46
		AT.2	<5	<5	<5	<10	<8	<15	23	3,61	0,15	1,32
		AT.4	b.d.l.	<5	21	<10	b.d.l.	<15	<5	1,63	0,00	1,69
		AT.5	<5	b.d.l.	<5	<10	<8	<15	34	3,13	0,09	1,80
		AT.7	<5	9	22	<10	b.d.l.	<15	<5	3,44	0,08	1,61
		AT.8	<5	b.d.l.	<5	<10	<8	<15	27	2,07	0,01	1,12
		AT.9	<5	b.d.l.	<5	<10	b.d.l.	<15	25	3,85	0,11	1,30
Al Magh ara	Safia	AT.12	12	7	27	<10	b.d.l.	<15	6	1,14	0,00	1,92
		Mg.1	<5	<5	<5	19	<8	<15	39	2,90	0,35	0,81
		Mg.3	<5	<5	5	16	<8	<15	44	2,90	0,39	0,83
Abu Zinema	Ataqa	Mg.5	<5	<5	<5	13	<8	<15	37	2,55	0,35	0,78
		AZ.1	<5	<5	<5	19	9	124	51	7,67	0,85	1,49
		AZ.5	<5	b.d.l.	<5	15	<8	95	30	7,25	0,48	1,46
		AZ.7	<5	b.d.l.	<5	<10	<8	b.d.l.	10	3,00	0,59	4,06
		AZ.8	<5	6	<5	14	<8	79	20	3,23	0,42	1,24

Table 6a: Pearsons correlation coefficient values of each pair of elements of the studied shale samples

	SiO ₂	Al ₂ O ₃	CaO	MgO	Fe ₂ O ₃	TiO ₂	P ₂ O ₅	Na ₂ O	K ₂ O	SO ₃	Sr	Ba	V	Ni	Cr	Zn	Cu	Zr	Rb	Cl	F
SiO ₂	1.00																				
Al ₂ O ₃	0.59	1.00																			
CaO	-0.89	-0.77	1.00																		
MgO	0.21	-0.07	-0.15	1.00																	
Fe ₂ O ₃	0.09	0.33	-0.28	0.16	1.00																
TiO ₂	0.57	0.79	-0.63	-0.19	0.13	1.00															
P ₂ O ₅	-0.02	-0.36	0.14	-0.13	-0.03	-0.20	1.00														
Na ₂ O	-0.06	-0.03	-0.07	0.27	0.21	-0.20	0.11	1.00													
K ₂ O	0.52	0.28	-0.50	0.18	0.09	0.48	0.08	0.12	1.00												
SO ₃	-0.14	-0.10	0.09	-0.03	-0.05	-0.12	0.00	-0.19	-0.11	1.00											
Sr	-0.41	-0.45	0.49	-0.07	-0.23	-0.24	0.39	0.13	-0.03	0.02	1.00										
Ba	0.36	0.00	-0.27	-0.08	-0.06	0.13	0.62	0.30	0.41	-0.23	0.12	1.00									
V	0.41	0.61	-0.53	0.440	0.46	0.24	-0.21	0.18	0.16	-0.16	-0.40	-0.02	1.00								
Ni	-0.13	0.29	0.00	0.28	0.54	0.15	-0.02	0.21	-0.05	-0.14	-0.12	-0.08	0.46	1.00							
Cr	-0.28	0.30	-0.09	0.11	0.27	0.14	-0.08	0.25	-0.13	-0.21	0.10	-0.17	0.52	0.61	1.00						
Zn	0.00	0.21	-0.16	0.34	0.30	-0.27	0.02	0.41	-0.05	-0.08	-0.24	0.14	0.37	0.64	0.28	1.00					
Cu	0.40	0.33	-0.36	0.00	-0.13	0.38	0.05	0.12	0.57	0.01	-0.13	0.29	0.18	0.03	0.05	0.06	1.00				
Zr	0.46	0.54	-0.43	-0.33	-0.06	0.87	0.00	-0.31	0.35	-0.08	-0.11	0.27	-0.10	0.04	-0.08	-0.08	0.27	1.00			
Rb	0.39	0.35	-0.41	0.31	0.12	0.41	-0.03	0.28	0.82	-0.24	-0.14	0.41	0.33	0.24	0.10	0.28	0.52	0.25	1.00		
Cl	-0.07	-0.21	-0.13	0.03	0.07	-0.11	0.00	0.59	0.01	-0.01	-0.03	0.21	-0.07	-0.10	-0.08	0.31	0.07	-0.10	0.07	1.00	
F	0.02	-0.36	0.13	0.26	-0.11	-0.35	0.35	0.12	0.01	-0.05	0.19	0.48	-0.18	-0.07	-0.23	0.20	-0.05	-0.19	0.12	0.07	1.00

Table 6b: Pearsons correlation coefficient of each pair of elements of the studied phosphate samples

	SiO ₂	Al ₂ O ₃	CaO	MgO	Fe ₂ O ₃	TiO ₂	P ₂ O ₅	Na ₂ O	K ₂ O	SO ₃	Sr	Ba	V	Ni	Cr	Zn	Cu	Zr	Rb	Cl	F
SiO ₂	1.00																				
Al ₂ O ₃		1.00																			
CaO			1.00																		
MgO				1.00																	
Fe ₂ O ₃		0.81			1.00																
TiO ₂		0.98			0.82	1.00															
P ₂ O ₅			0.66				1.00														
Na ₂ O			0.63					1.00													
K ₂ O		0.96			0.74	0.98			1.00												
SO ₃		0.81			0.91	0.82			0.74	1.00											
Sr			0.68				0.93			0.67	1.00										
Ba	0.50											1.00									
V		0.53				0.62			0.61	0.71			1.00								
Ni		0.96			0.69	0.91			0.91	0.71				1.00							
Cr					0.73			0.88							1.00						
Zn								0.93							0.86	1.00					
Cu			0.50														1.00				
Zr																0.67		1.00			
Rb																0.64		0.89	1.00		
Cl								0.79							0.70	0.87		0.55	0.58	1.00	
F							0.95				0.82						0.54			0.16	1.00

Appendix B

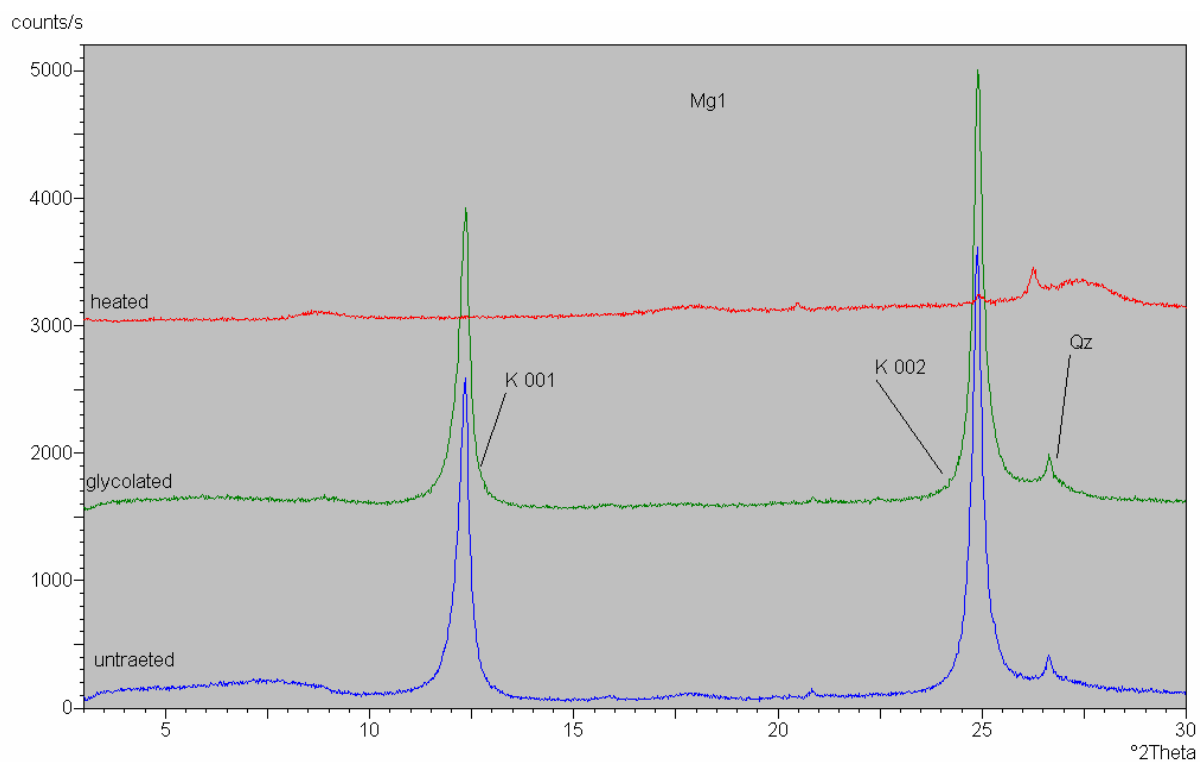


Fig.1: Representative profile of X-ray diffraction patterns for studied clays of Al Maghara coal mine

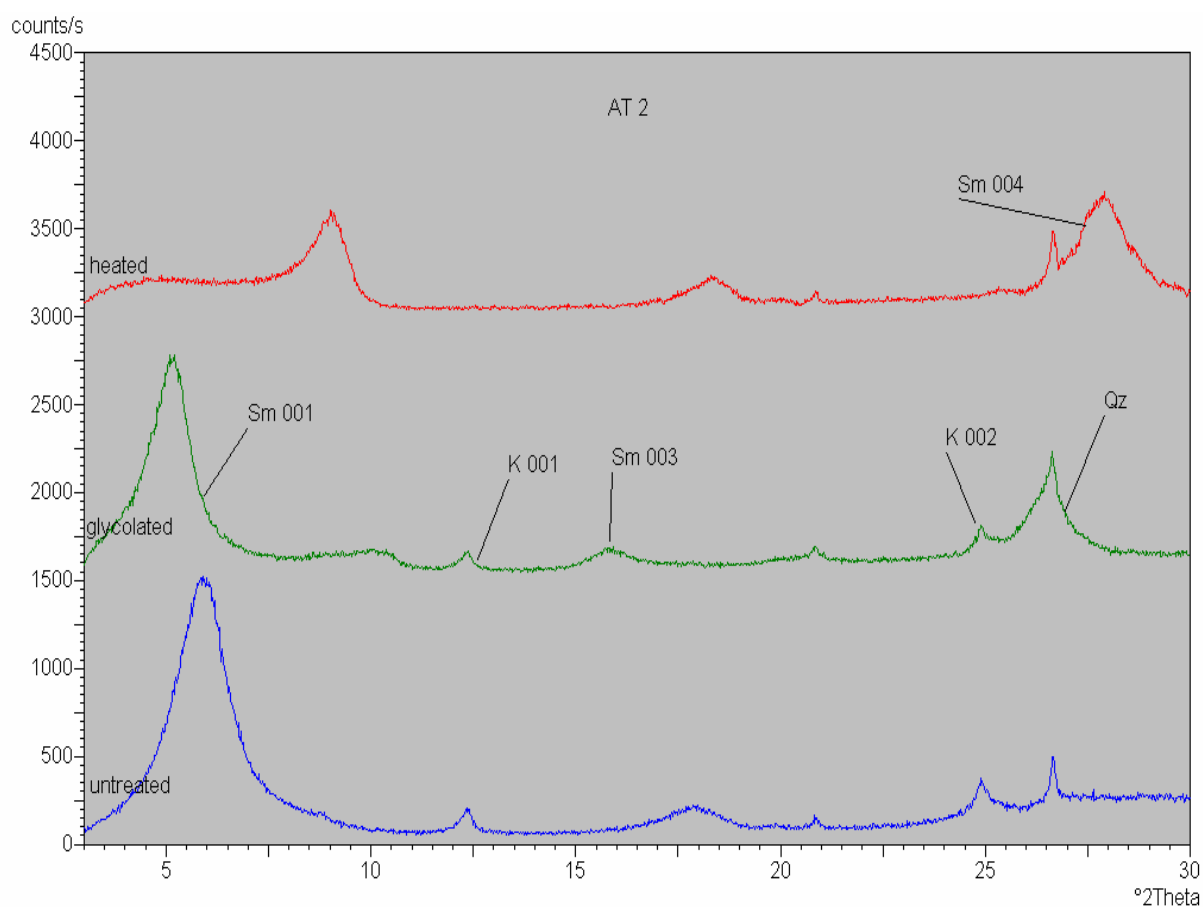


Fig.2: Representative profile of X-ray diffraction patterns for studied clays of Abu Tartur phosphate mine

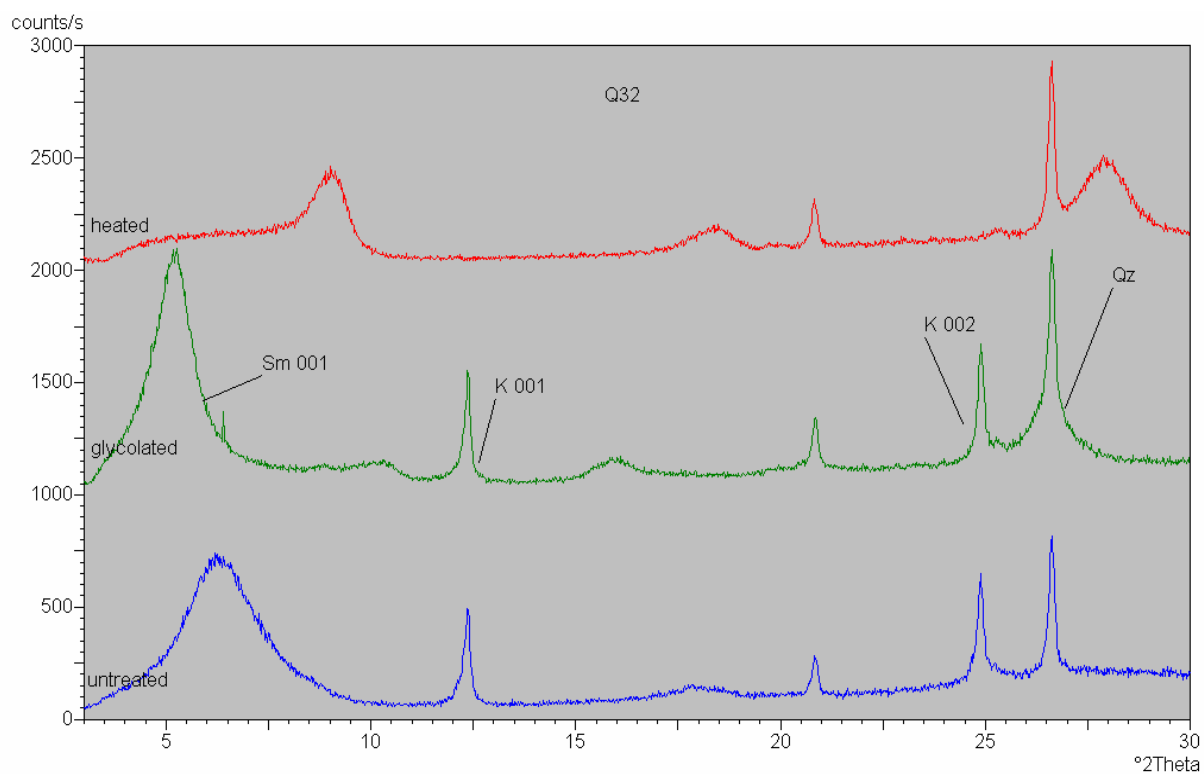


Fig.3: Representative profile of X-ray diffraction patterns for the studied clays of Quseir phosphate mine

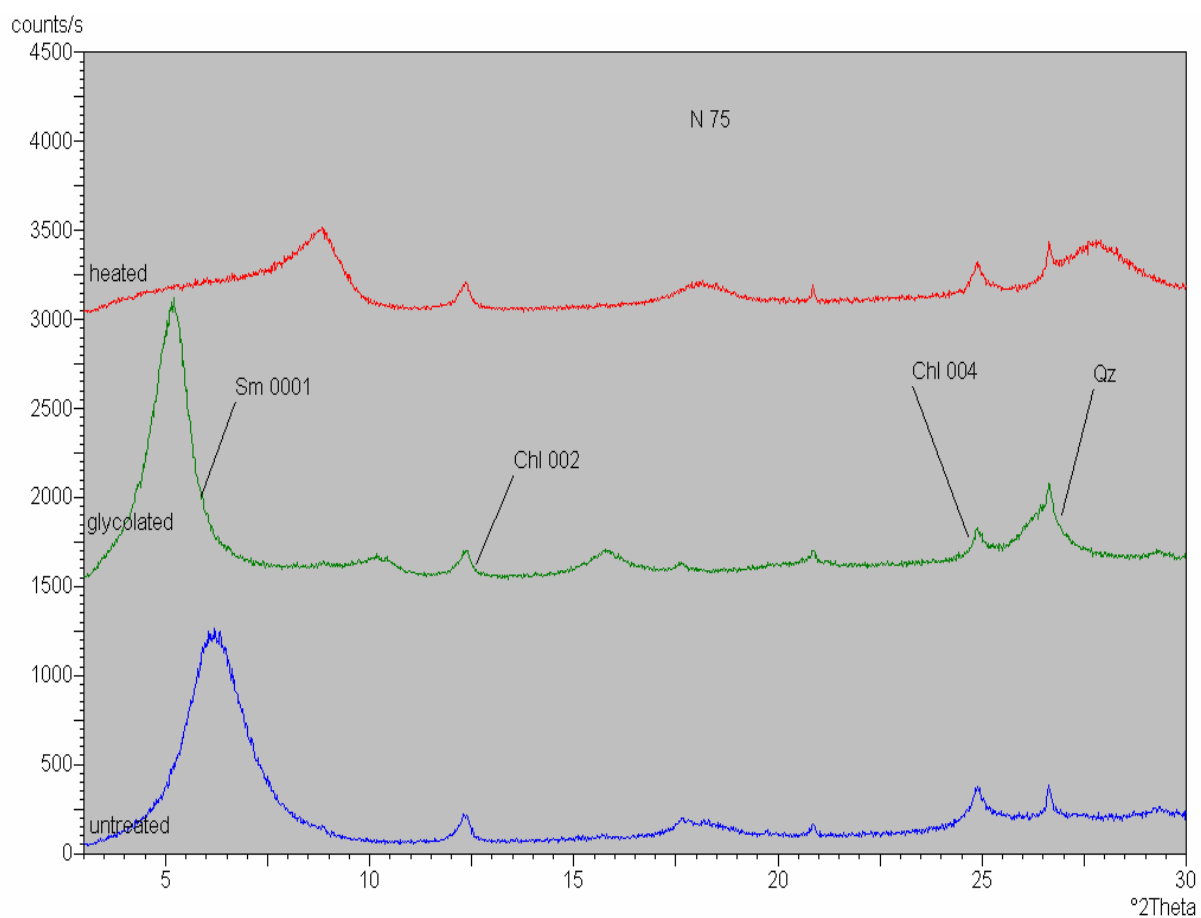


Fig.4: Representative profile of X-ray diffraction patterns for studied clays of Esna-Idfu, Nile Valley.

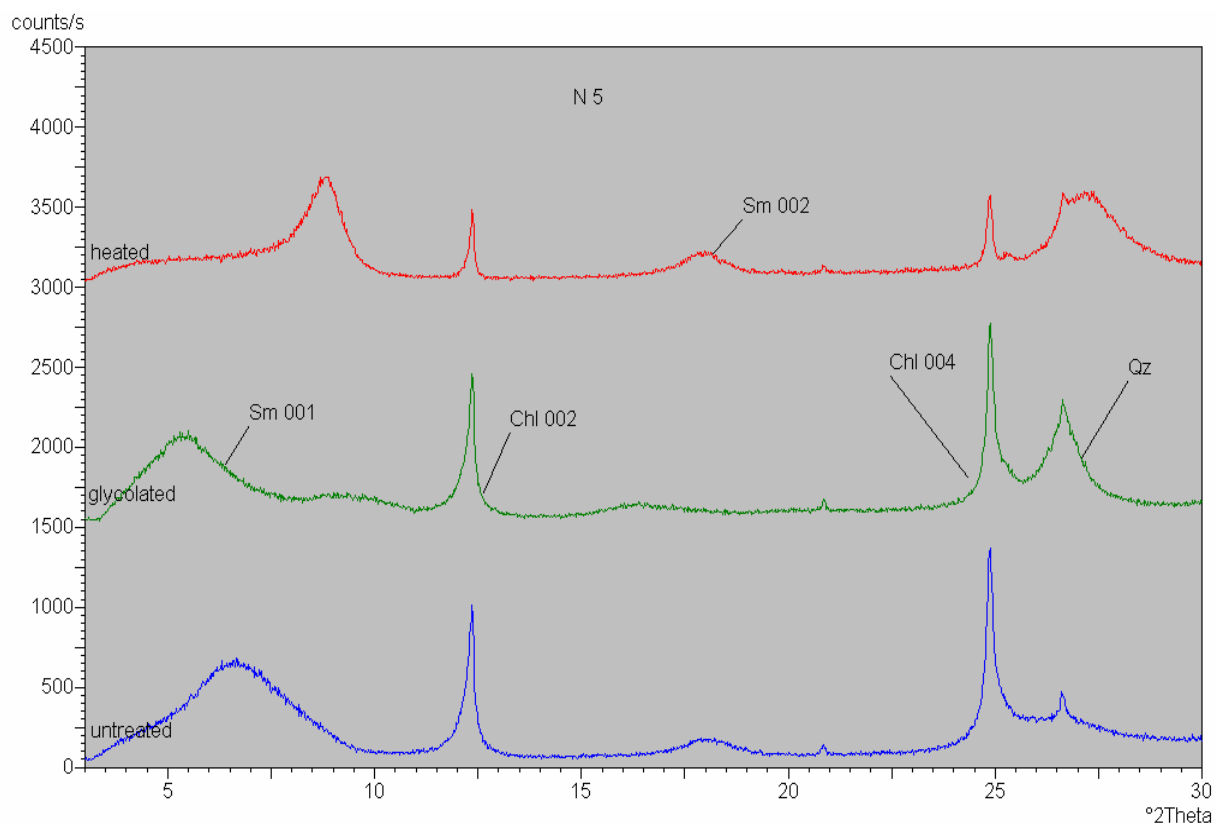


Fig.5: Representative profile of X-ray diffraction patterns for studied clays of Esna-Idfu, Nile Valley.

For abbreviations; Sm: smectite, K: kaolinite. Chl: chlorite, Qz: quartz.

Appendix C

Plate 1

- Fig. A: Photomicrograph of black shale of Duwi Formation in Abu Tartur phosphate mine shows quartz grains, monocrystalline, moderately to well sorted grains.
- Fig. B: Photomicrograph of black shale of Safa Formation in Al Maghara coal mine shows wisps of organic matter.

Plate 2

- Fig. A: SEM micrograph shows swirl texture with face to face arrangement of coarse detrital kaolinite in black shale of Safa Formation in Al Maghara coal mine.
- Fig. B: SEM micrograph shows swirl texture with face to face arrangement of coarse detrital kaolinite and detrital platelets of kaolinite with irregular edges in black shale of Ataqa Formation in Abu Zinema.

Plate 3

- Fig. A: Photomicrograph of black shale of Duwi Formation in Abu Tartur phosphate mine shows silty claystone.
- Fig. B: SEM micrograph shows smectite particles, have expanded, floored "cornflak" or "Okal leaf" like structure, in Duwi Formation in Abu Tartur phosphate mine.

Plate 4

- Fig. A: SEM micrograph showing the aggregates of euhedral pyritic grains in Duwi Formation in Abu Tartur phosphate mine.
- Fig. B: SEM micrograph showing aggregates of framboids of pyrite.

Plate 5

- Fig. A: Photomicrograph showing highly foraminiferal shale in Dakhla Shale in Esna-Idfu, Nile Valley.
- Fig. B: Photomicrograph showing highly foraminiferal shale in Dakhla Shale in Quseir mines.

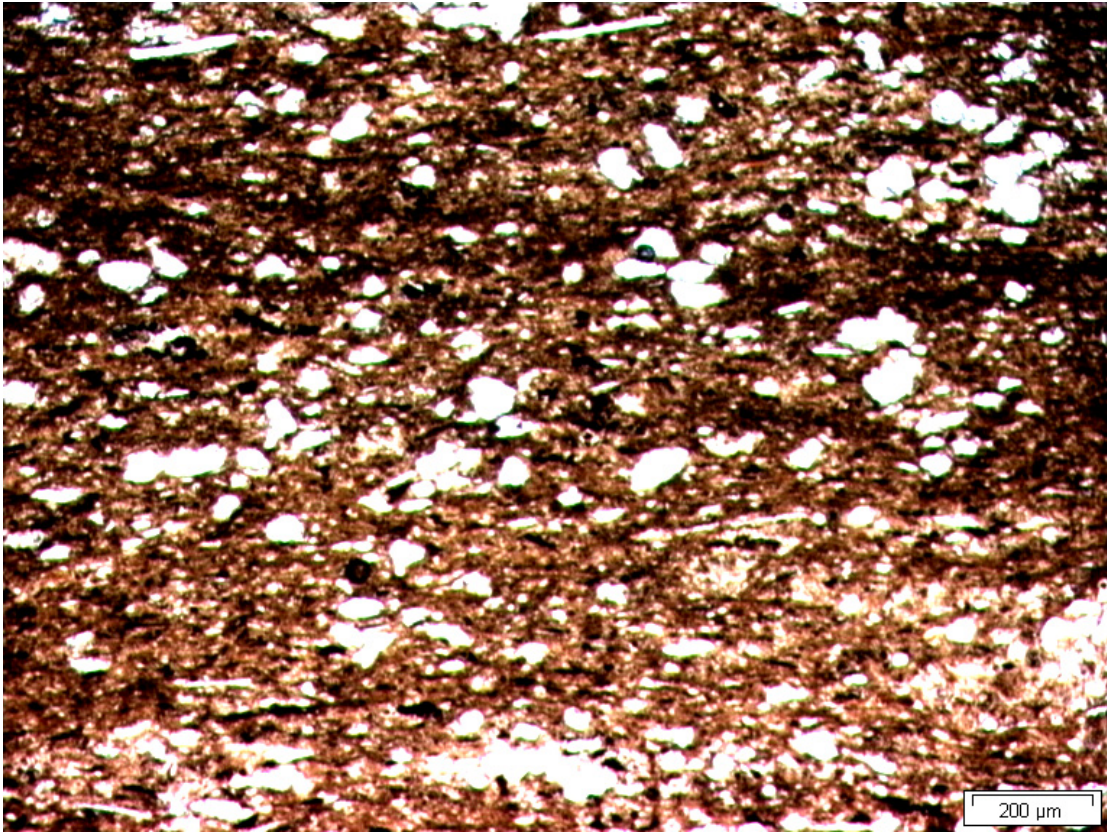
Plate 6

- Fig. A: Photomicrograph showing a micritic, microsparitic or sparitic matrix of the oyster limestone bed in Quseir mine.
- Fig. B: Photomicrograph showing micritic, microsparitic or sparitic, fossiliferous limestone of Tarawan Chalk in Esna-Idfu Nile Valley.

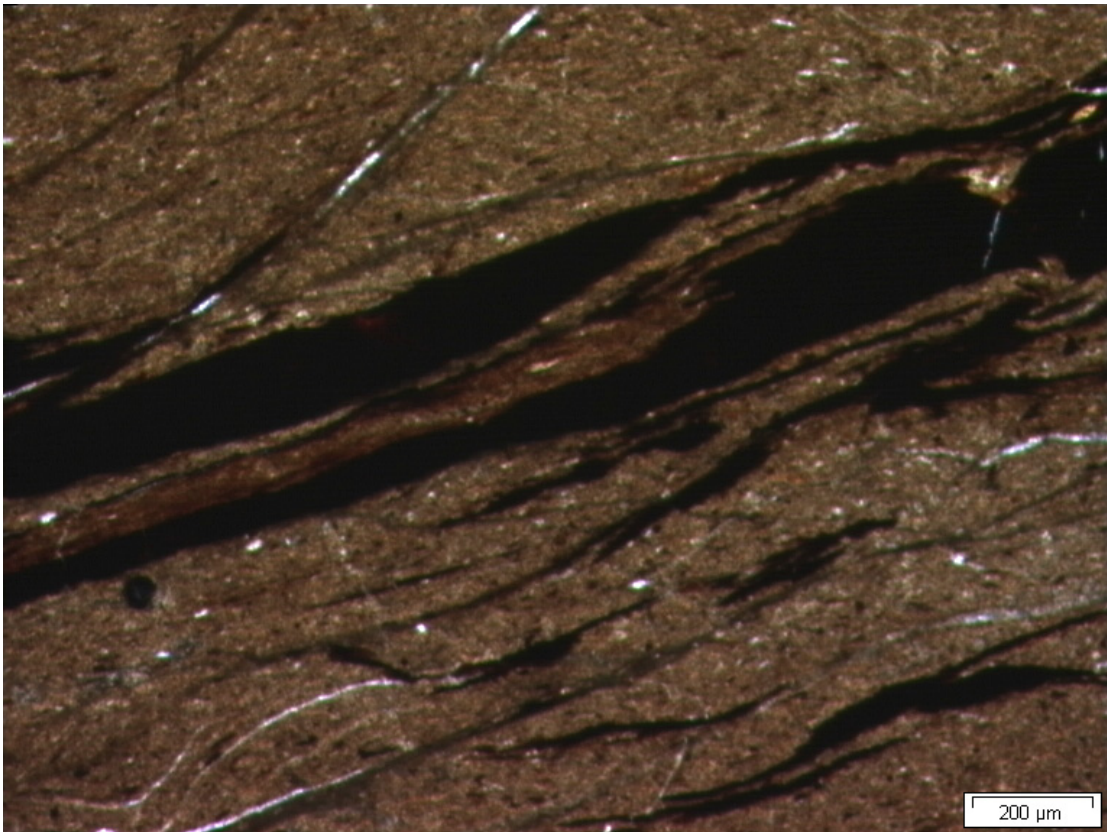
Plate 7

- Fig. A. Photomicrograph showing uncoated phosphate grains in Quseir phosphate mine
- Fig.B: SEM micrograph showing phosphate grains cemented by silica in Duwi Formation Esna-Idfu Nile Valley.
- Fig.C: SEM micrograph showing coated and uncoated phosphate grains cemented by calcite in Duwi Formation in Abu Tartur.

PLATE 1

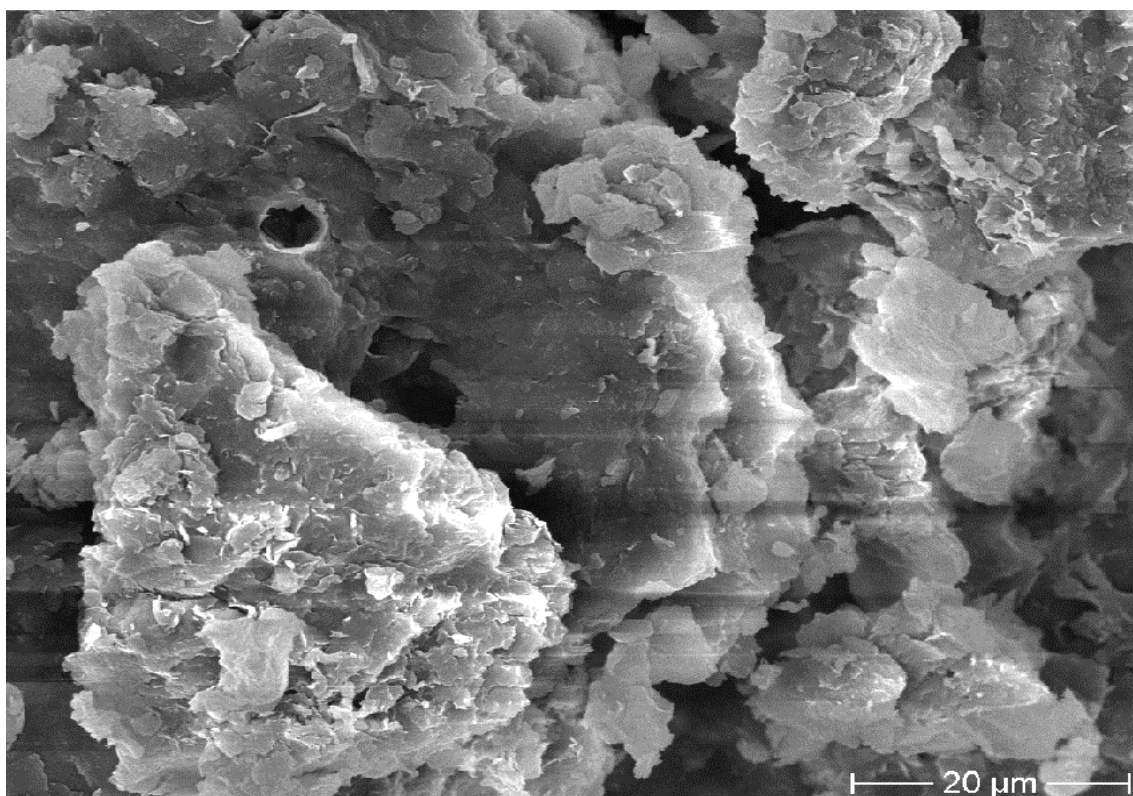


A

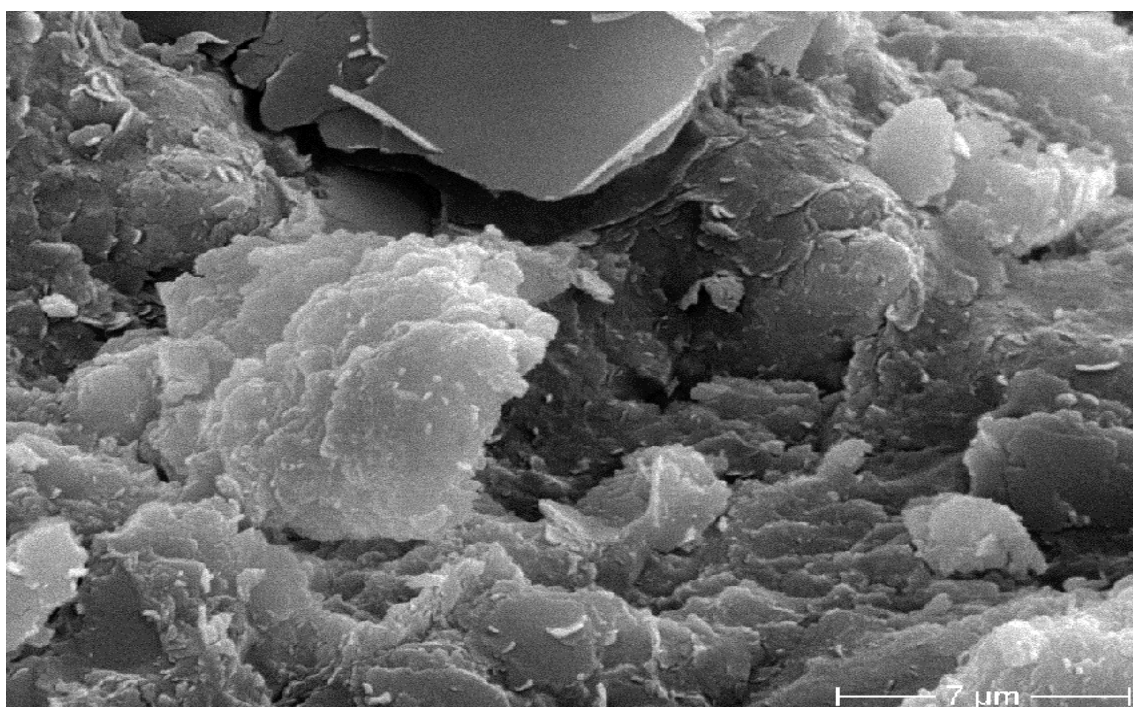


B

PLATE 2

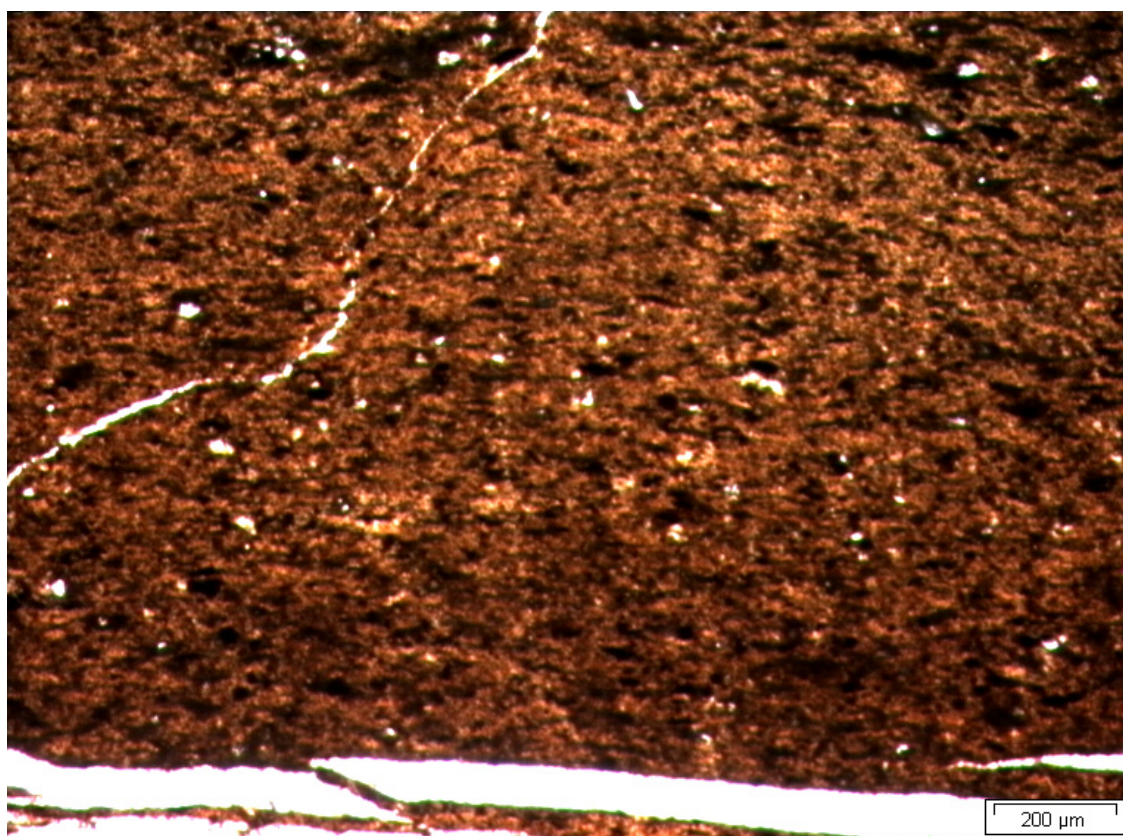


A

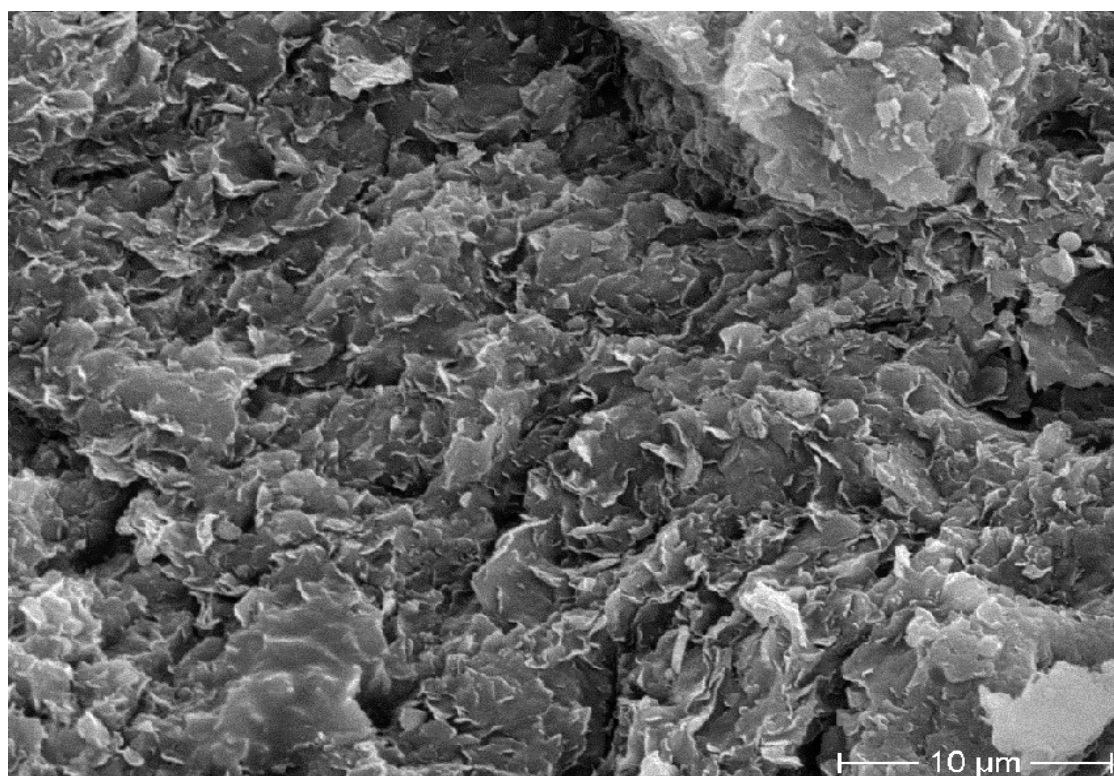


B

PLATE 3

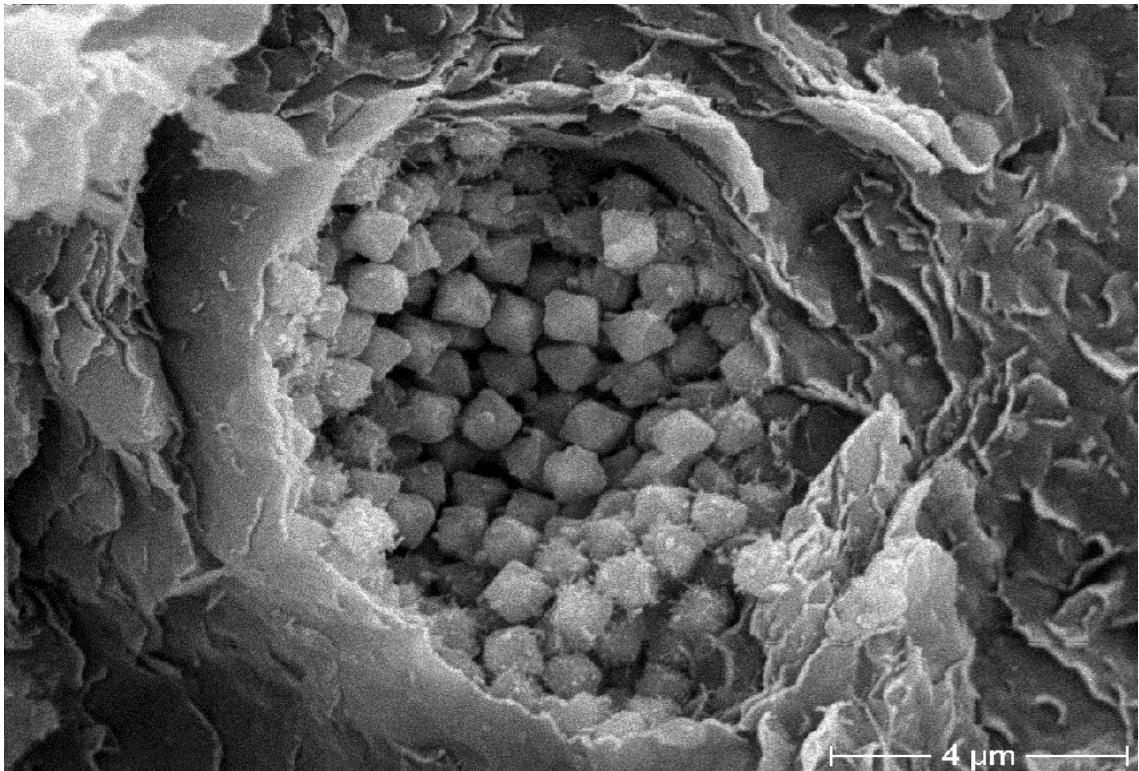


A

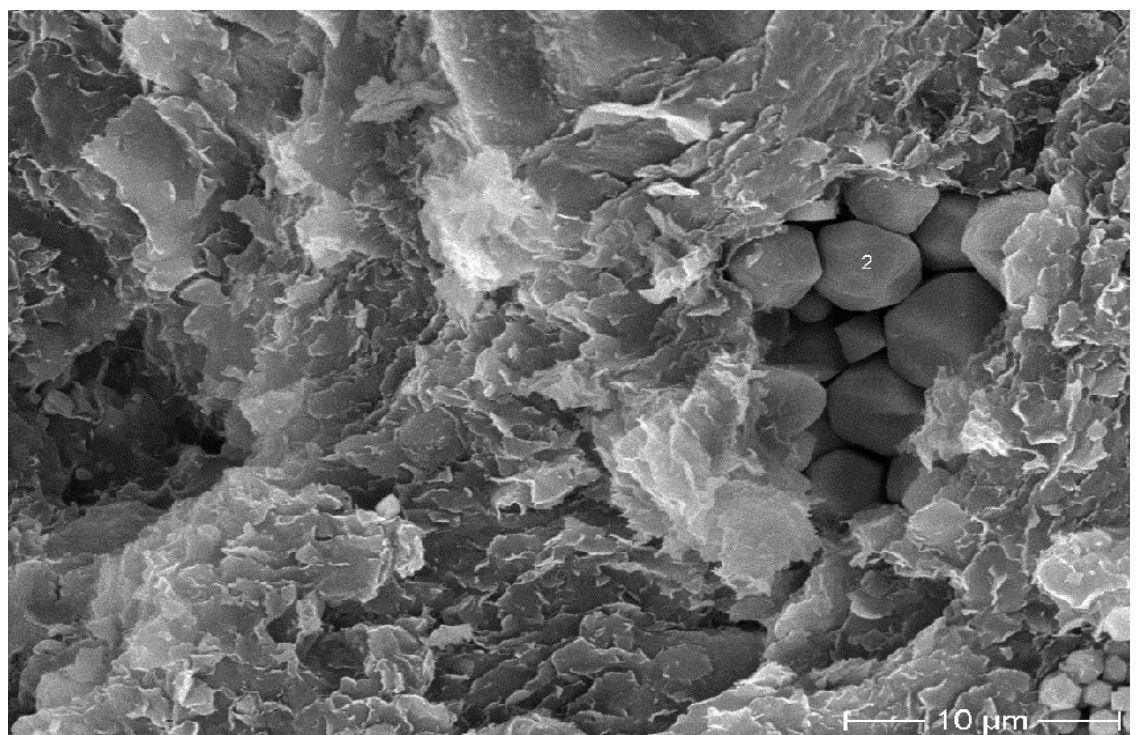


B

PLATE 4

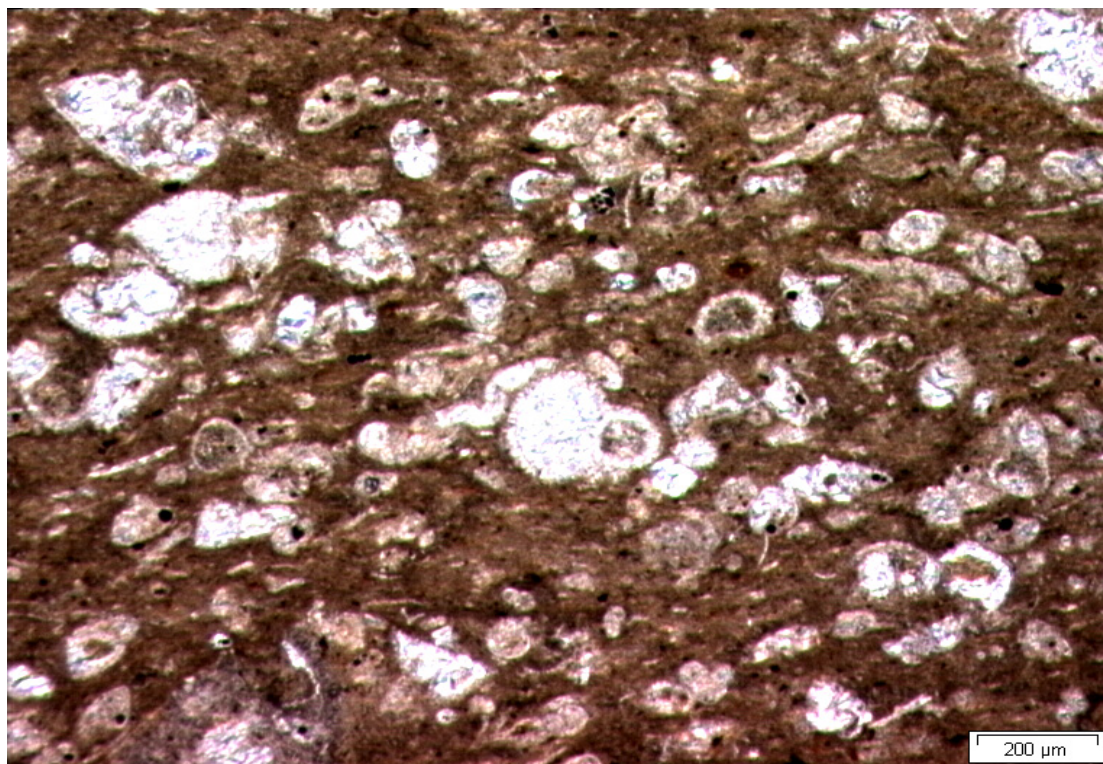


A

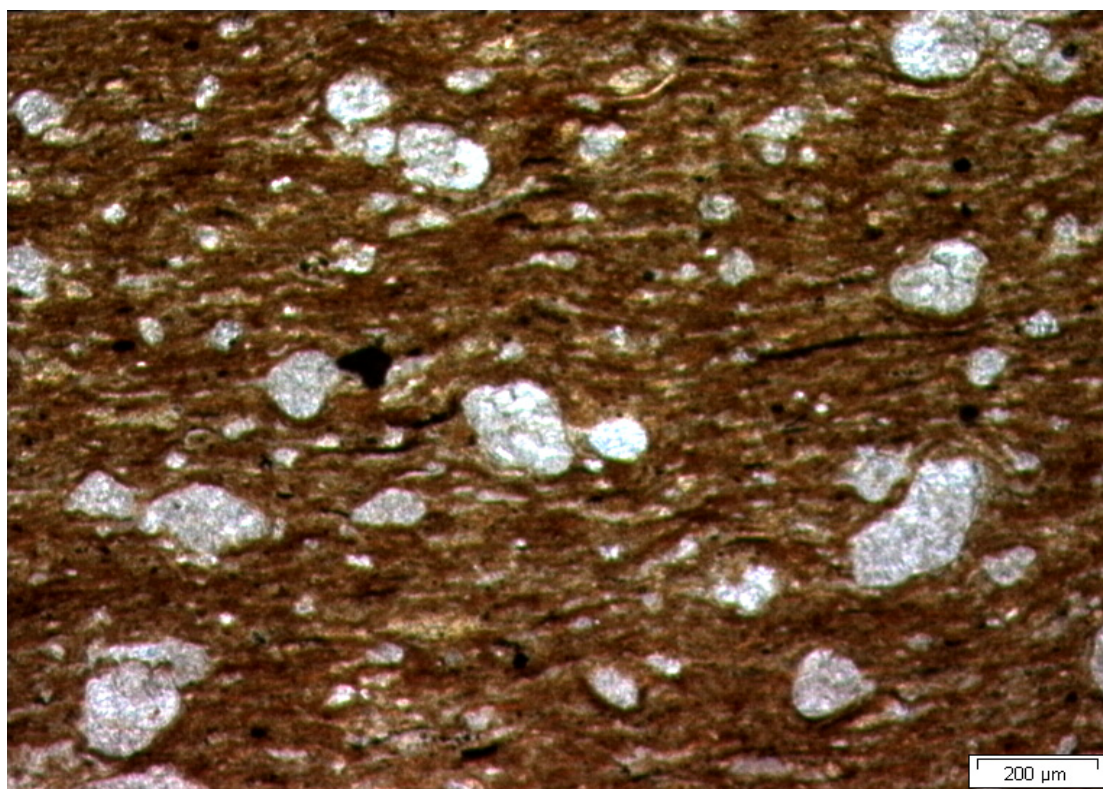


B

PLATE 5

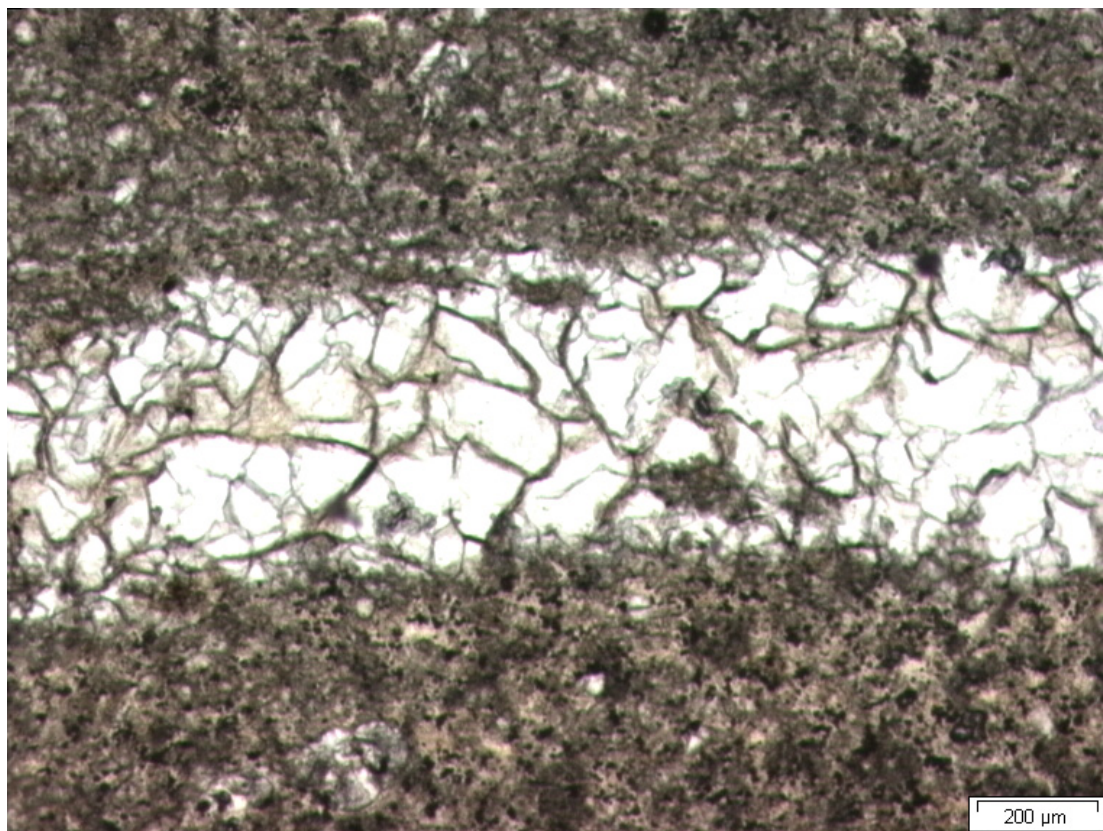


A

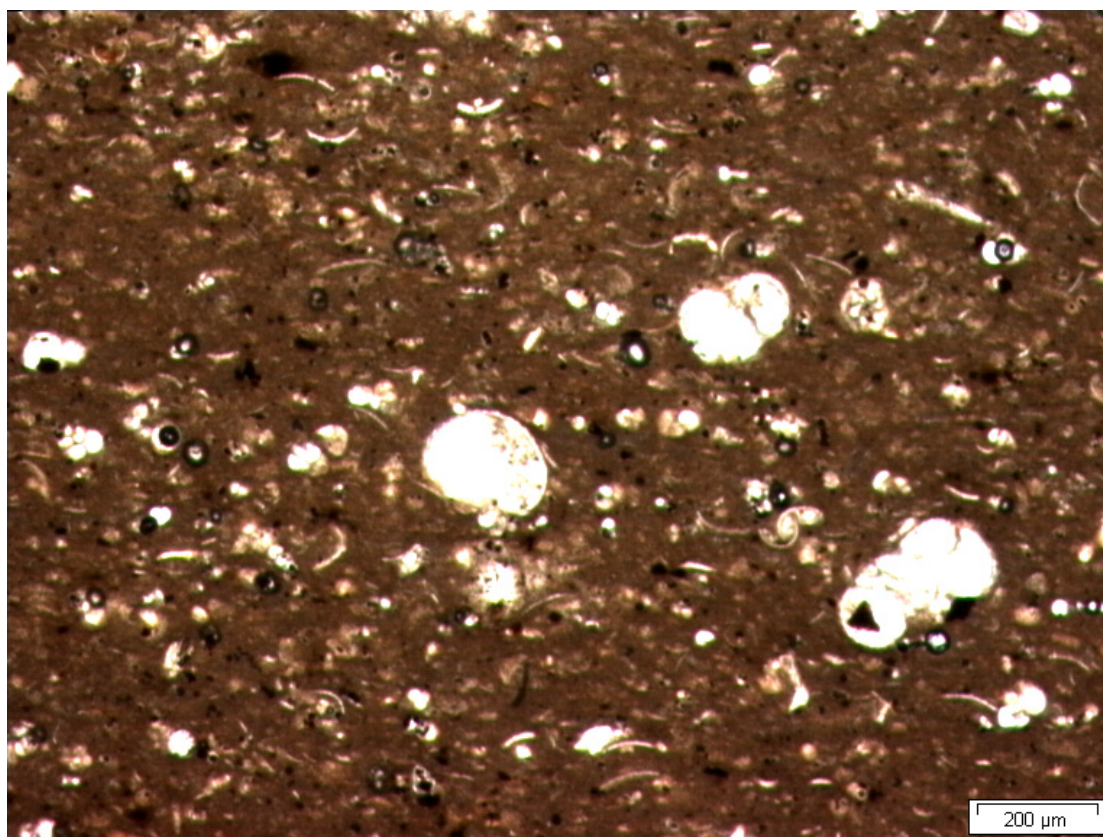


B

PLATE 6



A

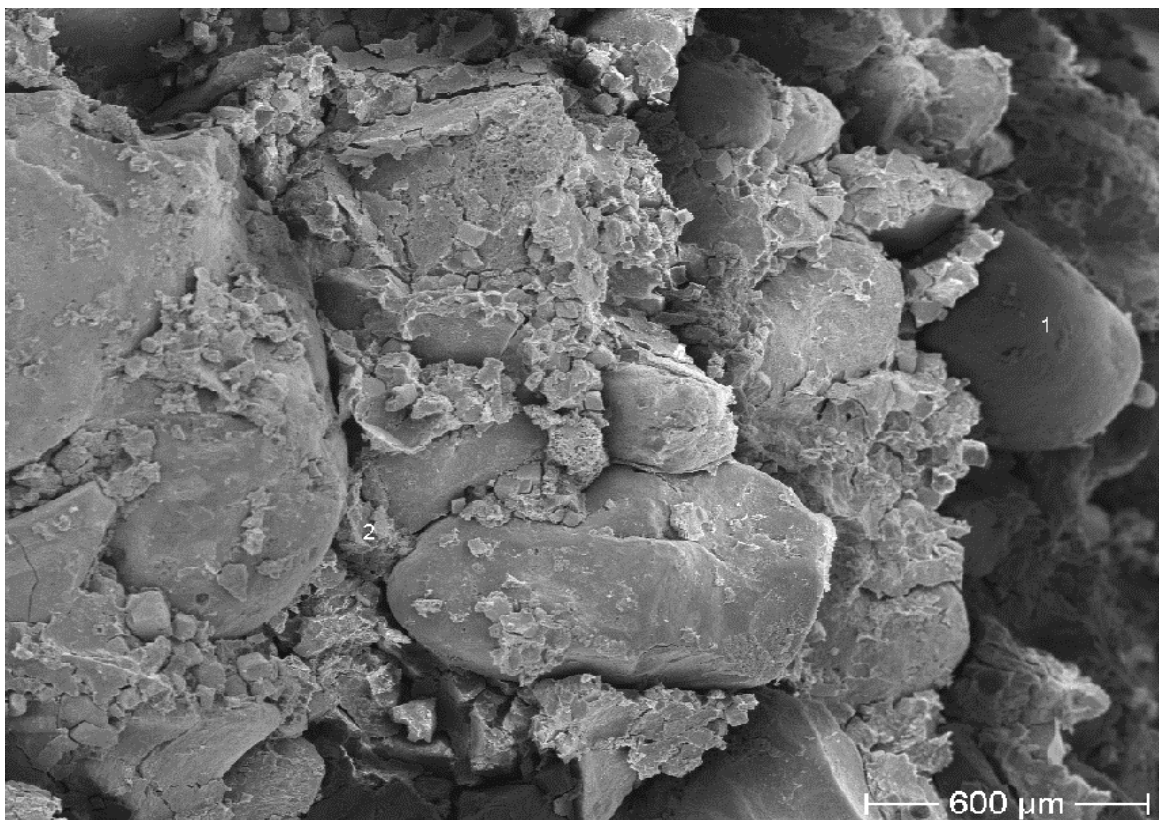


B

PLATE 7

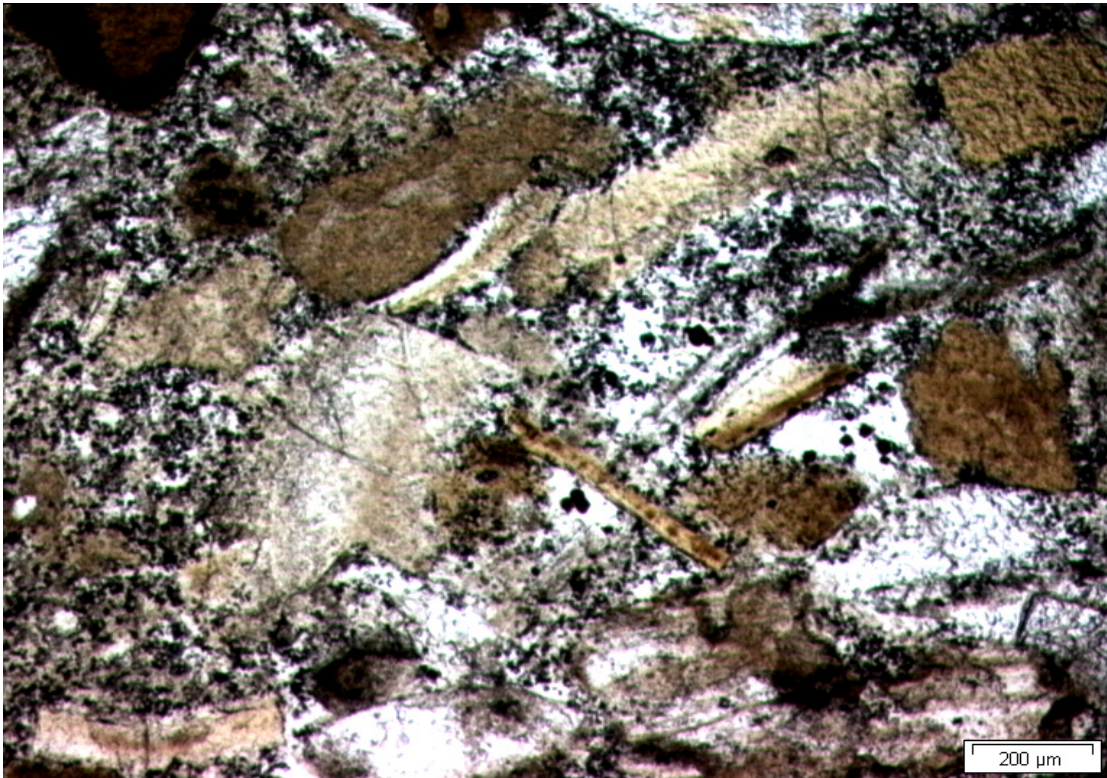


A



B

PLATE 7



C